FAA-74-24

REPORT NO. FAA-RD-75-174

AIRCRAFT L-BAND BALLOON - SIMULATED SATELLITE EXPERIMENTS
Volume I: Experiment Description and Voice and Data Modem Test Results

Peter D. Engels
Robert A. Wilson

OCTOBER 1975
FINAL REPORT

Prepared for
U.S. DEPARTMENT OF TRANSPORTATION
FEDERAL AVIATION ADMINISTRATION
Systems Research and Development Service
Washington DC 20591

Technical Report Documentation Page

1. Report No.	2. Government Accession No.	3. Recipient's Catalog No.
FAA-RD-75-174		

4. Title and Subtitle	5. Report Date
AIRCRAFT L-BAND BALLOON - SIMULATED SATELLITE EXPERIMENTS Volume I: Experiment Description and Voice and Data Modem Test Results	October 1975
	6. Performing Organization Code
7. Author(s) Peter D. Engels and Robert A. Wilson	8. Performing Organization Report No. DOT-TSC-FAA-74-24
9. Performing Organization Name and Address U.S. Department of Transportation Transportation Systems Center Kendall Square Cambridge MA 02142	10. Work Unit No. (TRAIS) FA311/R6153
	11. Contract or Grant No.
12. Sponsoring Agency Name and Address U.S. Department of Transportation Federal Aviation Administration Systems Research and Development Service Washington DC 20591	13. Type of Report and Period Covered Final Report Sept. 1971-Nov. 1973
	14. Sponsoring Agency Code

15. Supplementary Notes

16. Abstract

This report details the result of an experiment performed by the Transportation Systems Center of the Department of Transportation to evaluate candidate voice and data modulation systems for use in an L-Band Air Traffic Control System. The experiment was designed to evaluate performance in the presence of oceanic multipath, using a high altitude balloon carrying an L-Band transponder as a geostationary satellite simulator. The voice modems chosen were Delta Modulation, Pulse Duration Modulation and Adaptive Narrow-Band Frequency Modulation. The data modems used employed PSK modulation with coherent demodulation.

This is Volume I of a two-volume report. Volume II "CW Multipath Test Results and Analyses," FAA-RD-73-173, details the portion of the data dealing exclusively with the measurement of oceanic multipath.

17. Key Words	18. Distribution Statement
Multipath, Balloon Tests, Aerosat, Satellite ATC, Satellite Channel Characterization, Modems, Voice Systems, Digital Data Systems	DOCUMENT IS AVAILABLE TO THE PUBLIC THROUGH THE NATIONAL TECHNICAL INFORMATION SERVICE, SPRINGFIELD, VIRGINIA 22161

19. Security Classif. (of this report)	20. Security Classif. (of this page)	21. No. of Pages	22. Price
Unclassified	Unclassified	140	

Form DOT F 1700.7 (8-72) Reproduction of completed page authorized

PREFACE

As a result of detailed studies sponsored by the NASA and the Department of Transportation, a set of candidate voice and data modulation techniques were analyzed and experimental hardware was developed. At the invitation of the European Space Research Organization, a joint experiment was performed in Southern France during September and October of 1971, to evaluate these techniques. This report details the results of that experiment in two volumes. Volume I is titled "Experiment Description and Voice and Data Modem Test Results". Volume II is titled "Experiment Design and CW Tests".

The authors wish to acknowledge here the magnificent support provided by the Experiment Team, including: Robert Bland, Richard Waetjen, Michael Moroney, Franklin MacKenzie, Robert Brush, Robert Jones, Christopher Duncombe, Lee Tami, Andrew Caporale, and Joseph Golab. We would also like to acknowledge the leadership and support of Leo M. Keane.

CONTENTS

Section		Page
1	INTRODUCTION	1
2	EQUIPMENT DESCRIPTION	5
	2.1 Voice Modems	6
	2.1.1 CONSAT 4-Phase DELTA Voice Modem	6
	2.1.2 Suppressed Clock Pulse Duration Modulation	9
	2.1.3 Adaptive Narrow Band Frequency Modulation	16
	2.2 Data Modems	20
	2.2.1 Modulator	20
	2.2.2 Bell Demodulator	20
	2.2.3 Magnavox Demodulator	23
	2.3 Experiment Configuration	23
	2.3.1 Ground Station	23
	2.3.2 Balloon Transponder	23
	2.3.3 Aircraft Receiving System	27
	2.3.3.1 Antennas	27
	2.3.3.2 Low Noise Pre-Amplifiers	31
	2.3.3.3 L-Band - VHF Translator	31
	2.3.3.4 King Transceivers	31
	2.3.3.5 Demodulators	31
	2.3.3.6 Honeywell 5600 Instrumentation Recorder	31
	2.4 Laboratory Evaluation of Test Modems	32
	2.4.1 Voice Modem	32
	2.4.2 Data Model Laboratory Evaluation	34
	2.5 C/No Measurement	34
	2.5.1 C/No Measurements Unit	34
	2.5.2 C/No Calibration	37
3.	EXPERIMENT CONFIGURATION AND CONDITIONS	38
	3.1 Discussion of Data	38
	3.1.1 Laboratory Data	38
	3.1.2 Field Data	39

CONTENTS (CONT'D)

Section		Page
	3.2 C/No Measurements During Flight	45
	3.2.1 Field C/No Measurements	45
	3.2.2 CW Multipath Measurements	47
4	RESULTS AND CONCLUSIONS	64
	4.1 Discussion of Results	64
	Voice Modems - Field Results	72
	4.2 Conclusions	88
	4.3 Digital Data Modem Results	89
APPENDIX A -	MODEM DATA REDUCTION AND ANALYSIS	93
APPENDIX B -	A COMPARISON OF SATELLITE-TO-AIRCRAFT, BALLOON-TO-AIRCRAFT AND AIRCRAFT-TO AIRCRAFT MULTIPATH TESTS	102
APPENDIX C -	CONCLUSIONS	121
APPENDIX D -	SIMULATION OF FADING BANDWIDTH WITH AN AIRCRAFT-TO-AIRCRAFT LINK	123
APPENDIX E -	ELEVATION ANGLE θ VS ANGLE OF INCIDENCE ϕ	126
APPENDIX F -	REFERENCES	129

LIST OF ILLUSTRATIONS

Figure		Page
1-1	Experiment Configuration	2
2-1	Four-Phase Delta Voice Modulator (DCDM) w/4ϕ PSK	7
2-2	Four-Phase Delta Voice Modulator Receive System 4ϕ PSK	8
2-3	Performance of COMSAT Four-Phase Delta Voice Modem	10
2-4	PDM Modulator	12
2-5	PDM Modulator Timing Diagram	13
2-6	PDM Demodulator	14
2-7	PDM Demodulator Waveforms	15
2-8	ANBFM Modulator	17
2-9	ANBFM Demodulator	18
2-10	ANBFM Demodulator Frequency Response	19
2-11	Data Modulator	21
2-12	Bell Aerospace Data Demodulator	22
2-13	Magnavox Data Demodulator	24
2-14	Ground Station Block Diagram	25
2-15	Aircraft Receiving Station	28
2-16	Roll Plane Pattern -35° DICO Antenna	29
2-17	Laboratory Set-Up Block Diagram	33
2-18	Flight Tape Re-Record Set-Up	35
2-19	C/No Measurement Technique	36
3-1	Experiment Communications Links	41
3-2	Downlink Frequency Assignments	42
3-3	Experiment Geometry	44
3-4	Strip Chart Format	46

LIST OF ILLUSTRATIONS (CONT'D)

Figure		Page
3-5	C/No Calibration Curve	48
3-6	C/No Variation - 15° Elevation Angle	49
3-7	C/No Variation - 10° Elevation Angle	50
3-8	C/No Variation - 7° Elevation Angle	51
3-9	Block Diagram, CW Measurement System	53
3-10	AGC Variation with Signal Level	55
3-11	Cumulative Density of Signal, 8° Elevation Angles Test Run #1	56
3-12	Cumulative Density of Signal, 8° Elevation Angle	57
3-13	Cumulative Density, 12° Elevation Angle	58
3-14	Roll Plane Pattern - Zenith Antenna	61
3-15	AGC - Cumulative Density - Curve	62
4-1	Laboratory Intelligibility Curve, ANBFM	65
4-2	Laboratory Intelligibility Curve, PDM	66
4-3	Laboratory Intelligibility Curve, Delta	67
4-4	Comparison of Modem Performance	68
4-5	Harvard Sentence Intelligibility Vs. Word Intelligibility	70
4-6	Equivalent Sentence Intelligibility Vs. Carrier-to-Noise Ratio	71
4-7	15° Data, ANBFM	73
4-8	15° Data, PDM	74
4-9	15° Data, Delta-Mod	75
4-10	Comparison of 15° Data	76
4-11	10° Data, ANBFM	77
4-12	10° Data, PDM	78
4-13	10° Data, Delta-Mod	79

LIST OF ILLUSTRATIONS (CONT'D)

Figure		Page
4-14	Comparison of 10^{o} Data	80
4-15	7^{o} Data, ANBFM	81
4-16	7^{o} Data, PDM	82
4-17	7^{o} Data, Delta Mod	83
4-18	Comparison of 7^{o} Data	84
4-19	Intelligibility Comparison - 1000 Word List vs 256 Work List	87
4-20	Magnavox Data Modem - Bit Error Rate vs C/No	90
4-21	Bell Aerospace Data Modem - Bit Error Rate vs C/No	91
A-1	Voice Data-Curve Fitting Algorithm	100
B-1	Aircraft-Balloon Geometry	103
B-2a	F-Relative Doppler Shift Vs. θ Elevation Angle λ = 18 cm (L-Band)	107
B-2b	F-Relative Doppler Shift Vs. θ Elevation Angle (Same as B-2a) λ = 2.5 m (VHF)	108
B-3a	Δf Doppler Shift Vs. Elevation θ. λ = 18 cm (L-Band.	109
B-3b	Δf Doppler Shift Vs. Elevation θ. (Same as B-3a) λ = 2.5 m (VHF)	110
B-4a	Relative Doppler Shift Vs. Elevation Angle. λ = 18 cm. (L-Band)	111
B-4b	Relative Doppler Shift Vs. Elevation Angle. (Same as B-4a) λ = 2.5 m (VHF)	112
B-5	Normalized Fading Bandwidth Vs. Elevation Angle	115
B-6	B_s Fading Bandwidth Vs. Elevation Angle	116
B-7	Space Loss Difference in dB Vs. Elevation	119
B-8	Rate of Change of Elevation	120
D-1	Geometry of Aircraft-to-Aircraft Link	123
E-1	Elevation Angle θ vs Angle of Incidence for Satellite at 19323 n.m	128

LIST OF TABLES

Table		Page
2-1	UHF/L-BAND LINK ANALYSIS FOR BALLOON EXPERIMENT.....	26
2-2	GAIN AND MULTIPATH REJECTION WITH R-35° ANTENNA.....	30
3-1	SUMMARY OF VOICE DATA RECORDED.....	38
3-2	VOICE TEST SUMMARY.....	40
3-3	CW MULTIPATH TEST CONDITIONS.....	52
3-4	AVERAGE OBSERVED FADE LEVELS.....	59
4-1	C/NO VS INTELLIGIBILITY - LABORATORY DATA.....	69
4-2	RANGE OF VALID DATA.....	85
4-3	REQUIRED C/NO FOR AI = 0.3.....	86
4-4	REQUIRED C/NO FOR AI = 0.19.....	86
4-5	BIT-ERROR RATE VS C/NO (dB-Hz).....	92
B-1	CALCULATIONS FOR LOW ELEVATION ANGLE.....	106
B-2	NORMALIZED BANDWIDTH.....	114
B-3	SCATTER BANDWIDTH FOR L-BAND ELEVATION ANGLE AND SURFACE ROUGHNESS.....	114

1. INTRODUCTION

This report presents the results of an evaluation of candidate voice and data modulation schemes considered for use in an L-band satellite air traffic control system such as AEROSAT. The evaluation included field experiments in a high altitude balloon-simulated satellite environment and a set of controlled laboratory measurements.

The basic goal of this test program was to obtain performance data on selected modems operating in the presence of oceanic multipath. The modems were chosen for their potential applicability in an aeronautical satellite system, i.e., acceptable performance at low (43 dB-Hz) carrier-to-noise density ratios.

Figure 1-1 shows the basic operational configuration for the experiment. A high altitude balloon with an L-band transponder aboard was chosen to simulate a geostationary satellite. The signal transmission originated on the ground and was transmitted to the high altitude balloon, which transponded to the receiving station aboard a jet aircraft where it was demodulated and recorded for later evaluation.

The experiment was conducted jointly with the European Space Research Organization (ESRO), utilizing the French Balloon Launching Facility located at Aire Sure L'Adour, France. All balloons were provided by ESRO, who also provided the ground transmitting and balloon tracking facilities, and the balloon transponder. TSC provided the ground modulators for its portion of the experiment, and an instrumented jet aircraft which received, demodulated and recorded the necessary signals. The aircraft was a Convair 880 from the FAA NAFEC facility.

Evaluation of digital data was simply based on the bit-error rate as a function of carrier-to-noise power density. This technique is very straight forward and simple to implement. The evaluation of voice data is not quite as easily implemented. An extensive examination of voice transmission evaluation techniques

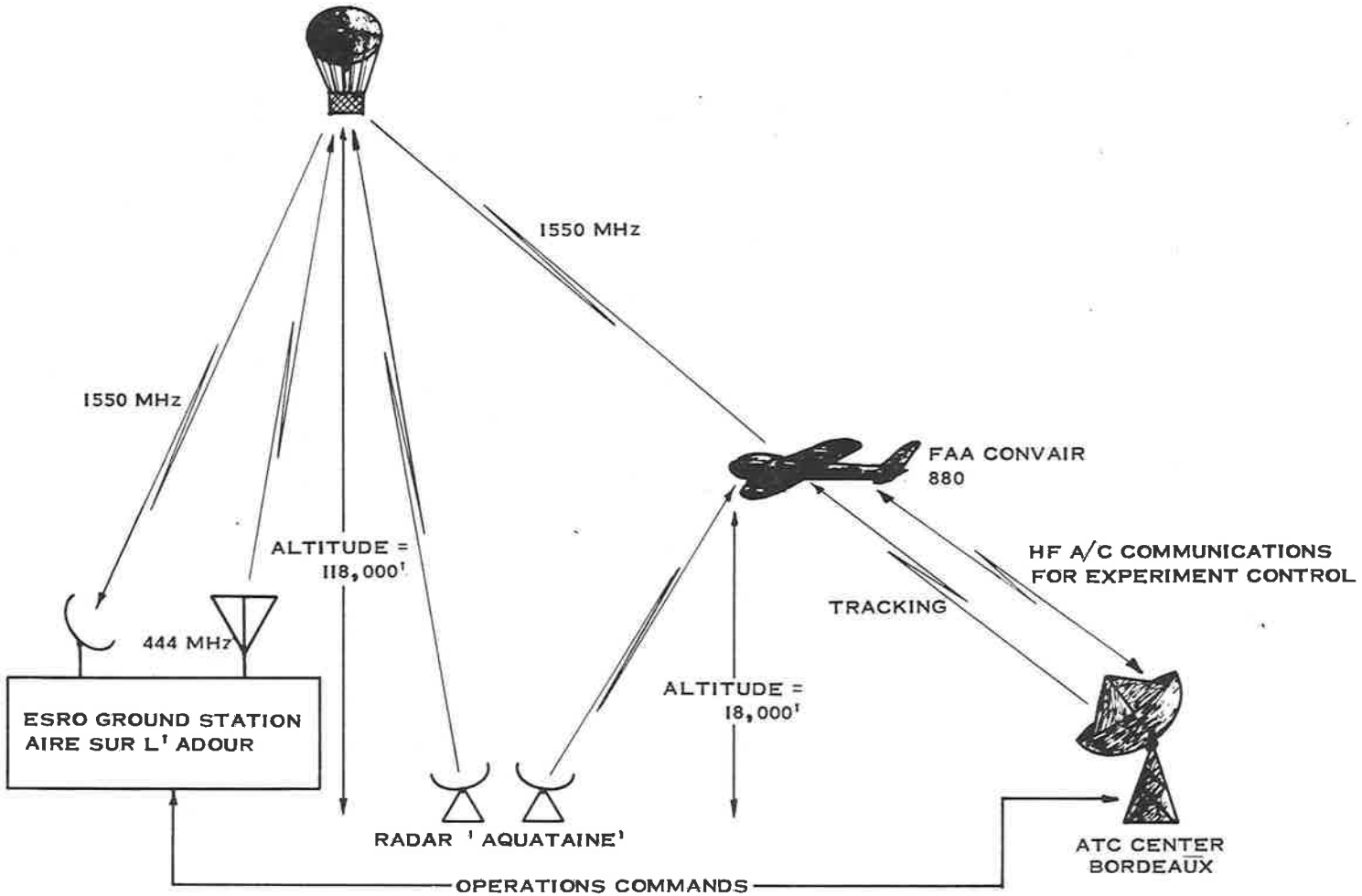

Figure 1-1. Experiment Configuration

was performed. The selected technique consisted of the transmission of standard word lists using phonetically balanced words.

The voice modulation schemes chosen for evaluation were as follows: 1) Variable Slope Delta modulation using four-phase PSK modulation. This modem was built by Comsat Research Laboratories. 2) Suppressed Clock Pulse Duration Modulation (PDM) using bi-phase PSK. This modem was built by Magnavox Research Laboratory. 3) Adaptive Narrow Band Frequency Modulation (ANBFM). This modem was built by the Bell Aerospace Co.

Two data modems were used. Both employed differentially Encoded Bi-phase PSK, transmitted at 1200 b/s, and used PN codes for detection of bit-errors. The two modems were built by Magnavox and Bell Aerospace respectively.

The report is organized into three major sections which appear in the following order:

Section 2.0 Equipment Description - This section describes the equipment used in both the field and laboratory evaluations of modem performance. Included is a detailed description of each modem. Section 2.0 also describes the equipment and techniques used for measurement of carrier-to-noise power density (C/No) during the experiment.

Section 3.0 Experiment Configuration and Conditions - This section contains a brief description of the overall operation, including experiment geometry and a summary of the flight data. The C/No measurements made during the experiments are presented to set forth the conditions under which the systems were evaluated.

Section 4.0 Results and Conclusions - Presented herein are the performance characteristics obtained from the laboratory and field evaluations of the various modems.

Also included are the following Appendixes:

Appendix A - Modem Data Reduction and Analysis - This section examines the available techniques for voice modem evaluation, provides the rationale for selection of the 1000 word PB list,

and describes the technique by which the recorded data was analyzed.

Appendix B - Balloon-Aircraft Geometry

This section provides an analysis of the Balloon-Aircraft geometry and a comparison with the Satellite-Aircraft geometry.

2. EQUIPMENT DESCRIPTION

The performance objective of AEROSAT Communications system is to provide a satellite capability which can attain the quality of voice and data communication service required of an operational air traffic control system. In terms of specific system performance requirements, the voice quality desired corresponds to an articulation index of approximately 50% at a link quality of C/No* = 43 dB-Hz. The data transfer quality desired is a bit-error rate of one part in 10^5 at a C/No = 43 dB-Hz.

The selection of a modem for transmission and reception of voice and data signals through a satellite is primarily constrained by the need to operate satisfactority with limited satellite power output consistent with the overall channel capacity system requirements. This constraint also pertains to the avionics elements in the system in order to minimize user cost and transmitter size. Accordingly, the modems selected for this test program were chosen for their ability to provide reasonable quality voice and low data rate data signals at low signal-noise ratios. The three candidate voice modems which were selected for test had demonstrated under laboratory conditions, satisfactory system performance. Since data communications are an important mode of operation, two PSK modulation data modems were also included for field evaluation.

The major emphasis in this experiment, however, was on performance of voice modems. Until quite recently, little effort has been expended on the problem of providing reasonable quality voice transmissions with low signal-noise ratios. In addition, aircraft communications have traditionally relied on voice almost exclusively.

*Throughout this report, the abbreviation C/No is used to denote "carrier-to-noise-power-density ratio."

2.1 VOICE MODEMS

2.1.1 COMSAT 4-Phase DELTA Voice Modem

The delta modulated four-phase PSK modem was built at COMSAT Laboratories. The delta modulator used was capable of delivering good quality speech at 18 kbit/sec.

The transmit and receive units of the system are shown in Figures 2-1 and 2-2 respectively. Referring first to the transmit unit, the audio signal, limited by filtering to the band from 200 to 2500 Hz is supplied to the digitally controlled delta modulator (DCDM). In a delta modulated system, instead of absolute signal amplitude being transmitted at each sampling instant only the changes in signal amplitude are encoded. In Variable Slope Delta, the step size fed to the comparator circuit is controlled by the previous history of the signal amplitude. This companding action provides the system with an ability to follow rapid changes in the input signal and to some degree prevents slope overload.

The delta modulator is operated at a clock rate of 18 kHz and provides an 18 kilobit per second binary signal at its output. This is supplied to a differential binary coder which encodes the differences between bit pairs into two 9 kilobit per second binary signals designated P and Q. These are next supplied to a pair of mixers which phase modulate a 70.000 MHz carrier oscillator so that the carrier is shifted by 90° by ± 1. The mixer outputs are summed to form the four-phase PSK modulated IF carrier. Also, a pilot at a frequency of either 69.989 or 70.011 MHz is added at a level 10 dB below the carrier. Provision of two possible pilot frequencies, one 11 kHz below and the other 11 kHz above the 70.000 MHz carrier is provided to accommodate the possibility of spectrum inversion. At this point, the 70 MHz IF carrier and the pilot are supplied to the ESRO designed up-converter.

The receive unit, shown in Figure 2-2, is designed to accept the received signal at a frequency of 10 MHz. The signal is first processed by an AFC loop which translates it to a center frequency of 512 kHz. This translation is accomplished by locking onto the

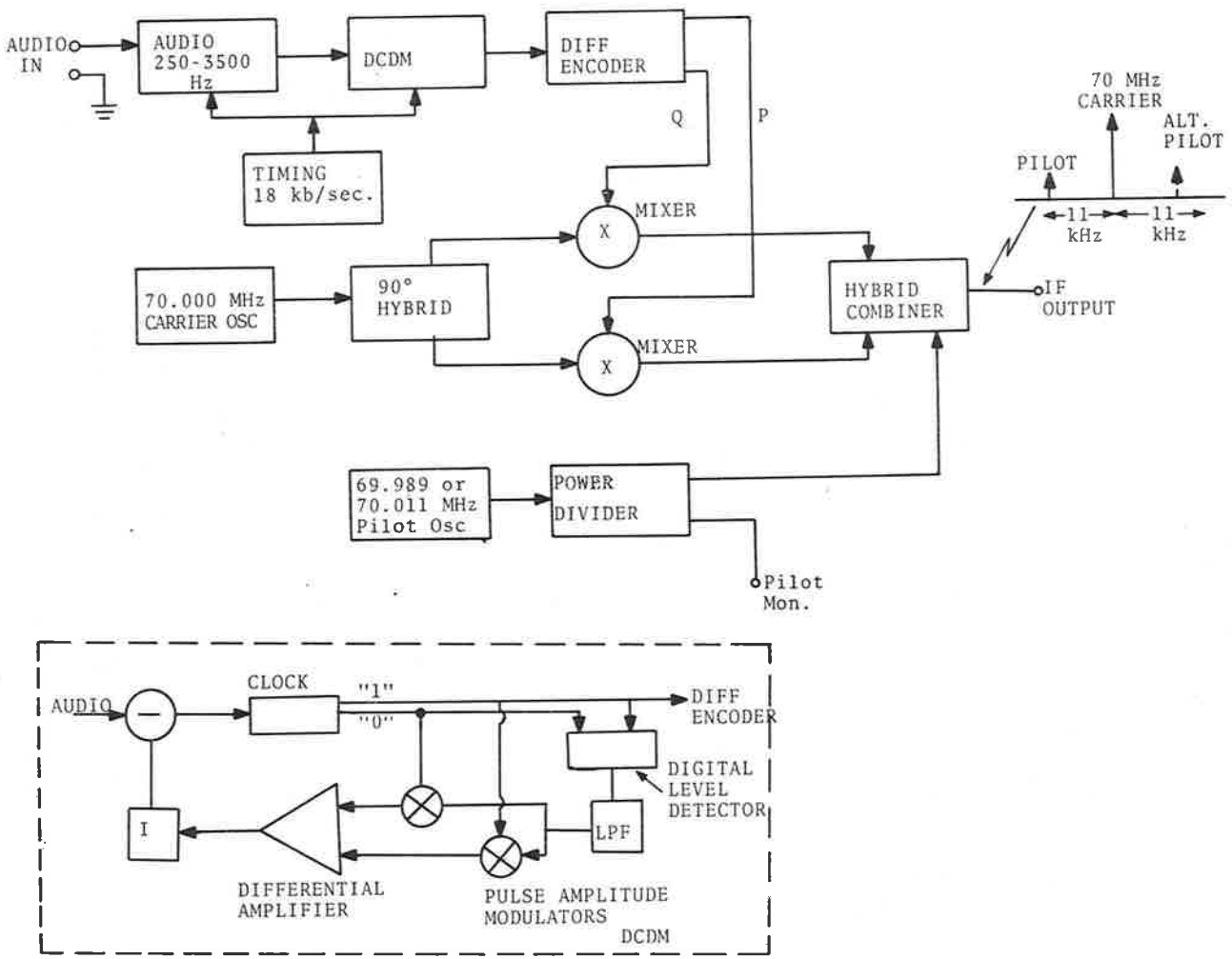

Figure 2-1. Four-Phase Delta Voice Modulator (DCDM) w/4ϕ PSK

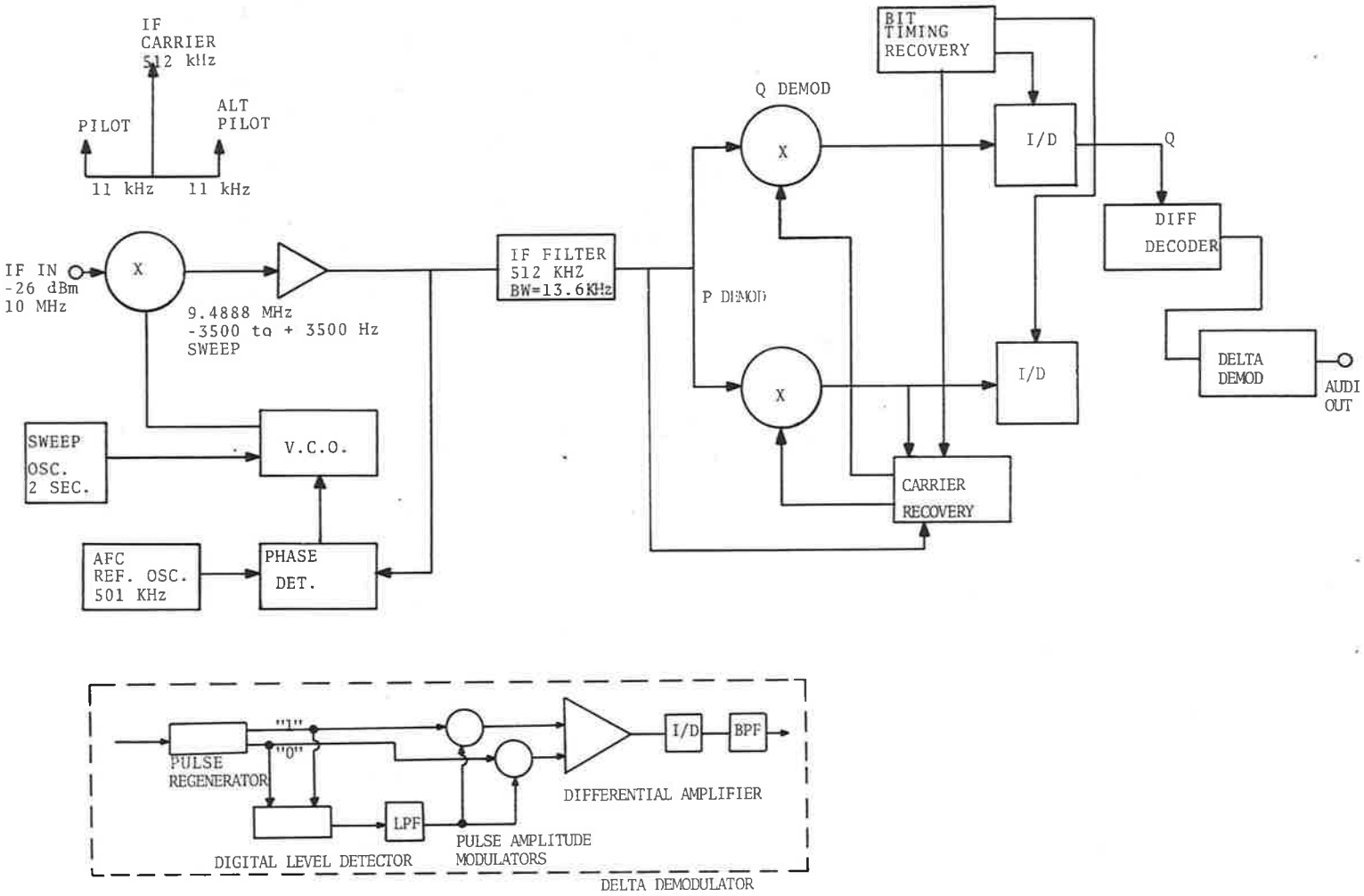

Figure 2-2. Four-Phase Delta Voice Modulator Receive System 4ϕ PSK

pilot tone which is translated to a frequency of 501 kHz. A crystal controlled 501 kHz frequency reference oscillator, which is compared to the incoming pilot in the phase detector, is used for this purpose. The local oscillator for the input mixer is derived from a VCO that is frequency controlled by the phase detector output. The VCO is swept over a frequency range of 7000 Hz every two seconds to provide for carrier acquisition. The 512 kHz IF is followed by a four-phase PSK coherent demodulator which segments the P and Q binary signals. Carrier recovery is accomplished by a remodulator loop. Bit timing recovery is accomplished by processing the Q channel transitions. The P and Q signals are next processed by an integrate and dump (I/D) circuit and then drive a differential decoder and the delta demodulator. The delta modulator audio output is bandpass filtered to the range from 250 to 2500 Hz.

The performance of the four-phase PSK modem used in the delta modulation system, measured in terms of the signal energy-to-noise density ratio, and also in terms of carrier power-to-noise density ratio is shown in Figure 2-3. Also shown is the theoretically ideal performance curve. It can be seen that a departure of 3 to 3.5 dB from theoretical is apparent in the performance of the modem used with the delta modulation system. The cause of this departure is believed by COMSAT Labs to be due to inter-symbol interference limitations imposed by the bandpass filters used in the transmit unit. By incorporating improved filtering with the four-phase PSK modem or by going to two-phase PSK which is less severely influenced by filter design, a performance departing only 1.0 dB from theoretical should be expected. Thus, the curves of AI versus C/No given in this report can be expected to improve by 2 dB by appropriate modification of the modem (Reference 1).

2.1.2 Suppressed Clock Pulse Duration Modulation

The PDM/PSK modulator (designed and built by Magnavox Research Labs) generates a carrier which is PSK modulated by a 7.2 kHz clock. This clock in turn has been modulated by the voice signal such that the clock pulse width is a function of the voice signal amplitude.

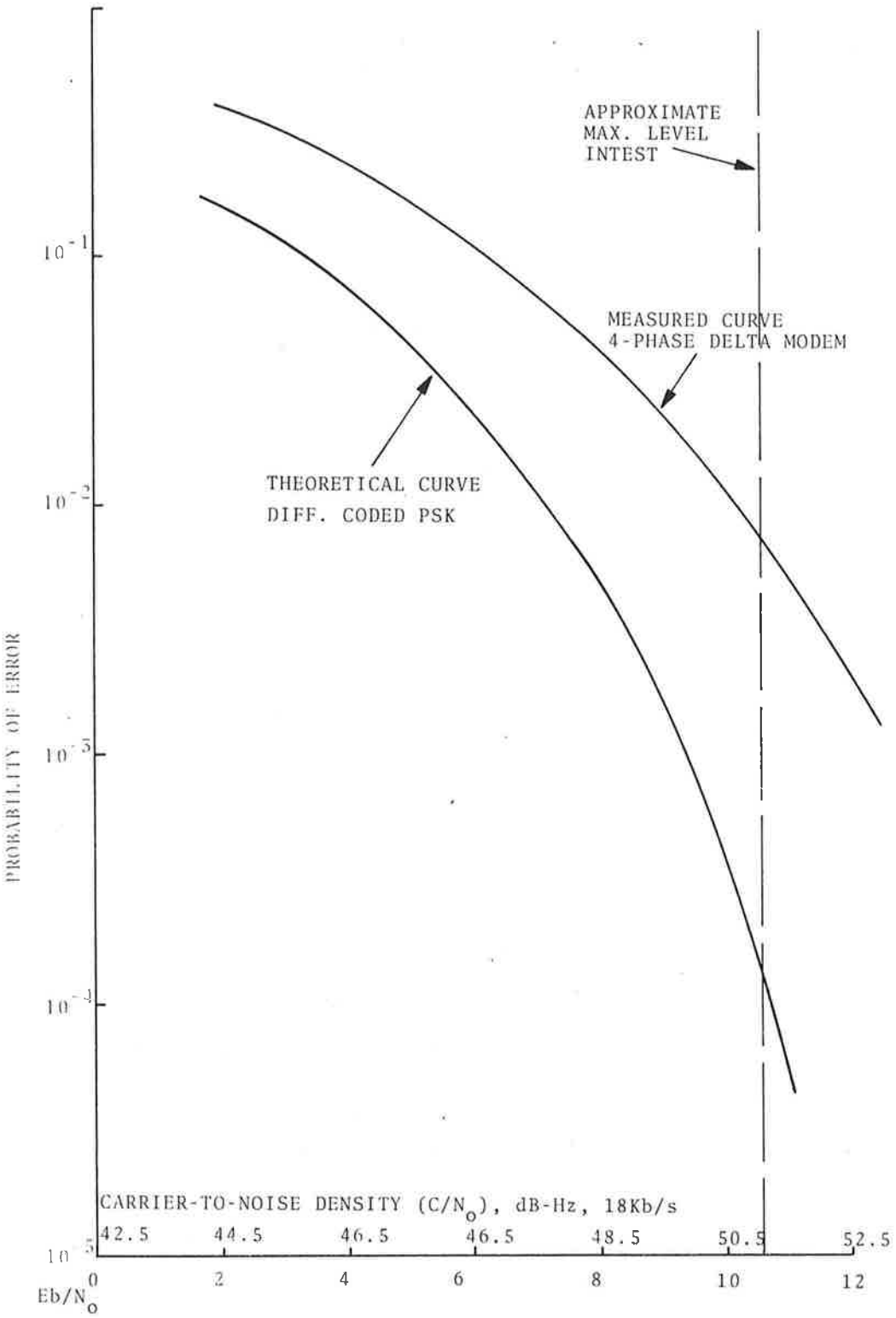

Figure 2-3. Performance of COMSAT Four-Phase Delta Voice Modem

A simplified block diagram of the PDM modulator is shown in Figure 2-4. The input voice signal is amplified and filtered to a 2.5 kHz bandwidth. The filtered signal is sampled at the clock rate and the amplitude value is held until the next clock pulse. This sampled value is then compared in a differential comparator with a ramp signal generated at the clock frequency.

The output from this comparator is a train of pulses in which the leading edge occurs at the fall of the ramp. The duration of each of these pulses is proportional to the input signal amplitude. Essentially no information (except clock) is contained in the leading edge of the pulses. The signal bandwidth is reduced by eliminating this leading edge and transmitting only the fall of each PDM pulse. This is accomplished in an Exclusive - or. A sample timing diagram of this entire scheme is presented in Figure 2-5. The 7.2 kHz PDM modulated clock is then bi-phase modulated at 70 MHz and up-converted to RF for relay through the satellite.

In the demodulator, the IF signal is tracked by a Costas loop synchronous demodulator and then processed by an integrate and dump filter. The dc value of each integrated sample is held by the sample and hold circuit until the next sample time, thus producing at its output a replica of the originally transmitted audio signal. The output of the sample and hold is low-pass filtered to a 2.5 kHz bandwidth and then amplified. The operation of the PDM demodulator shown functionally in Figure 2-5 may be best understood by referring to the block diagram of Figure 2-6. The chart is scaled to Figure 2-7 and shows the waveform at various points in the demodulator. A stored 7.2 kHz clock at the receiver which has been derived from the coder clock toggles the flip flop. The true output of the flip flop is AND-gated with the recovered data while the complementary output is AND-gated with the inverted data. The outputs of the two AND-gates are combined in the OR gate producing the original PDM data as developed at the comparator in the modulator.

The output of the OR gate drives the integrate and dump filter which produces the signal shown in the timing chart. The output of the I&D is examined by the sample and hold circuit just

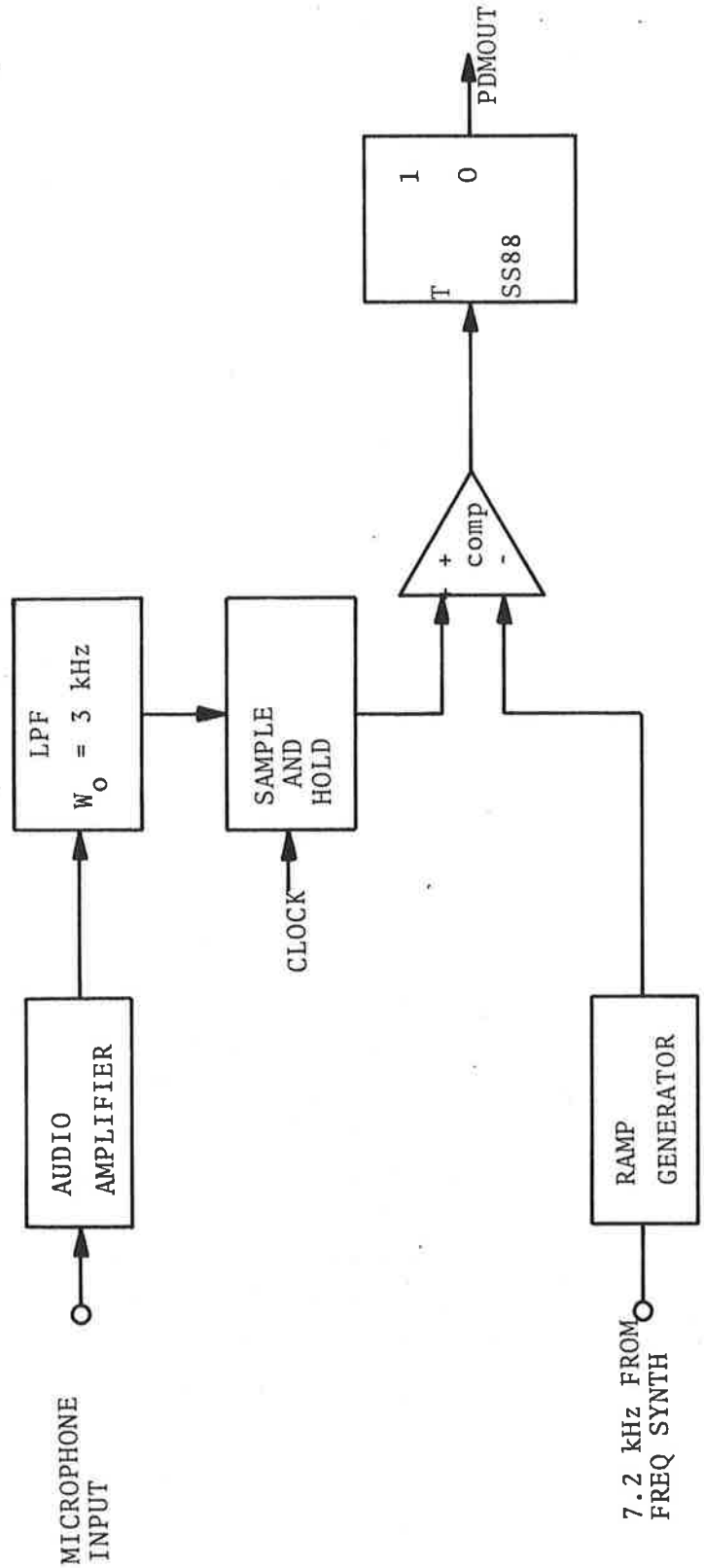

Figure 2-4. PDM Modulator

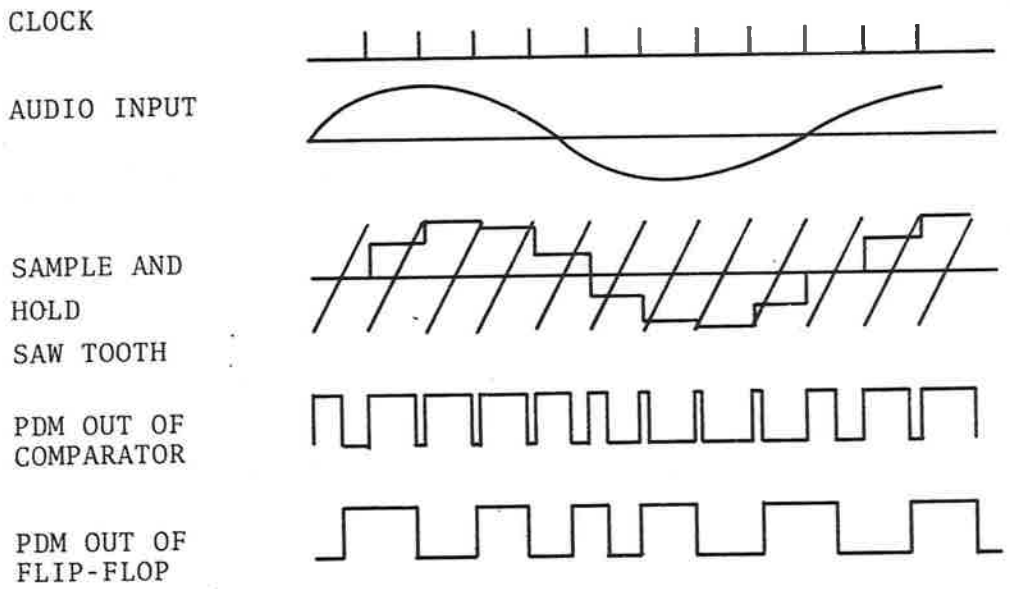

Figure 2-5. PDM Modulator Timing Diagram

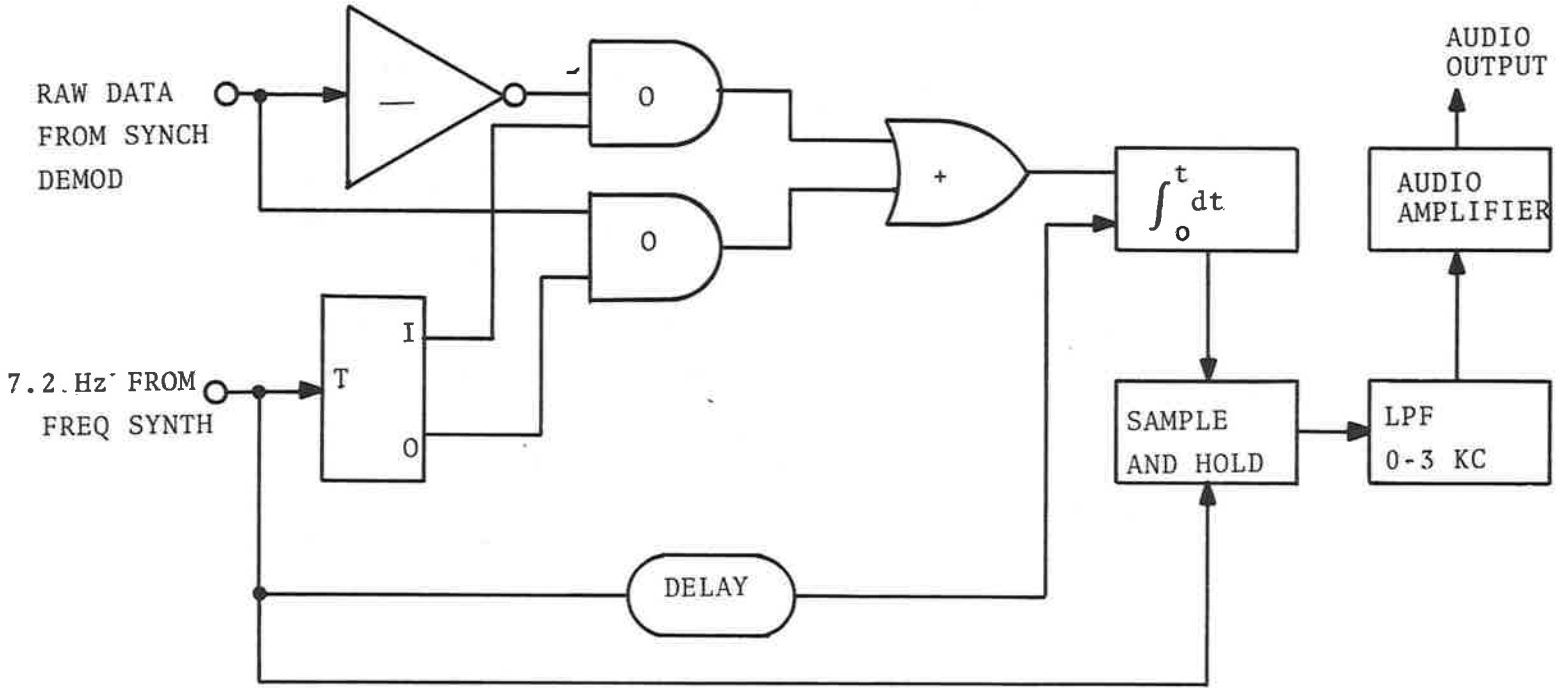

Figure 2-6. PDM Demodulator

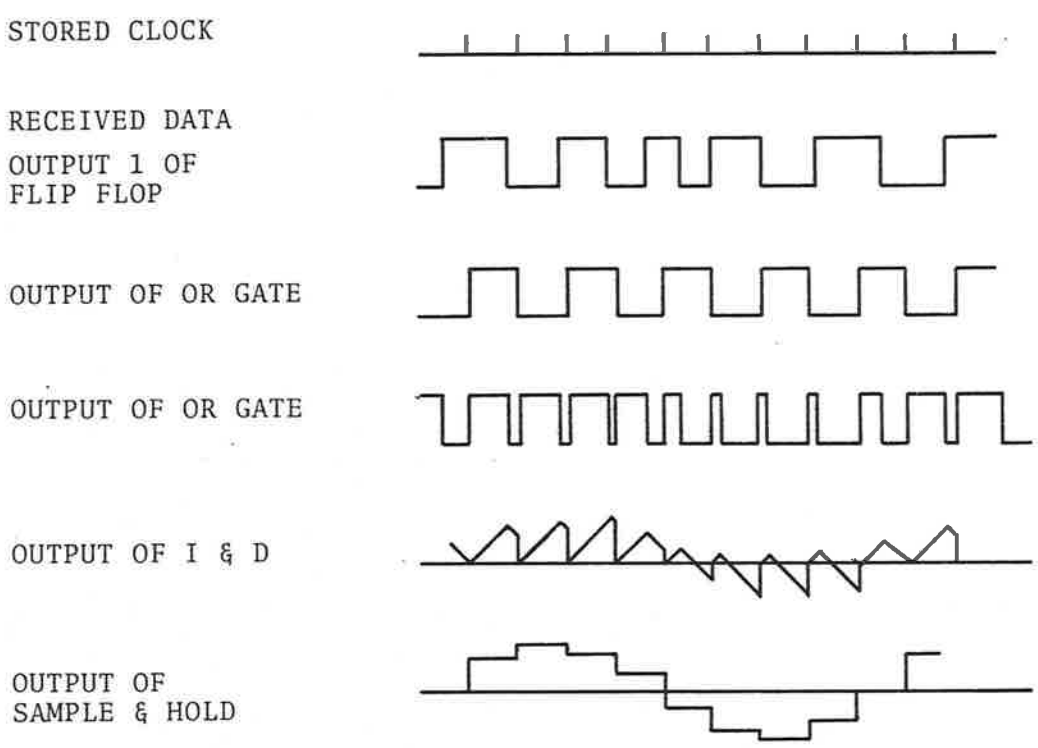

Figure 2-7. PDM Demodulator Waveforms

before the I&D is dumped, producing a stair-step version of the original input signal. This is then low pass filtered, with a cut-off frequency of 2.5 kHz, to produce the demodulated replica of the voice signal.

2.1.3 Adaptive Narrow Band Frequency Modulation

The Narrow Band FM modulator (designed and built by Bell Aerospace Co.) frequency modulates a voltage controlled oscillator which is limited to a deviation of ±1.5 kHz. Prior to modulation the voice signal is filtered to a 300-3500 Hz bandwidth. Since in an FM system the demodulation noise voltage increases with frequency, noise masking of the high frequency portion of the voice spectrum can be decreased by the use of pre-emphasis. The ANBFM modulator utilizes a pre-emphasis network on the voice signal in which the gain increases at 6 dB per-octave from 300-3500 Hz. At 3500 Hz the gain of this network falls off at 6 dB/octave. In order to prevent over-deviation of the carrier, peak clipping is employed. The amplitude of the signal reaching the VCO is limited to 12 dB below peak value. The output of the VCO is translated to 70 MHz and up-converted to RF. Figure 2-8 is a block diagram of the ANBFM modulator. Included in the ANBFM modulator is a circuit to detect pauses in the voice signal. During these pauses a gating signal was transmitted. This gating signal was used to determine the proper time (aboard the aircraft) for making carrier-to-noise power density measurements. At the receive station the ANBFM system uses a modulation-tracking phase lock loop to demodulate the FM signal. The demodulator is shown in Figure 2-9. Limiting of the IF occurs prior to the PLL demodulator resulting in a loop bandwidth which changes as a function of input carrier-to-noise density. This effect is illustrated in Figure 2-10, which is a set of parametric curves illustrating the change in loop bandwidth as a function of closed loop gain and C/No. The threshold at which the PLL will lose lock is dependant on the loop bandwidth and the received carrier-to-noise ratio. Thus by reducing the closed loop bandwidth with decreasing input signal-to-noise ratio the threshold at which the loop loses lock is extended. The 3 dB

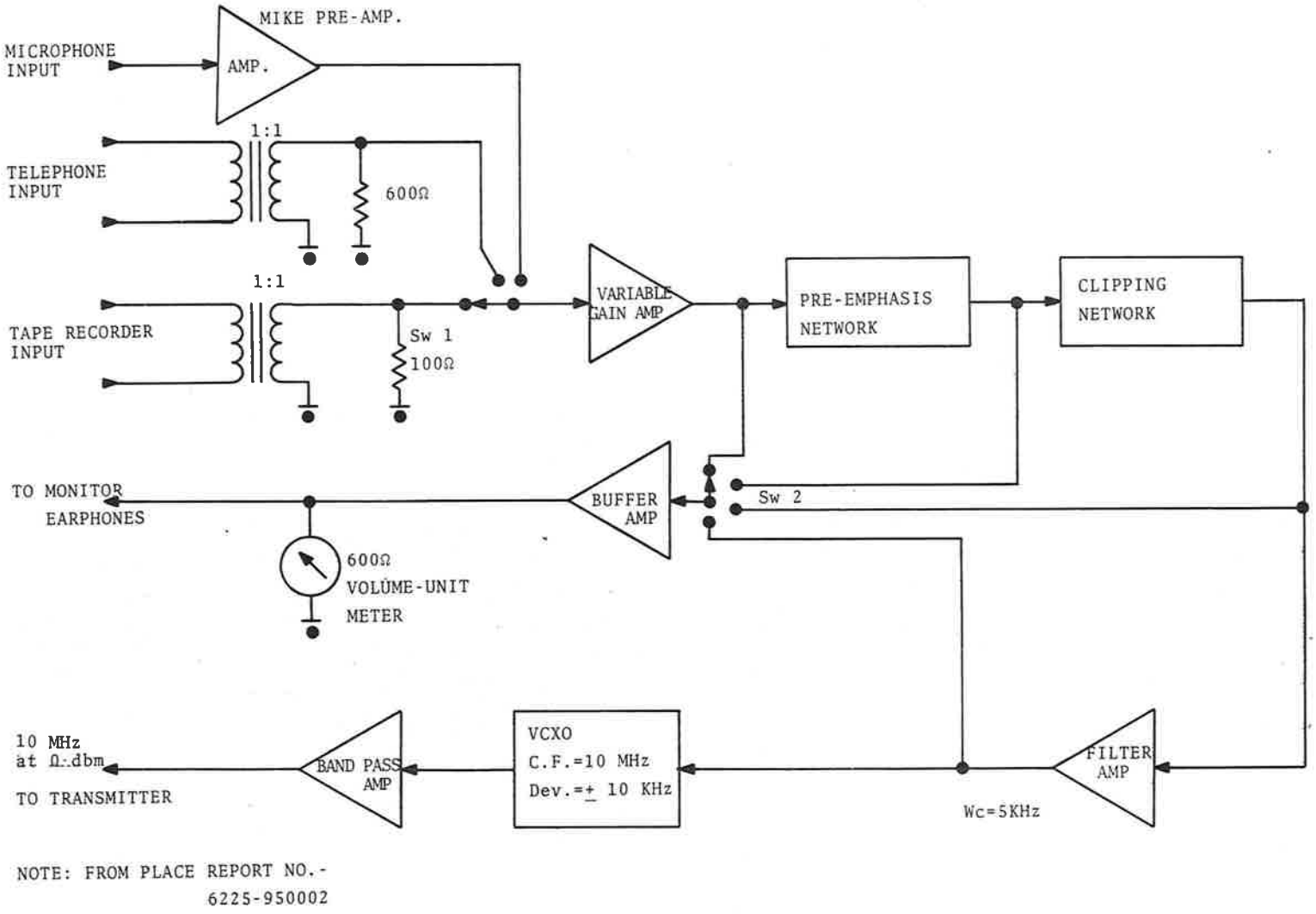

NOTE: FROM PLACE REPORT NO.-
6225-950002

Figure 2-8. ANBFM Modulator

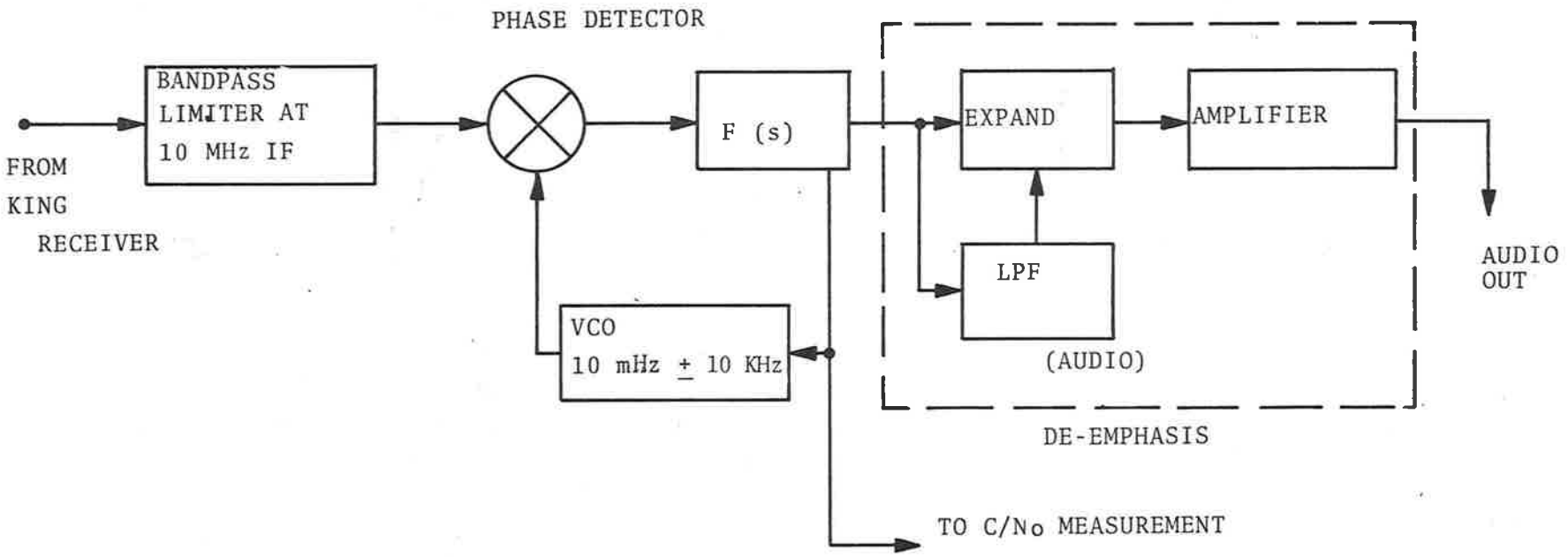

F(s)- 3 pole active
Loop Filter

Figure 2-9. ANBFM Demodulator

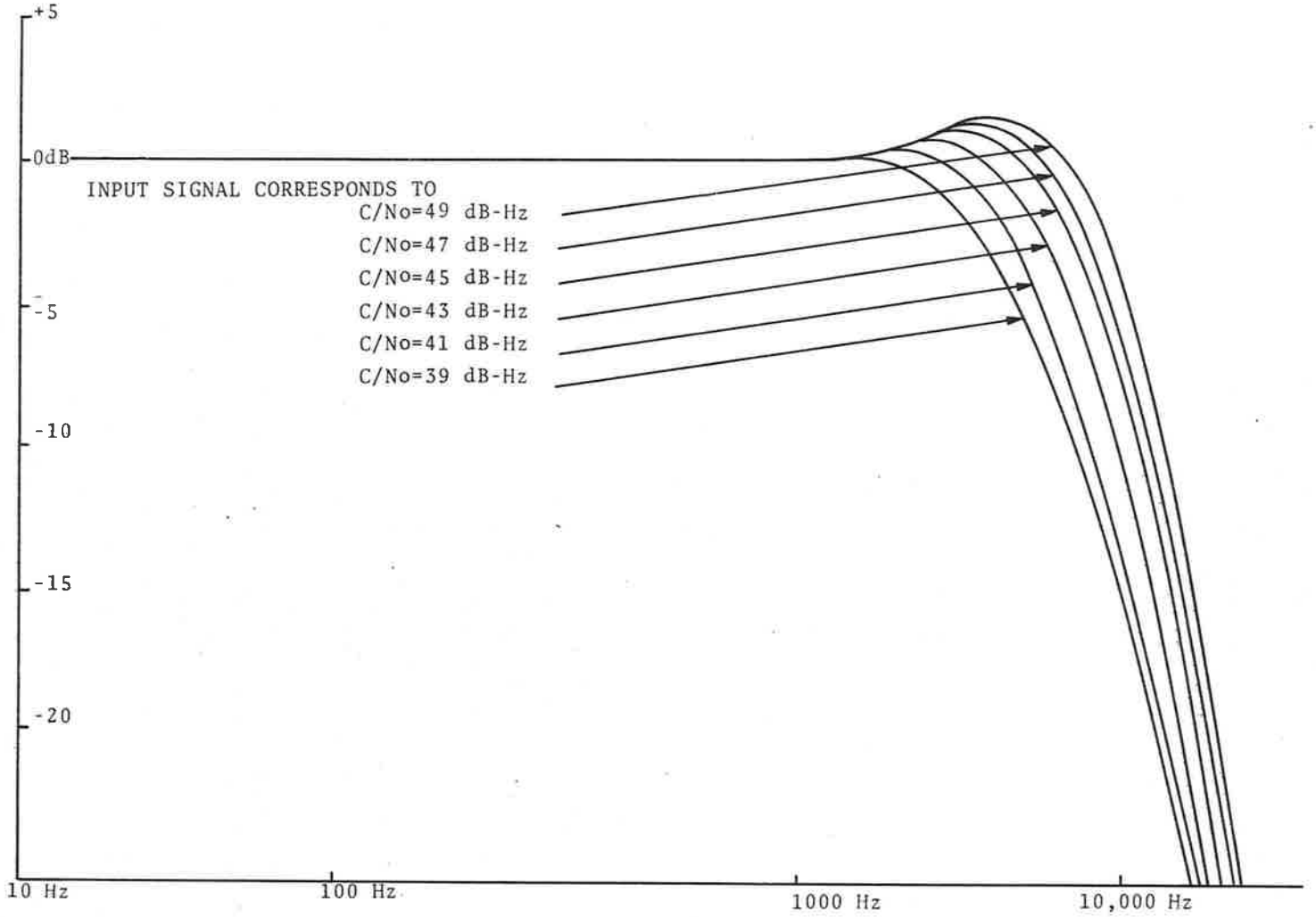

Figure 2-10. ANBFM Demodulator Frequency Response

loop bandwidth is 3.5 kHz with a 49 dB-Hz input C/No. The PLL demodulator loop filter contains a three pole active filter with a frequency response chosen to optimize the closed loop response of the PLL for the average speech power spectrum. Following demodulation, the audio signal is fed to a low pass filter and amplifier combination to provide the proper offset to the pre-emphasis employed at the modulator.

2.2 DATA MODEMS

Two data modems were provided for the experiment. Both transmitted differentially encoded, bi-phase modulated (PSK) data signals at 1200 b/s. Demodulation was by use of a Costas loop synchronous demodulator. Both transmissions then, were differentially encoded, coherently demodulated PSK (DECPSK).

2.2.1 Modulator

The modulator was identical for both units. Referring to Figure 2-11 data signals were generated in a 7-stage maximal length shift register. They are then differentially encoded, and bi-phase (PSK) modulate the 70 MHz carrier. The 7-stage shift register generates a 127 bit pseudo-noise (PN) sequence. This sequence is used to measure bit-error rate at the demodulator.

2.2.2 Bell Demodulator

This unit (Figure 2-12) consists of a synchronous demodulator utilizing a phase-locked loop, followed by a timing or bit synchronization loop, which locks to the clock component of the incoming bit stream. The timing loop output then serves as the syncronous timing signal to an integrate-and-dump matched filter, whose output is a filtered replica of the data stream. To accomplish bit-error detection, a local code generator is contained in the domodulator. This circuit generates a replica of the 127 bit PN code which is modulated on the carrier. A code correlator syncronizes the local code to the incoming code. Once local code synchromization is complete, the correlator compares the two codes

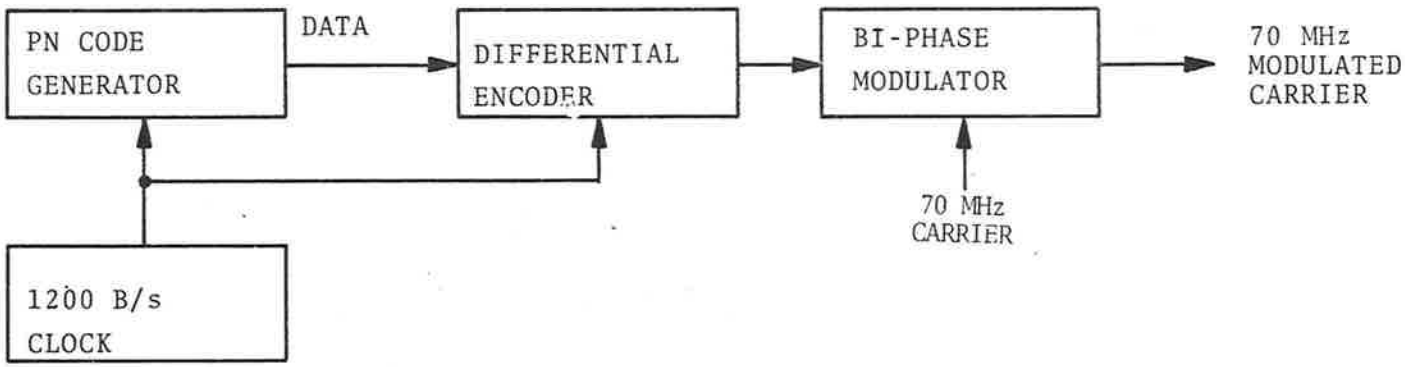

Figure 2-11. Data Modulator

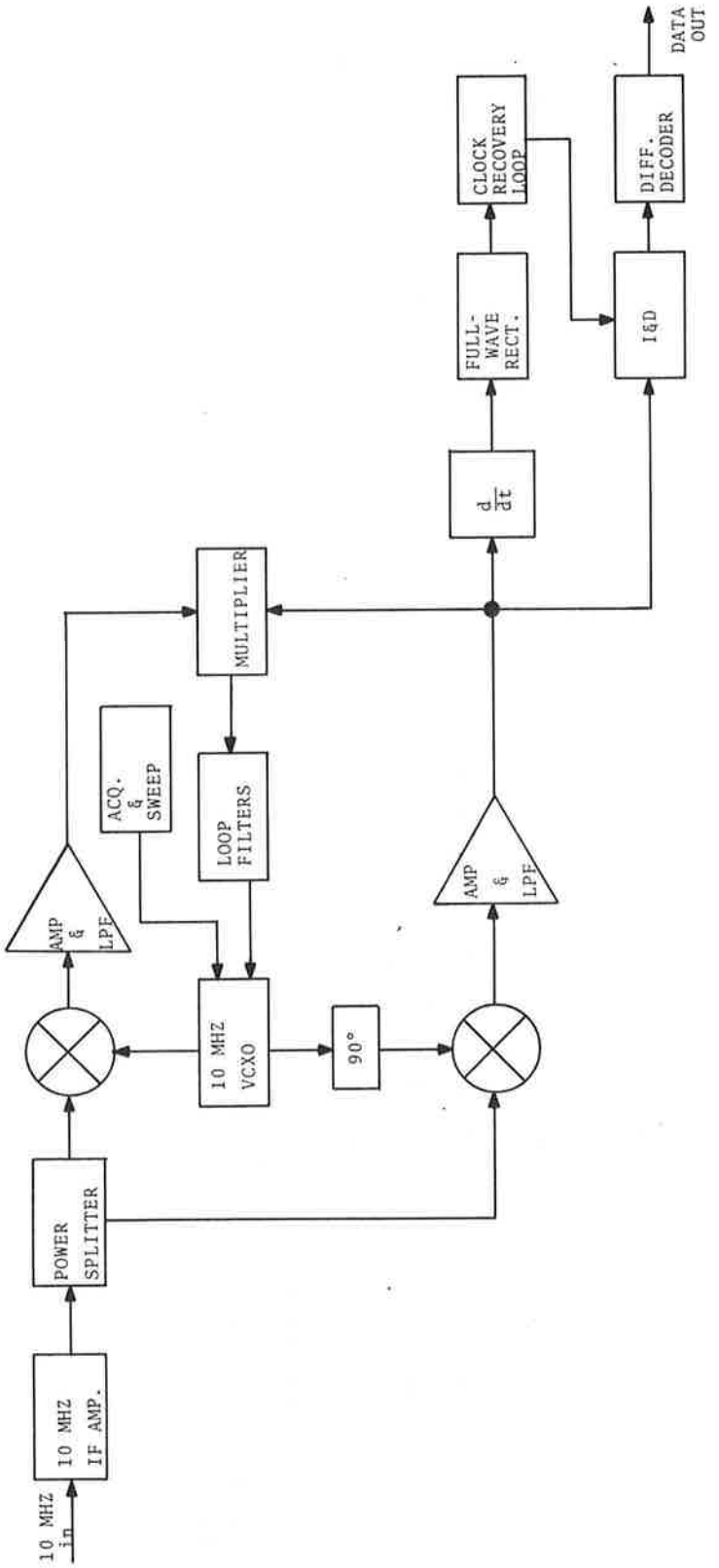

Figure 2-12. Bell Aerospace Data Demodulator

continuously, and generates an error pulse whenever an error is detected.

2.2.3 Magnavox Demodulator

This unit (Figure 2-13) is functionally identical to the Bell Demodulator. However, the demodulator and timing are derived from the circuitry in the PDM demodulator. To this has been added the necessary output, timing, I and D, and code matching circuitry described in paragraph 2.2.2.

2.3 EXPERIMENT CONFIGURATION

2.3.1 Ground Station

The ground station equipment was located in the ESRO van. The TSC ground equipment provided 70 MHz interfaces to ESRO hardware for frequency translation to 444 MHz, the up-link frequency to the balloon. The equipment configuration is illustrated in Figure 2-14.

At the ground station the modulated signals were transmitted to the balloon and relayed to the aircraft as an FDM spectrum. For voice tests the previously recorded word tape was played back on an Ampex AG-500 tape recorder and fed to the three voice modulators. Following modulation of the individual sub-carriers, the three voice channels were frequency multiplexed together and translated to 444 MHz. They were then power amplified and transmitted to the balloon. The individual up-link frequency assignments and the transmitted up-link power are also shown in Figure 2-14.

2.3.2 Balloon Transponder

The balloon transponder used for this experiment was supplied by ESRO.[2] Table 2-1 summarizes the UHF/L-band link power budget used in all voice and data testing. The transponder used simple frequency translation and employed a class C power amplifier. The bandwidth of the transponder was approximately 400 kHz, with an

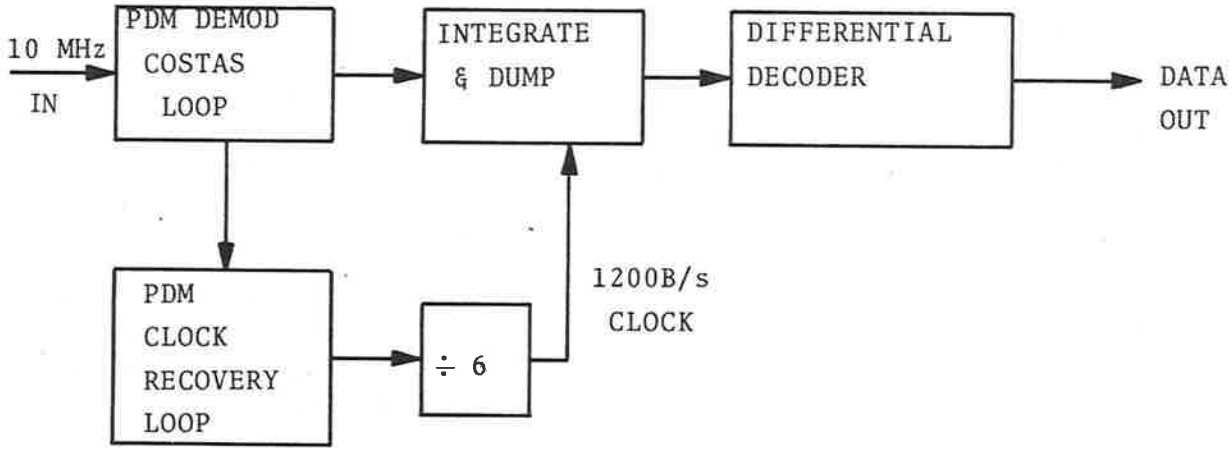

Figure 2-13. Magnavox Data Demodulator

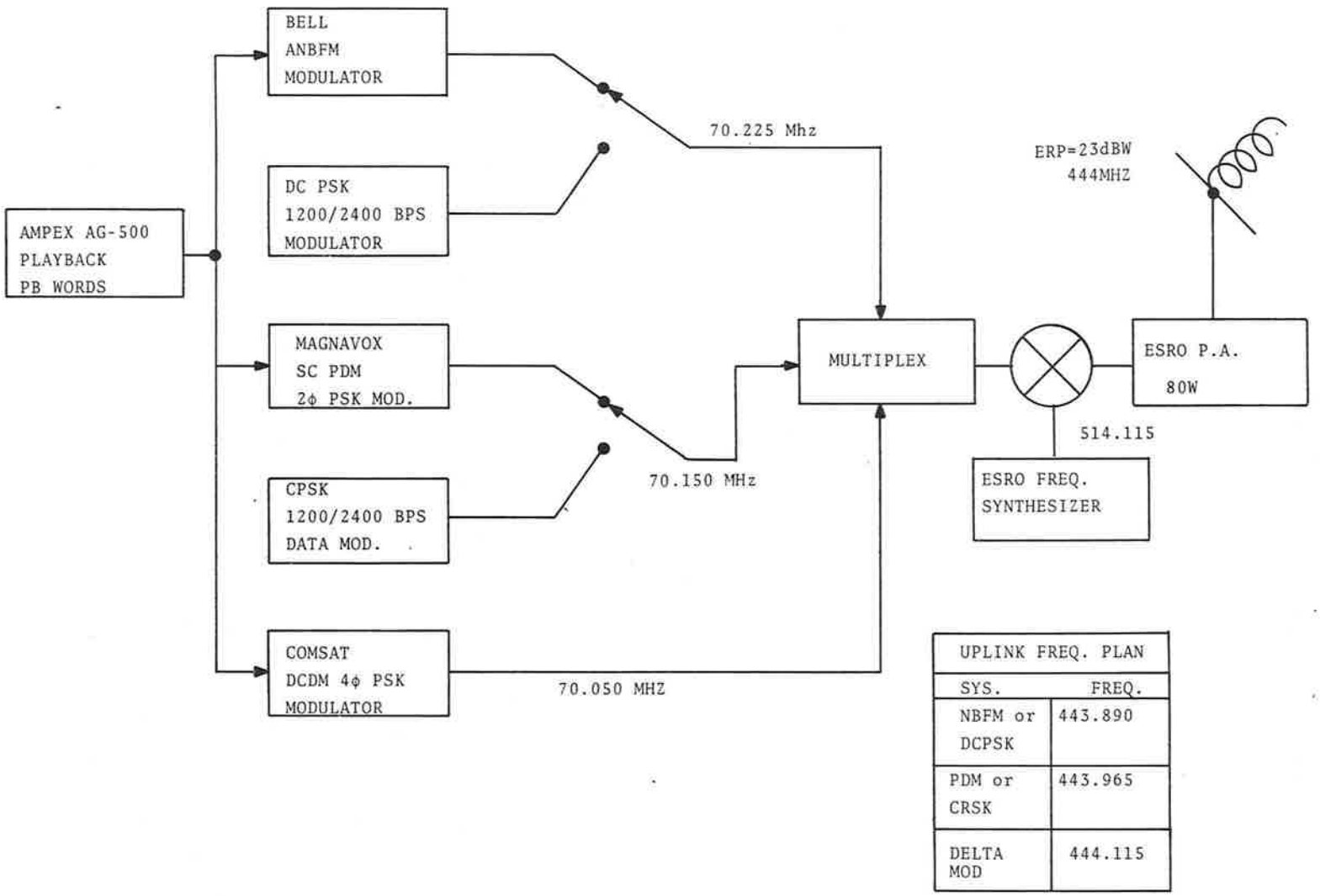

Figure 2-14. Ground Station Block Diagram

TABLE 2-1. UHF/L-BAND LINK ANALYSIS FOR BALLOON EXPERIMENT

BALLOON TRANSPONDER OUTPUT POWER	+31.5 dBm
BALLOON TRANSPONDER ANTENNA GAIN	+ 3.0 dB
CABLE & POLARIZATION LOSSES	- 3.5 dB
SPACE LOSS (BALLOON 120,000 FT; EL. ANGLE = 5°)	-149 dB
AIRCRAFT ANTENNA GAIN (35° OFFSET, 5° EL. ANGLE)	0 dB
AIRCRAFT RECEIVED SIGNAL POWER	-118.0 dBm
AIRCRAFT NOISE POWER DENSITY (NOISE TEMP. = 525°K)	-171.4 dBm/Hz
RECEIVED CARRIER-TO-NOISE DENSITY (C/No)	53.4 dB-Hz

NOTE: The System Noise Temperature is Calculated as:

$$Ts = \frac{T_A}{L} + \frac{290(L-1)}{L} + 290\,(NF-1)$$

T_A = ANTENNA TEMPERATURE = 150°

L = LOSS FROM ANTENNA TO PREAMP. = 0.5 dB

NF = PREAMP NOISE FIGURE = 3.5 dB

output center frequency of 1550.480 MHz. The balloon antenna was a right-hand circularly polarized spiral, with an antenna pattern carefully chosen for uniformity of coverage within the geometry constraints of the experiment.

2.3.3 Aircraft Receiving System

The aircraft receiving system configuration is shown in Figure 2-15. The system consisted of a set of low gain L-band antennas, a low noise preamplifier associated with each antenna, a dual channel L-band to VHF translator, King Radio Co. Satcom transceiver (ARINC characteristic 566), the voice and data demodulators, and an instrumentation recorder. Instrumented with the ANBFM demodulator was a technique for direct measurement of C/No. This scheme will be discussed in Section 2.5.

2.3.3.1 Antennas - Three antenna systems were initially available for use in the voice and data experiment. A Boeing orthogonal mode crossed slot antenna was flush mounted on top of the aircraft fuselage above the wing. Two DICO low-gain slot dipole antennas were also flush mounted and 35° offset from the top antenna. A medium-gain phased array antenna designed and built by Elecma was installed in the radome of the Convair 880. All antennas were right-hand circularly polarized. Unfortunately, installation problems occurred with both the Boeing and Elecma antennas and no meaningful data was obtained with either of these antenna systems. All data obtained during the French tests was obtained on the right or left 35° DICO antenna. Figure 2-16 shows the gain pattern in the roll plane for the DICO antenna obtained on a model of the Convair 880 scaled to 1/10. Since the experiment geometry was constrained to circular flight paths which were tangential to a radial to the balloon, this pattern gives a best overall estimate of antenna gain in both the direct and indirect paths. Table 2-2 presents the direct and indirect gain and approximate multipath rejection for the elevation angles for which data was obtained.

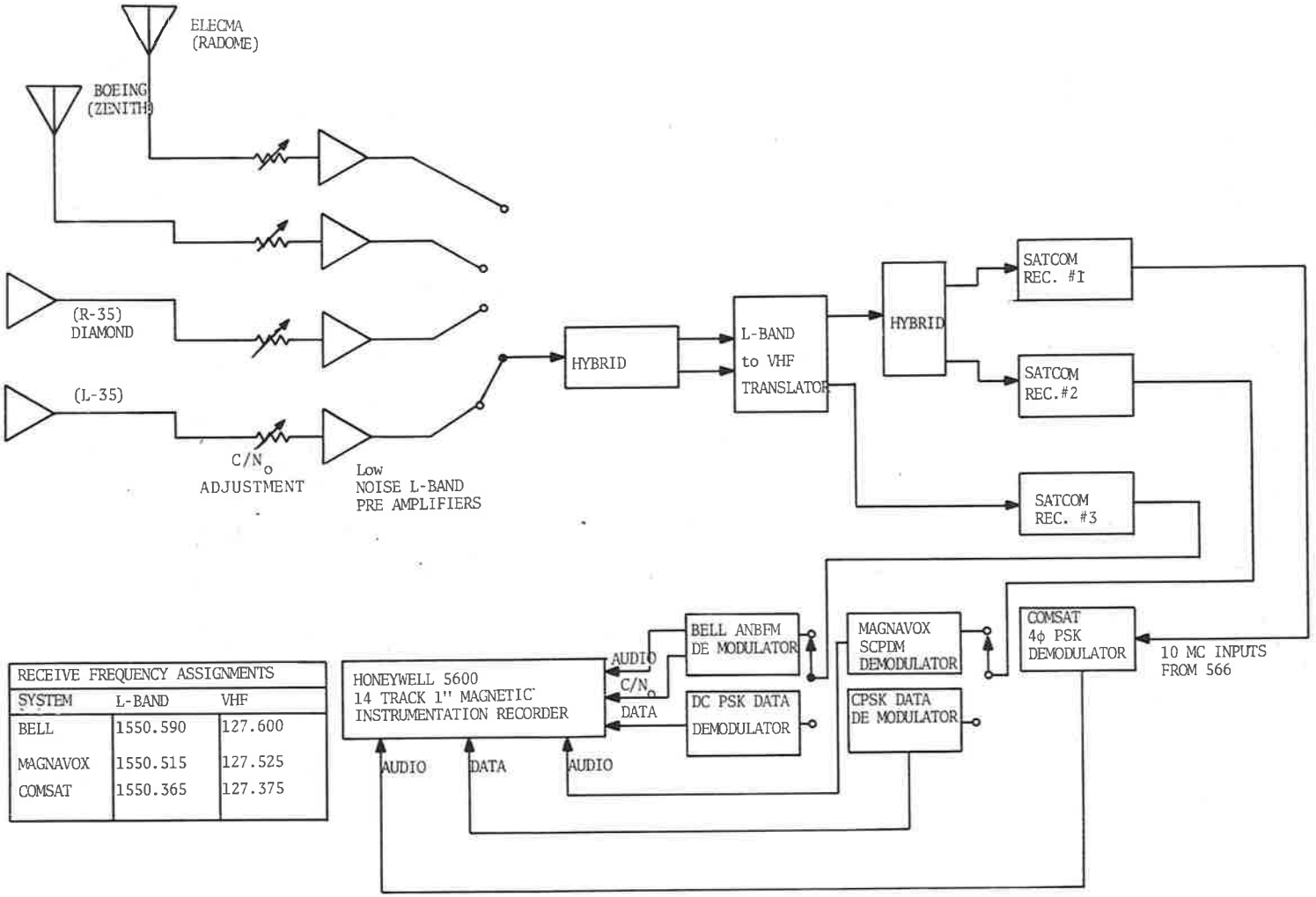

RECEIVE FREQUENCY ASSIGNMENTS		
SYSTEM	L-BAND	VHF
BELL	1550.590	127.600
MAGNAVOX	1550.515	127.525
COMSAT	1550.365	127.375

Figure 2-15. Aircraft Receiving Station

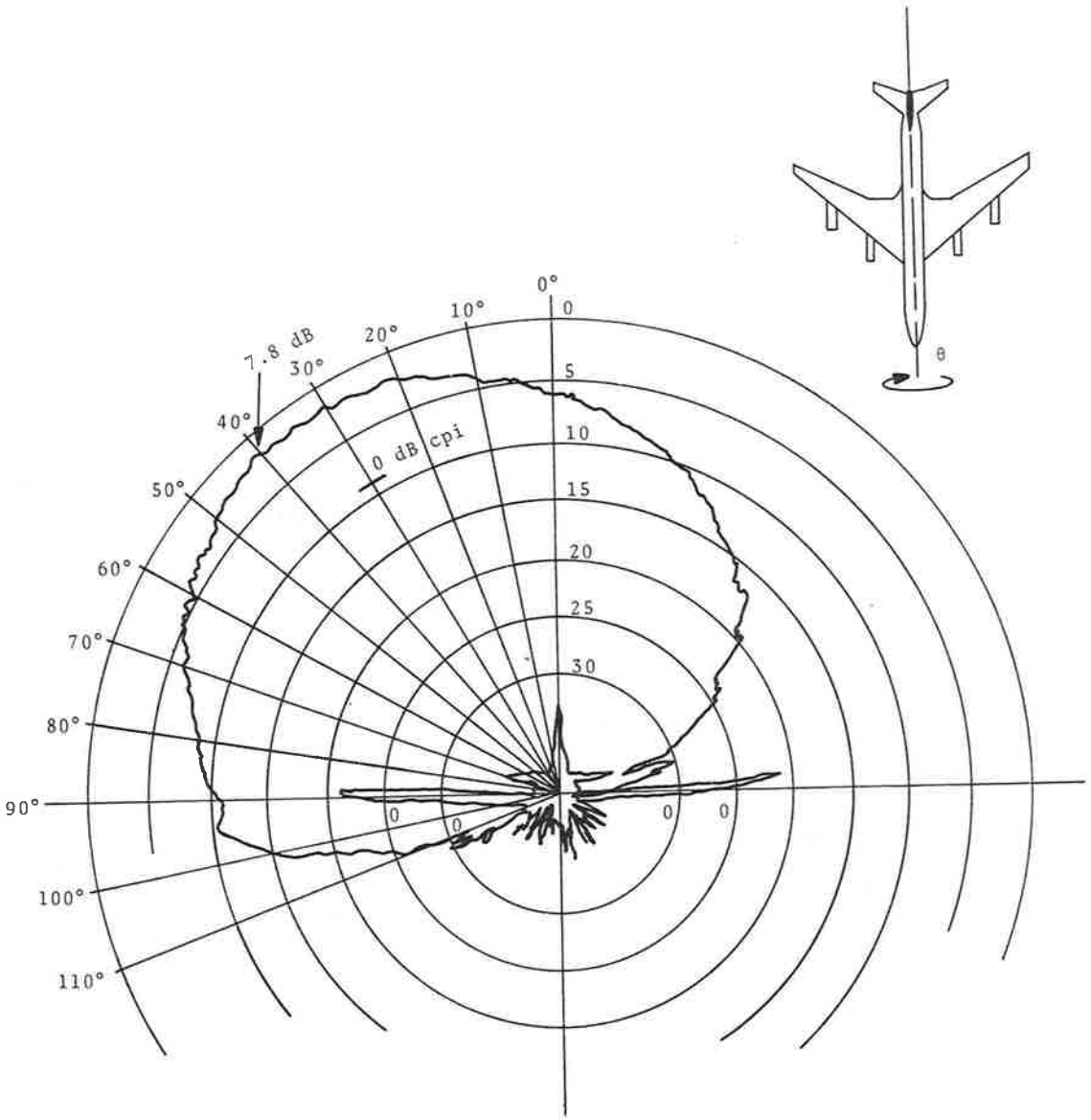

Figure 2-16. Roll Plane Pattern -35° DICO Antenna

TABLE 2-2. GAIN AND MULTIPATH REJECTION WITH R-35° ANTENNA

ELEVATION ANGLE	GAIN	MULTIPATH REJECTION
+15°	+2 dB	13 dB
+10°	+1 dB	6 dB
+ 7°	+0.5 dB	3.5 dB
- 7°	-3 dB	
-10°	-5 dB	
-15°	-11 dB	

2.3.3.2 Low Noise Pre-Amplifiers - Following each antenna system was a low noise high gain L-band preamplifier. These preamplifiers were designed and built by Avantec. The nominal noise figure for each preamplifier was 3.5 dB and the gain was 25 dB.

2.3.3.3 L-Band - VHF Translator - The output of the pre-amplifier is split and fed to a dual channel L-band to VHF translator. This translator was of conventional design with nominal gain of 20 dB in each channel and a noise figure of less than 8 dB. Channel 1 of the translator was used with the King transceiver which is connected to the ANBFM demodulator. Channel 2 was split in power and used with the King transceivers connected to the PDM and Delta demodulators.

2.3.3.4 King Transceivers - The transceivers used to down convert the 127 MHz output of the translator to a 10 MHz IF for all demodulators were ARINC specification 566 Satcom transceivers, produced by King Radio. The only modification made to these transceivers was the incorporation of manual gain adjustment and a 10 MHz buffered output.

2.3.3.5 Demodulators - The demodulators were described in Section 2.1.

2.3.3.6 Honeywell 5600 Instrumentation Recorder - All test signals derived during the experiment were recorded on a Honeywell Model 5600 analog tape recorder. These signals included the demodulated voice signals as well as C/No measurements. This unit had a capability of recording 14 tracks of information simultaneously on 1" magnetic tape. The information bandwidth for recording FM was dc to 1.25 kHz, and the direct record bandwidth was 50 Hz to 18 kHz.

2.4 LABORATORY EVALUATION OF TEST MODEMS

2.4.1 Voice Modems

Following the field experiments in the fall of 1971, all aircraft and ground station equipment including the voice and data modems were transported to the communications laboratory at TSC in order to reduce and analyze the field data and to make an evaluation of voice and data modems under purely thermal noise conditions. The field system was completely duplicated including losses between the L-band pre-amplifier and the translator, so as to ensure that the laboratory equipment configuration noise temperature was identical with that used in the field. The laboratory equipment configuration is shown in block diagram in Figure 2-17. This configuration was used to prepare tape recordings of the word list played through each of the three modems. To prepare these tapes, a modem and input C/No was chosen and the set-up was configured for these conditions. Previously recorded master tapes of the word lists are played back on tape recorder No. 1 and are fed to the appropriate modulator. Tape recorder No. 2 simultaneously records the words in a clear channel and the demodulated words from the output of the chosen system. The Ampex tape recorders were 1/4" tape 1/2 track studio quality recorders. The use of recorders of this quality essentially guaranteed distortion-less recordings and would thus introduce no degradation of intelligibility in the playback and re-recording process.

The use of 1/4" magnetic recording tape and 1/2 track recording format was necessary for the recorder interface with the U.S. Army Electronic Proving Grounds (USAEPG) who scored the word intelligibility of these tapes. In order to maintain a consistent tape format for evaluation of tapes at USAEPG, it was also required that the 1" magnetic tapes recorded in the field be re-recorded. This re-recording was necessary not only to have the words recorded on 1/4" tape, but also to increase the spacing between words from 1.5 seconds to 4 seconds. The 1.5 second spacing between words is considered insufficient timing for proper listener response in scoring the tapes. The scheme used to re-record the 1" tape

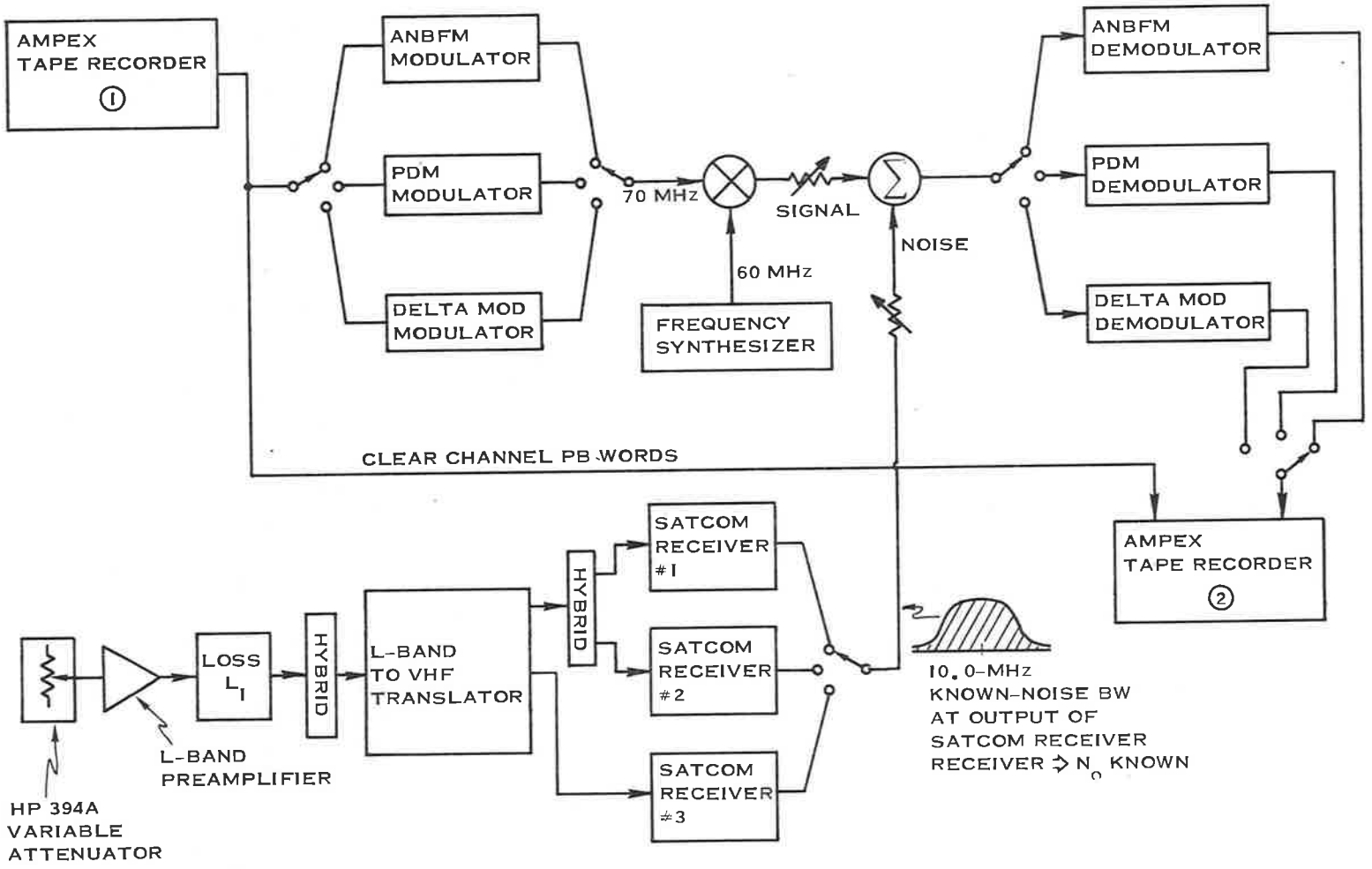

Figure 2-17. Laboratory Set-Up Block Diagram

produced in the field to 1/4" magnetic tapes with proper word spacing is shown in Figure 2-18.

2.4.2 Data Modem Laboratory Evaluation

The test set-up for laboratory evaluation of the data modems is essentially identical to that described for the voice modems. In this case, however, the signal input was a PN code, and the output consisted of error counts as C/No was varied.

In the data modulator, a 127 bit PN code was generated. Each demodulator contained a local code generator, code correlator, and error detector. The error detector compared the two codes, and generated a pulse whenever an error was detected. The error pulses were counted for a set time period and the bit-error rate was derived from counts per unit time. In the balloon experiment, a similar procedure was used, except that the error pulses were recorded on magnetic tape, for playback and analysis at TSC.

2.5 C/NO MEASUREMENT

During both the flight tests and the laboratory evaluation of the modems C/No measurements were made and recorded. This section briefly describes the theory of operation of the measurement equipment used during the flight tests and the subsequent C/No calibration techniques used when preparing the laboratory tapes.

2.5.1 C/No Measurements Unit

As part of the Bell ANBFM demodulator circuitry, a technique for direct measurement of C/No was implemented. This scheme is shown in Figure 2-19. It consists of measuring the rms phase jitter of the VCXO control voltage. The control voltage is fed to an audio band pass filter (800 $\pm$150 Hz) to measure the signal content in this range. The output of this band pass filter is gated by the analog voice gate. The gate detects the presence or absence of a word. During the absence, the gate closes, sending the filter output to a circuit which measures its rms voltage. The voltage from the rms detector is then low pass filtered (1 Hz

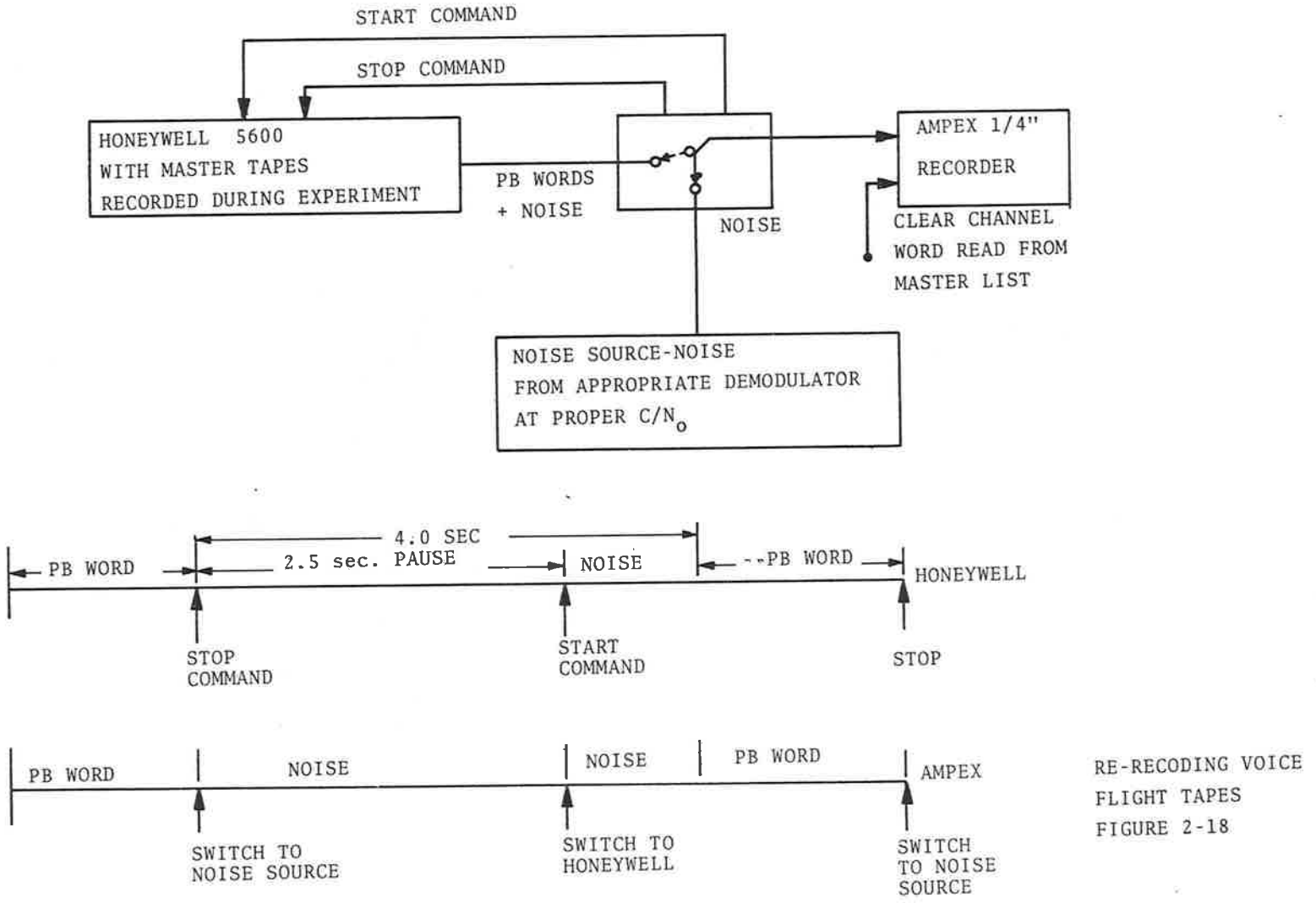

Figure 2-18. Flight Tape Re-Record Set-Up

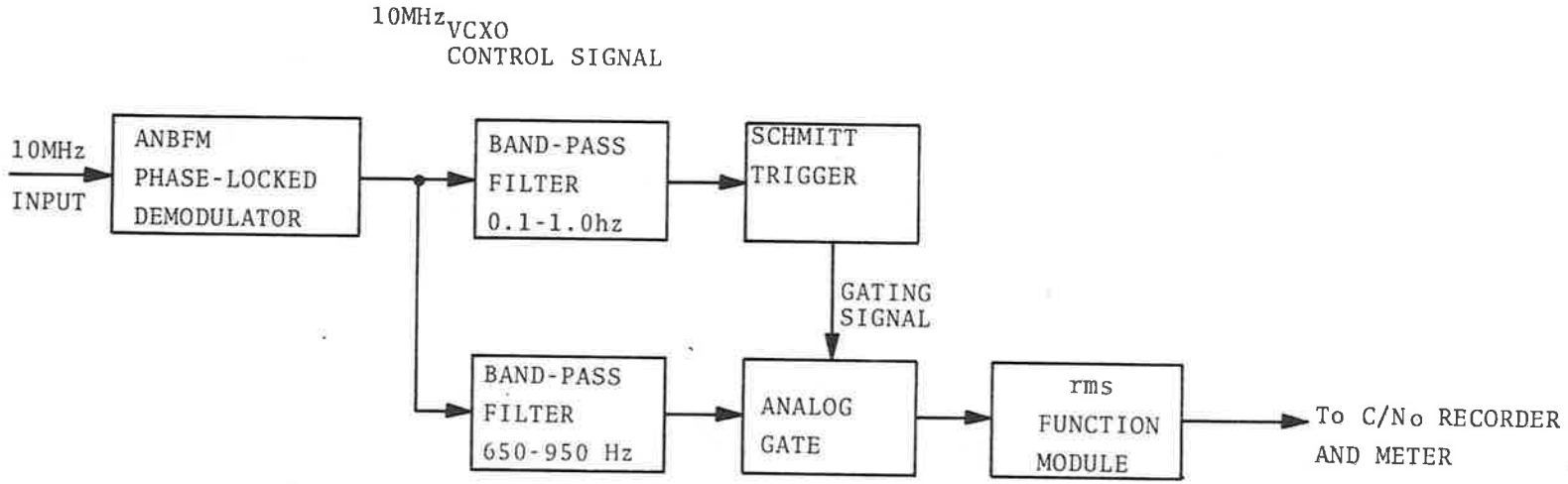

Figure 2-19. C/No Measurement Technique

time constant), amplified and set to the Honeywell analog tape recorder. It can be shown that for rms phase jitter less than approximately 13°, this voltage is a linear function of the input C/No.[3] A simple calculation shows that for the Bell phase lock loop demodulator, the loop phase jitter is less than 13° for any input C/No greater than 43 dB-Hz. Below 43 dB-Hz the relationship becomes non-linear. It is still possible to calibrate this scheme below 43 dB-Hz; however, since the output voltage becomes non-linear with decreasing C/No, the sensitivity of the measurement becomes less. Invariably, between 39-40 dB-Hz the loop looses lock and the measurement becomes meaningless.

2.5.2 C/No Calibration

To calibrate the C/No measuring technique, it was necessary to know precisely the equivalent noise bandwidth of the output 10 MHz IF filters of the King SATCOM receivers. The frequency response of these filters was precisely measured and the noise bandwidth calculated. Given the noise bandwidth and the noise power, the noise density (No) is precisely known. The noise bandwidth of SATCOM receiver 1 was found to be 16 kHz. Referring to Figure 2-17, a 0 dB signal-to-noise ratio at the output of the signal and noise summer represents 42 dB-Hz carrier-to-noise power density (C/No) at the input to the Bell demodulator and C/No meter. For calibration purposes the synthesizer output at 10 MHz is fed to the summer. This avoids any error due to spurious and harmonics produced at the output of the mixer from down conversion of the 70 MHz modulator signal. Calibration of the C/No meter was done daily during the preparation of the laboratory voice tapes. Following calibration, the 10 MHz source from the GR synthesizer was replaced by the 70 MHz source from the modulator, down converted to 10 MHz. The carrier and noise powers were then adjusted to the desired C/No (from measurement) and the appropriate voice tapes were recorded.

3. EXPERIMENT CONFIGURATION AND CONDITIONS

3.1 DISCUSSION OF DATA

3.1.1 Laboratory Data

Using the equipment set up described in Section 2.4, Table 3-1 shown below summarizes the data recorded for each of the modems for each evaluation condition:

TABLE 3-1. SUMMARY OF VOICE DATA RECORDED

C/No	NUMBER OF WORD GROUPS RECORDED	APPROXIMATE TOTAL RECORDING TIME
54	6	30 Mins
52	24	120 Mins
50	24	120 Mins
48	24	120 Mins
46	24	120 Mins
44	24	120 Mins
42	24	120 Mins
40	24	120 Mins

The master tape recordings of the words used in the laboratory evaluation were prepared with four different speakers. They each made a complete recording of 1000 pb words using four different word orders. The tapes were recorded in the same format as the original 1000 word tape used in the field. (No carrier phrase and a four second pause between words). The speakers chosen had a non-regional accent and the ability to maintain a constant speech level throughout the recording of each fifty word group.

In preparing the laboratory recordings for a particular C/No and modem (both training tapes and actual evaluations) word groups from all four speakers were equally used. The evaluation then more closely resembles a real world situation in which different speakers with different voice characteristics would use the system.

3.1.2 Field Data

The data obtained in the field is summarized in Table 3-2 in terms of antenna used, running time and approximate elevation angle. Outputs from all three modems were recorded simultaneously during all of the field tests. For all of the field tests, a single master tape was used. This tape was recorded by a single speaker. The original form of the tape included the entire 1000 pb words each with its own carrier sentence. The format was "Would you please write the word (word No. 1) now" pause "Would you please write the word (word No. 2) now" pause... Since useable flight time in the balloon experiment was at a premium it was decided to record only the actual word followed by a 1 - 1-1/2 second pause rather than the entire carrier phase. With the entire phrase and pause of the original tape only one word every seven to eight seconds could be recorded. By a cut and splice technique the carrier phrase was removed from all except the first word of each word group and the playing time per word was reduced to approximately two to three seconds. This new tape, consisting of words followed by a short pause (1-1/2 seconds) was actually used in the field tests. This greatly increased the efficient use of the available flight time. As seen in Table 3-2 all voice data was obtained on two successive flights on September 23 and September 24, 1971. The communications link for experiment control and experiment operation are given in Figure 3-1. The frequency assignments for the three voice systems are shown in Figure 3-2. Briefly, the experimental communications link operated as follows: All three voice signals originate at the ground station at Aire Sur L'Adour and were frequency multiplexed onto a 444 MHz uplink carrier. This signal was received at the balloon and translated to a center frequency of 1550.480 MHz, then retransmitted to the receiving station aboard the Convair 880. The L-band signal was also monitored at the ground station in order to be certain this link was operating correctly. The received signal at the aircraft was down converted to 127 MHz, split and sent to the appropriate receivers and demodulators.

TABLE 3-2. VOICE TEST SUMMARY

DATE	RUN NO.	ANTENNA	APPROX. TEST TIME	ELEVATION ANGLE
9/23/71 (AM)	TEST RUN	L-35°	6 min.	15°
	1	R-35°	8 min.	
	2	L-35°	8 min.	
	3	R-35°	8 min.	
	4	L-35°	8 min.	
	5	R-35°	8 min.	
	6	L-35°	8 min.	
	7	R-35°	8 min.	
	8	L-35°	8 min.	
9/24/71 (AM)	1	R-35°	8 min.	7°
	2	L-35°	15 min.	
	3	L-35°	10 min.	
	4	R-35°	10 min.	
	5	L-35°	10 min.	
	6	R-35°	10 min.	
9/24/71 (AM)	1	L-35°	8 min.	10°
	2	R-35°	8 min.	
	3	L-35°	8 min.	
	4	R-35°	8 min.	
	5	L-35°	8 min.	

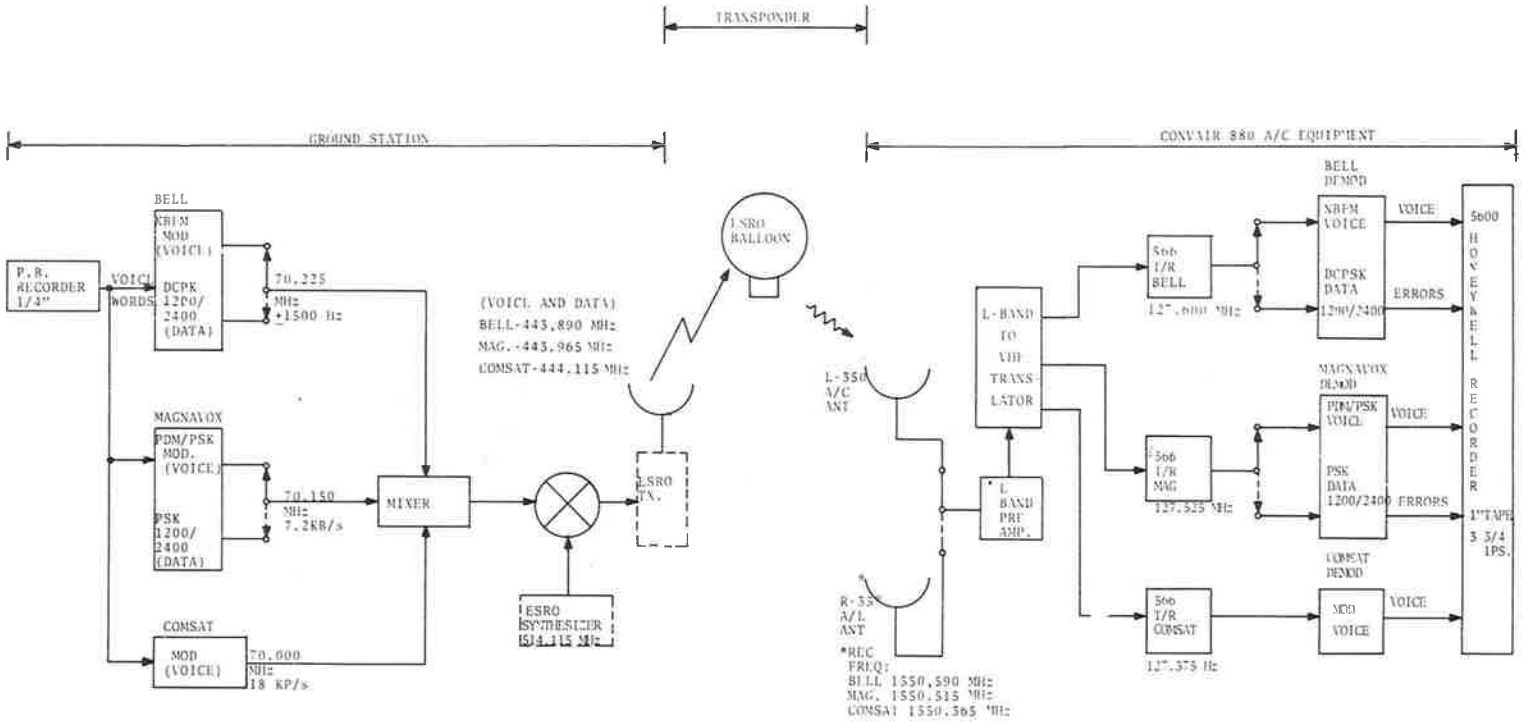

Figure 3-1. Experiment Communications Links

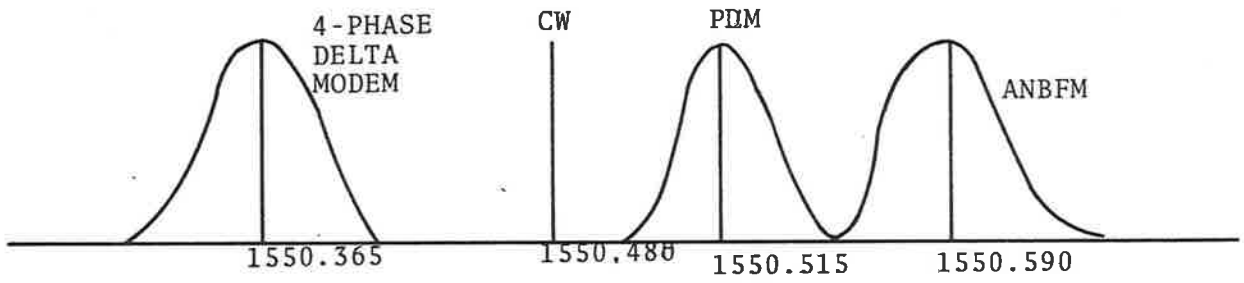

Figure 3-2. Downlink Frequency Assignments

A secondary communications link was in operation throughout the experiment. This link was the experiment control and operation communications. Information was gathered from the ATC center at Bordeaux concerning the locations of the balloon and test aircraft and used to determine where to position the aircraft in order to maintain a particular elevation angle during a given test. Communications to the aircraft as to positioning and operations (e.g., start and stop of a test run) were conducted over the normal aircraft h.f. and VHF channels.

Figure 3-3 is a scale drawing of the Experiment Geometry showing the test range and graphically describes the nature of the test runs. On a typical flight test, the sequence of events is as follows:

1. Launch balloon from Aire Sur L'Adour.
2. Convair 880 takeoff from Pau airport to station over Bay of Biscay.
3. Determine aircraft position with respect to drift of balloon by the ATC center in Bordeaux.
4. Determine highest elevation angle flight possible and position aircraft for start of test run.
5. Make test run (average duration 8 mins for 10 and 15° elevation angles and maximum of 15 minutes for an elevation of 7°).
6. Reposition aircraft.
7. Continue test runs until balloon position is out of test range.
8. Release transponder from balloon.
9. Convair 880 return to Pau airport.

The usable test time for the balloon flights was between 2 and 5 hours, of which about 50 percent was for voice and data tests; the remainder was for CW multipath testing. Although constant elevation angle flights were desired, this was not possible in practice. Instead, as shown in Figure 3-3, flights were

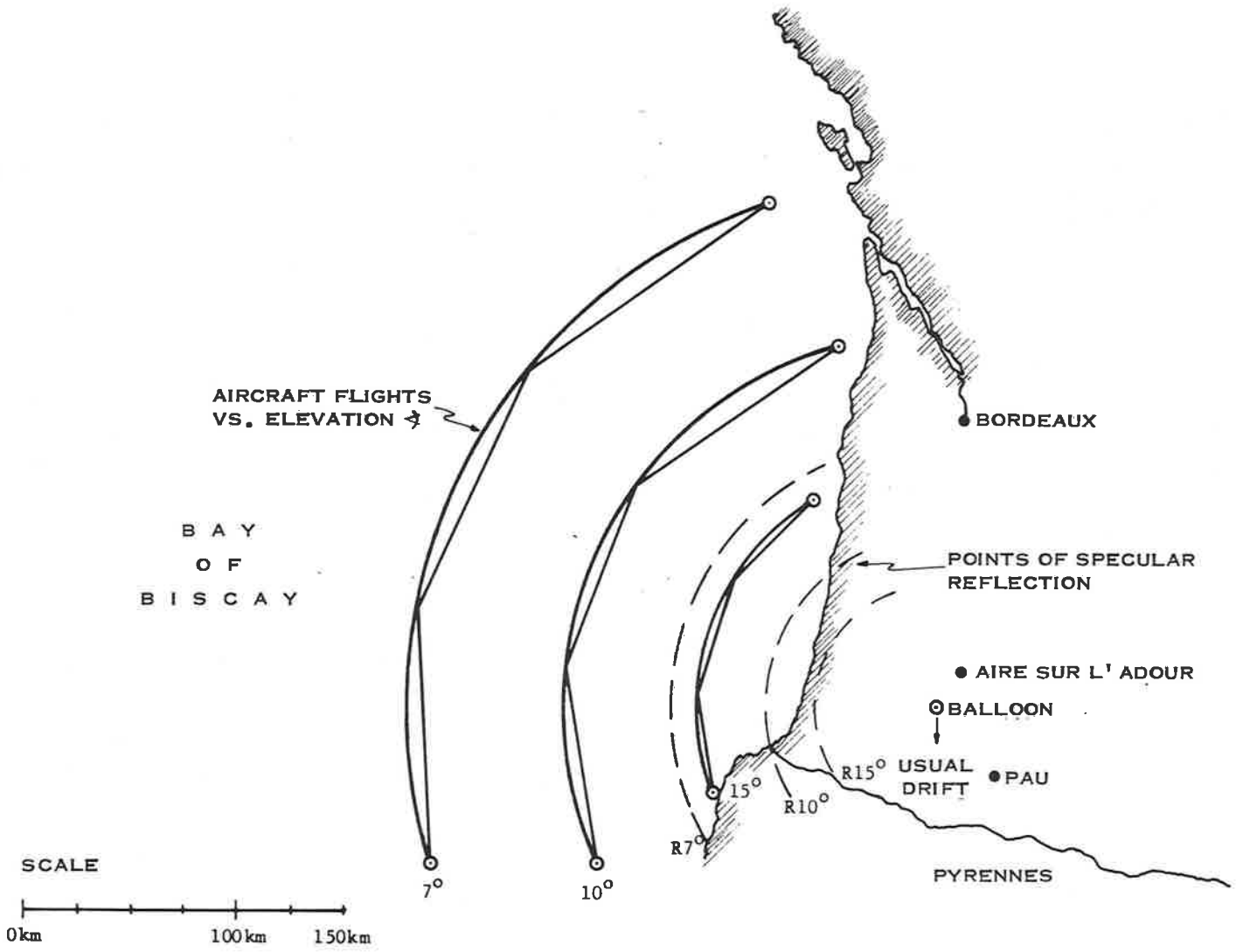

Figure 3-3. Experiment Geometry

straight-line paths between points of constant elevation angle. In addition, the balloon was drifting and real-time correction for this drift was not possible. However, a few simple calculations show that for test runs at the elevation angles used in our experiment, a (typical) balloon drift of 8 knots either towards or away from the aircraft resulted in an error in the elevation angle of no more than $\pm 1/4$ of a degree. Furthermore, if we assume the airspeed of the 880 as 425 knots, then the error introduced in flying a straight line for 10 minutes at 10° elevation is no more than approximately 1°. The knowledge of the actual balloon and aircraft position from the ATC radars introduced errors of the same magnitude. Therefore, it is reasonable to assume the elevation angle was known to $\pm 1°$ for any particular test run.

Sea state conditions during the tests were not precisely measured. However, from observations made of the test range prior to and shortly after the test flights, it is known that the conditions for the test period of interest (9/23 and 9/24) were essentially calm with flat seas. (Sea State 0 - 1.)

3.2 C/NO MEASUREMENTS DURING FLIGHT

3.2.1 Field C/No Measurements

All measurements were recorded on a 14-track instrumentation recorder and were later re-recorded in strip chart form in the laboratory to determine the actual C/No. A sample of the strip chart format is shown in Figure 3-4. The C/No circuits were designed to measure noise power in a very small band and provide a voltage which was proportional to the noise power in this band. However, the time constant of the final low-pass filter (one second) did not allow the filter capacitor to completely charge up within a given cycle. As a result of this interaction, the conversion of strip chart values of voltage to actual C/No could not be directly accomplished. Instead, the time constant of the measuring circuit was next determined and simple analysis showed that the desired d.c. value could be determined as depicted in Figure 3-4. Thus values of A and B were determined from the strip charts.

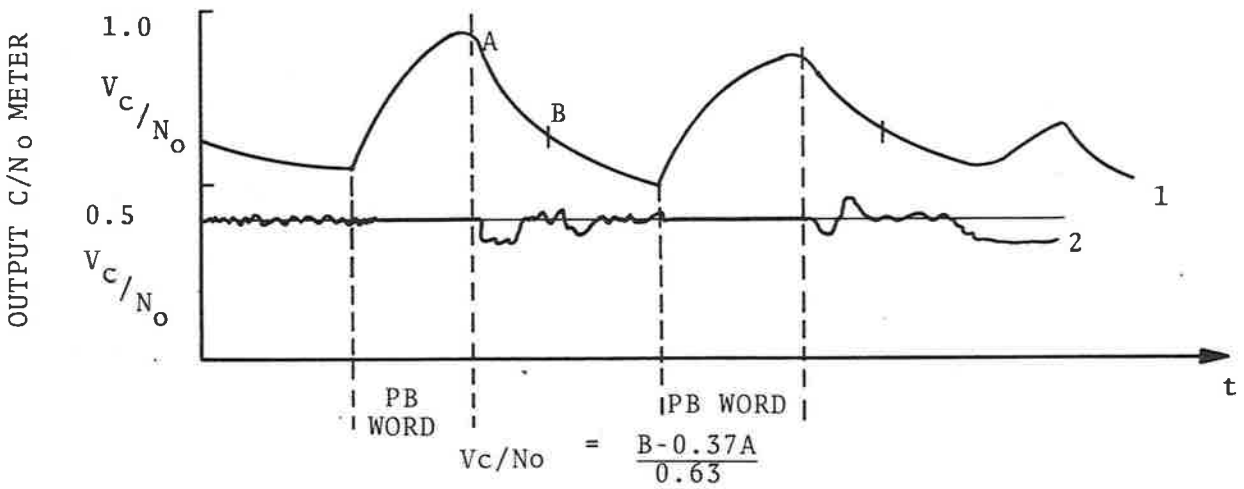

CURVE 2-Represents Vc/No sample and hold circuit been operative

CURVE 1-Actual C/N_o waveform recorded

Figure 3-4. Strip Chart Format

The calculation was then converted to C/No via a calibration curve relating voltage to C/No. This calibration curve is shown in Figure 3-5. This curve represents the mean value of a series of 35 separate calibrations (from 38-56 dB-Hz) of the voice equipment taken over a period of 2 months in the laboratory. Also shown in this curve is the one-sigma variation of the calibration over this period. As can be seen, the mean values represent less than a 1/2 dB variation in the calibration. Since some statistical analysis was desired on these C/No measurements, a computer program was written to convert the values of A and B to C/No values. The conversion was done in 1/2 dB increments. A histogram of these C/No values was then determined and a time plot was made. Figures 3-6 through 3-8 are representative of C/No conditions for 15, 10 and 7 degree elevation angle flights as indicated on the figures. As seen in these figures the input C/No was sampled at approximately once every two seconds. However, this sampling rate is not fixed and is determined by the word rate. It is obvious that substantial variation occurred in the recorded values of C/No. Typically, on the 7° runs, the variation was 10 dB peak-to-peak. The probable cause of this variation is discussed in the following section.

3.2.2 CW Multipath Measurements

The following results are presented to indicate the degree of fading measured in a typical CW L-band aircraft-to-balloon link on antennas identical to those used in the voice experiment. This data is from a previous set of tests conducted on the U.S. West Coast in May, 1971. The data is given for elevation angles of 10°, 12°, and 14°. A summary of the test conditions is presented in Table 3-3. Figure 3-9 is a block diagram of the measurement scheme used to obtain the data presented herein. The reference antenna was either the zenith antenna or 35° offset antenna as used in the voice and data experiments. The CW signal is amplified and then detected and down converted in the L-band phase lock loop receiver. The coherent AGC of this receiver is A/D converted at 64 samples per second and recorded with other flight data on a digital tape recorder. This AGC voltage can be related to input signal level

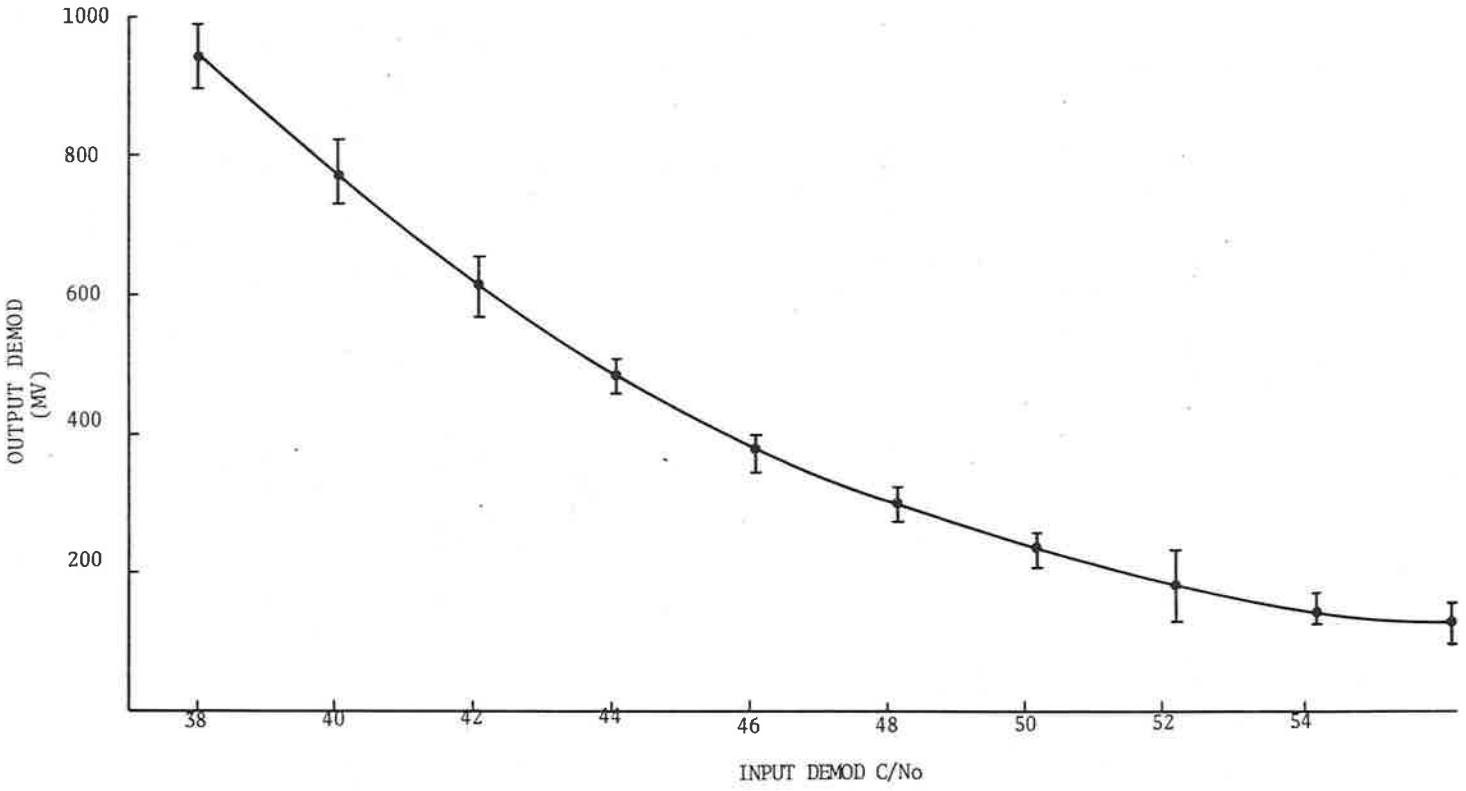

Figure 3-5. C/No Calibration Curve

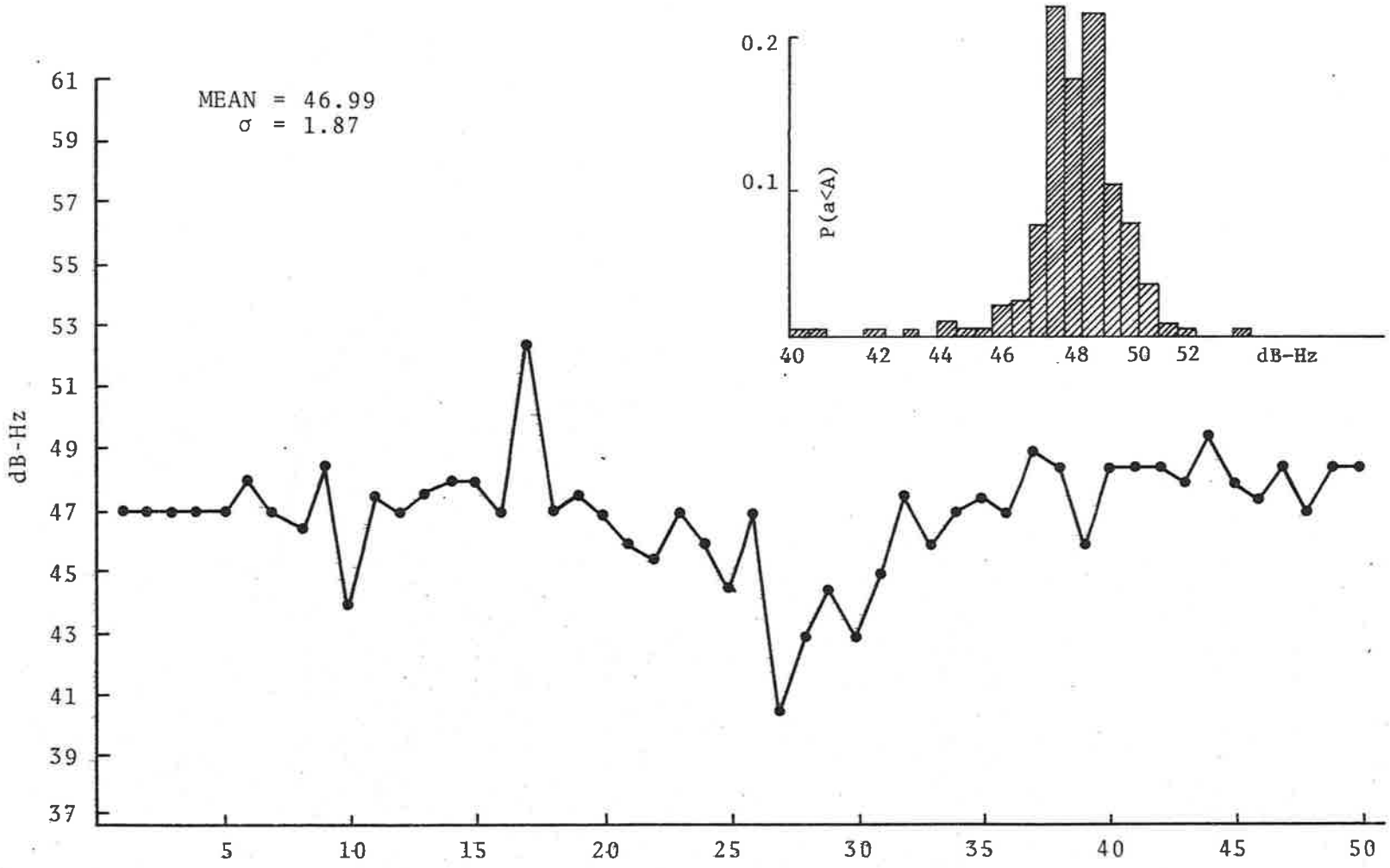

Figure 3-6. C/No Variation - 15° Elevation Angle

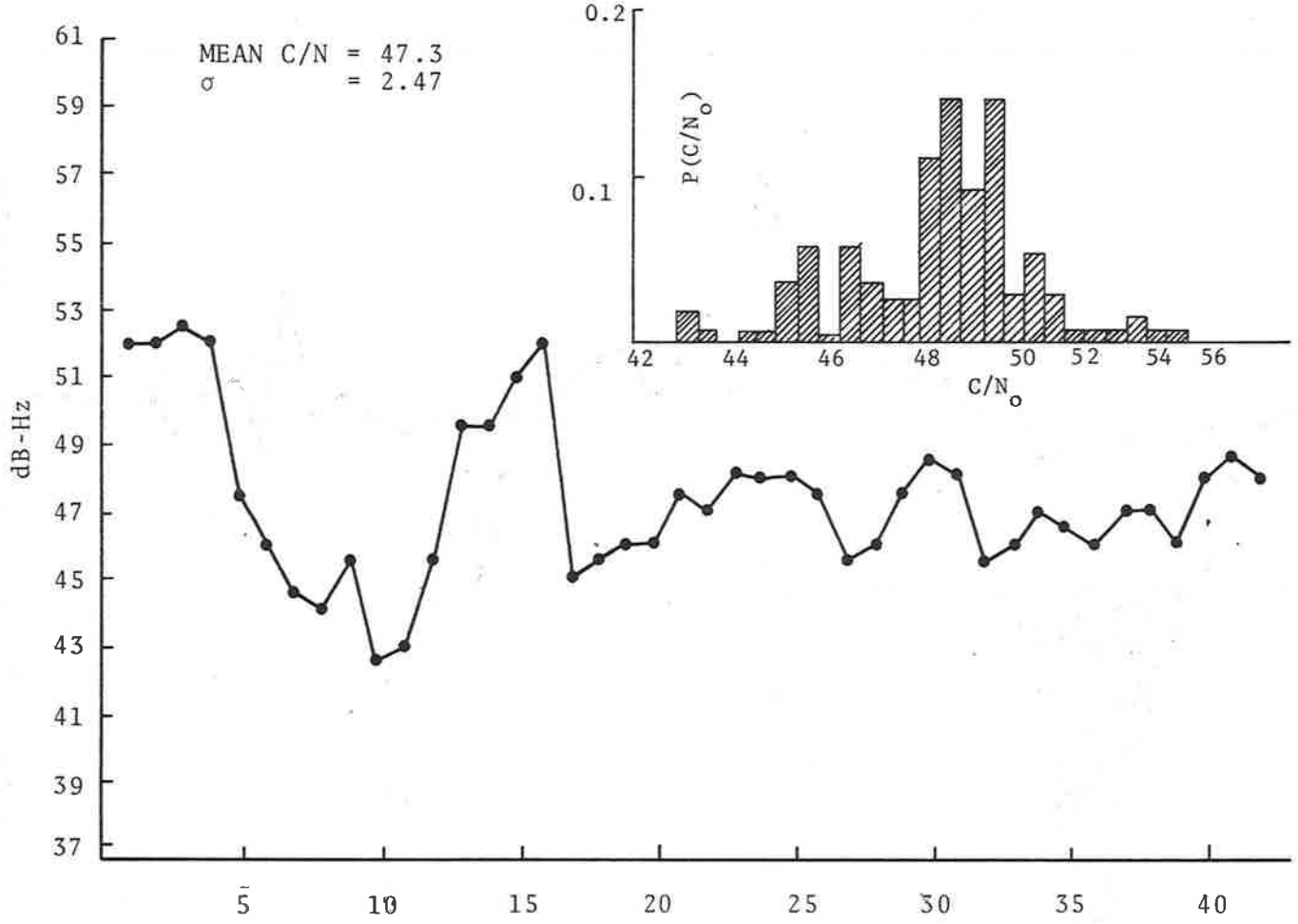

Figure 3-7. C/No Variation - 10° Elevation Angle

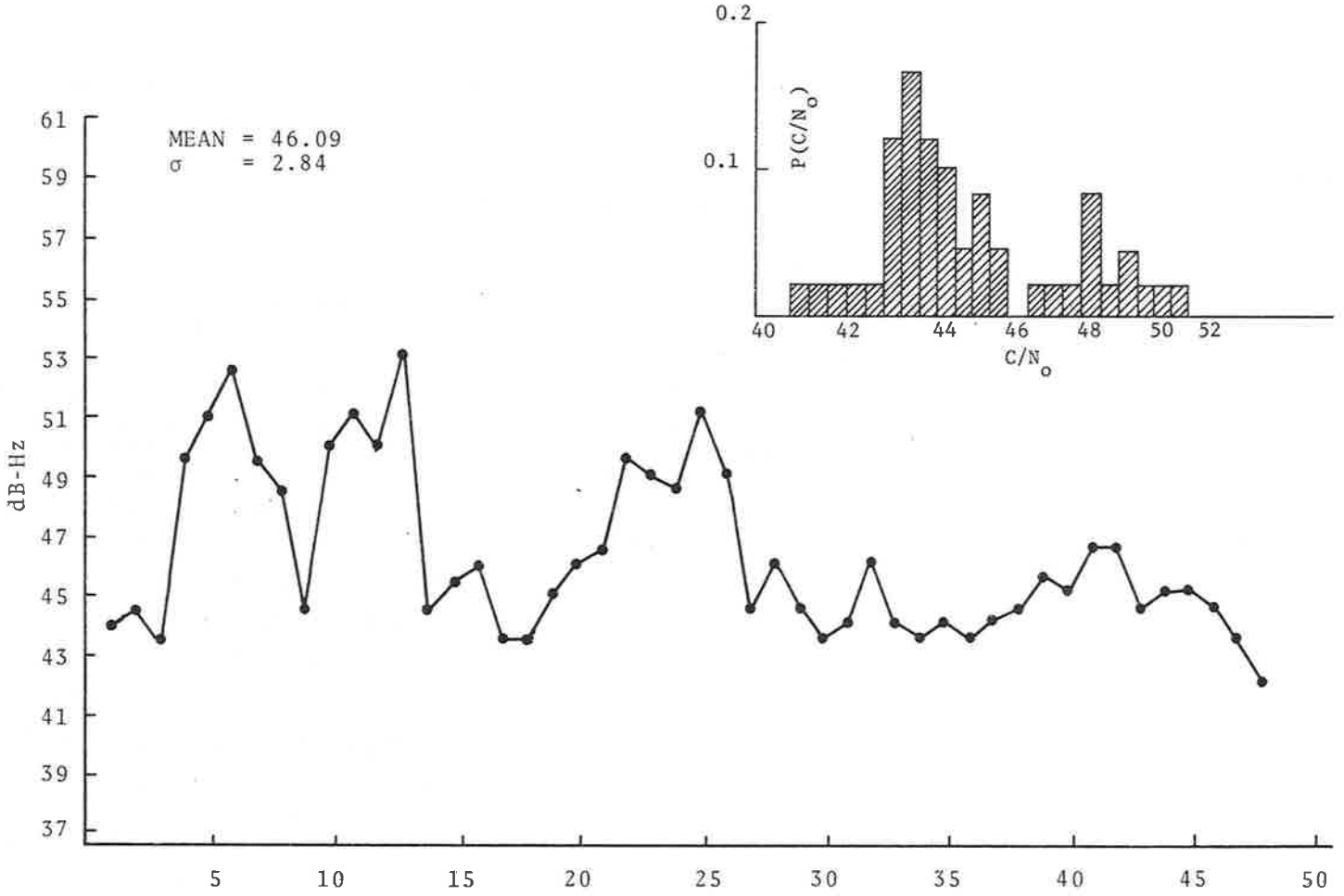

Figure 3-8. C/No Variation - 7° Elevation Angle

TABLE 3-3. CW MULTIPATH TEST CONDITIONS

DATE: May 24, 1971
BALLOON ALTITUDE: 102,000 ft.
AIRPLANE ALTITUDE: 18,000 ft.
AIRSPEEC: 418 KNOTS
Sea State: 2 ft. SIGNIFICANT WAVE HEIGHT
80 ft. WAVELENGTH
ON TOP OF 9 ft. SWELLS 400 ft. WAVELENGTH

CW MULTIPATH DATA TAKEN:

Elevation	ANTENNAS USED	LENGTH OF DATA
Test Run 1. 10.0° - 10.3	Zenith Ant., Starboard Side Antennas	20 mins.
2. 10.0° - 10.3	Zenith Ant., Starboard Side Antennas	20 mins.
3. 12°	Zenith Ant., Starboard Side Antennas	11 mins.
4. 14°	offset Ant. Port Antenna	20 mins.

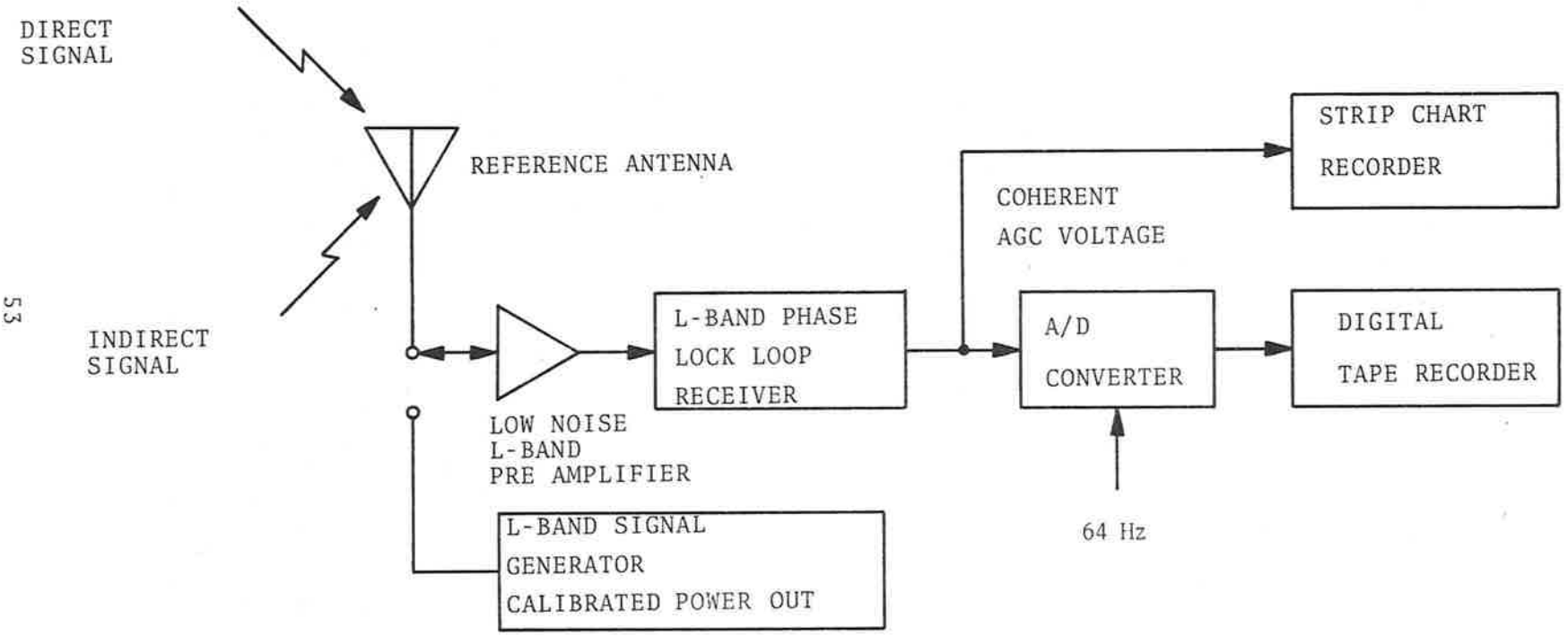

Figure 3-9. Block Diagram, CW Measurement System

by the calibration curve shown in Figure 3-10. Since we know that the noise figure of the entire receiving system is 3.5 dB and the external sky temperature is approximately 150°k then these input signal powers can be converted to C/No values as shown on the AGC calibration curve. Figures 3-11 through 3-13 are cumulative density curves or received signal amplitude as measured by the coherent AGC. The antenna used, balloon-to-aircraft elevation angle and the time of measurement is indicated on each curve. These cumulative density curves were obtained by a single histogram approach to viewing the data samples. Each three minute segment of data represents 11,520 data smaples taken at 64 samples per second. Because of the low sample rate, an estimate of the bandwidth of the input signal was obtained from fast Fourier transforms of the raw analog data (which was recorded separately) and averaging the magnitude squared of these transforms. The resulting average bandwidth obtained was approximately 13 Hz. Therefore, the sample rate of 64 sps was more than adequate to prevent aliasing. Table 3-4 presents the average fading level observed 1% of the time for the antennas and elevation angles indicated.

Some possible causes for signal fading are discussed below.

A. Aircraft Roll - The roll of the aircraft results in a change in the antenna gain in both the received direct signal and the received indirect signals. This change in gain would appear as a slow variation in the signal strength.

B. System Noise - Receiver thermal noise and sky noise changes may result in some variations of the measured AGC output voltage.

C. Changes in Balloon Transponder Output Signal Power.

D. Signal Reflections - from the skin of the aircraft.

E. Oceanic Multipath - specular, diffuse or both.

A simple investigation was made into causes A, B, and C for both the CW measurements and the C/No measurements of the voice experiment.

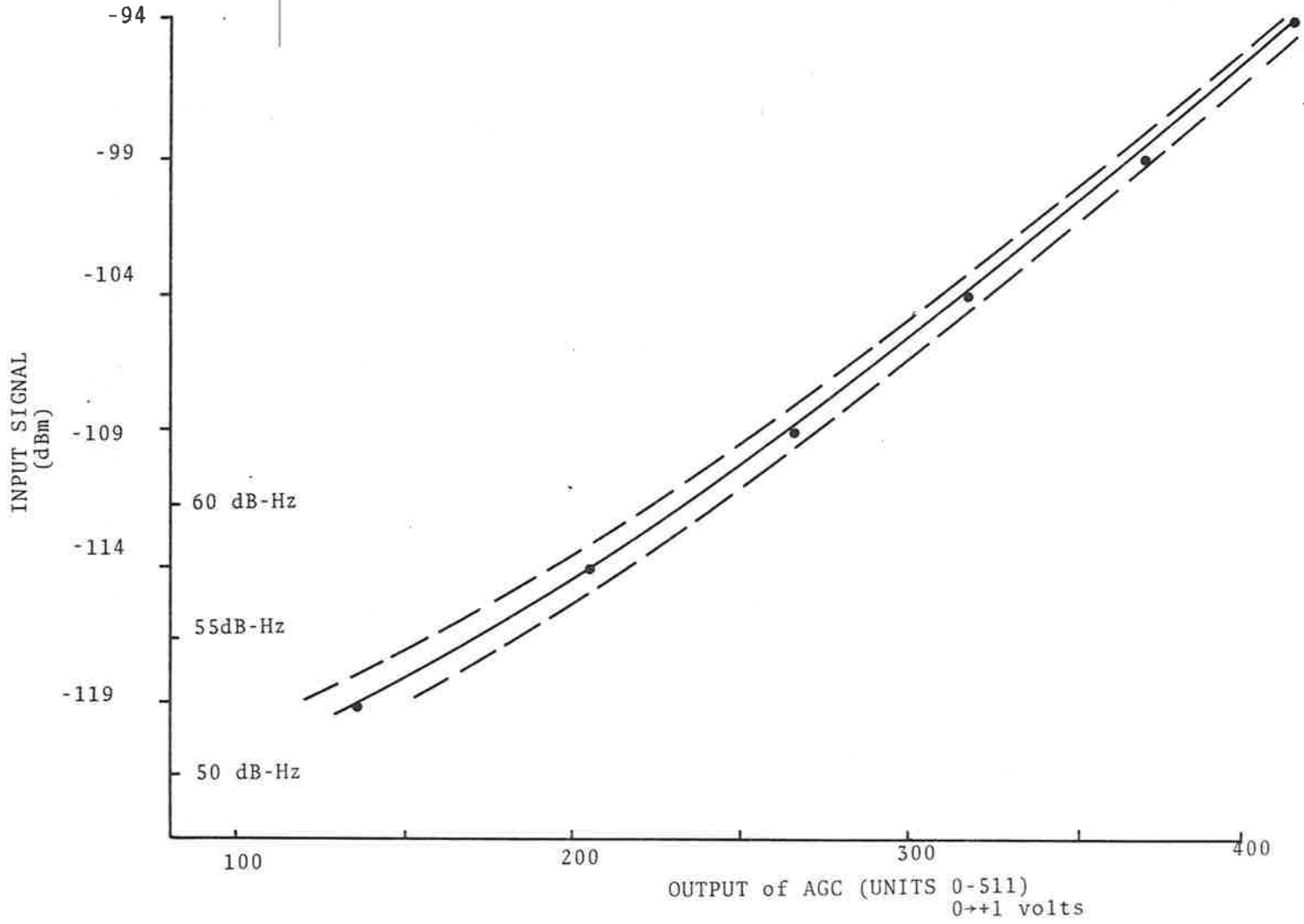

Figure 3-10. AGC Variation with Signal Level

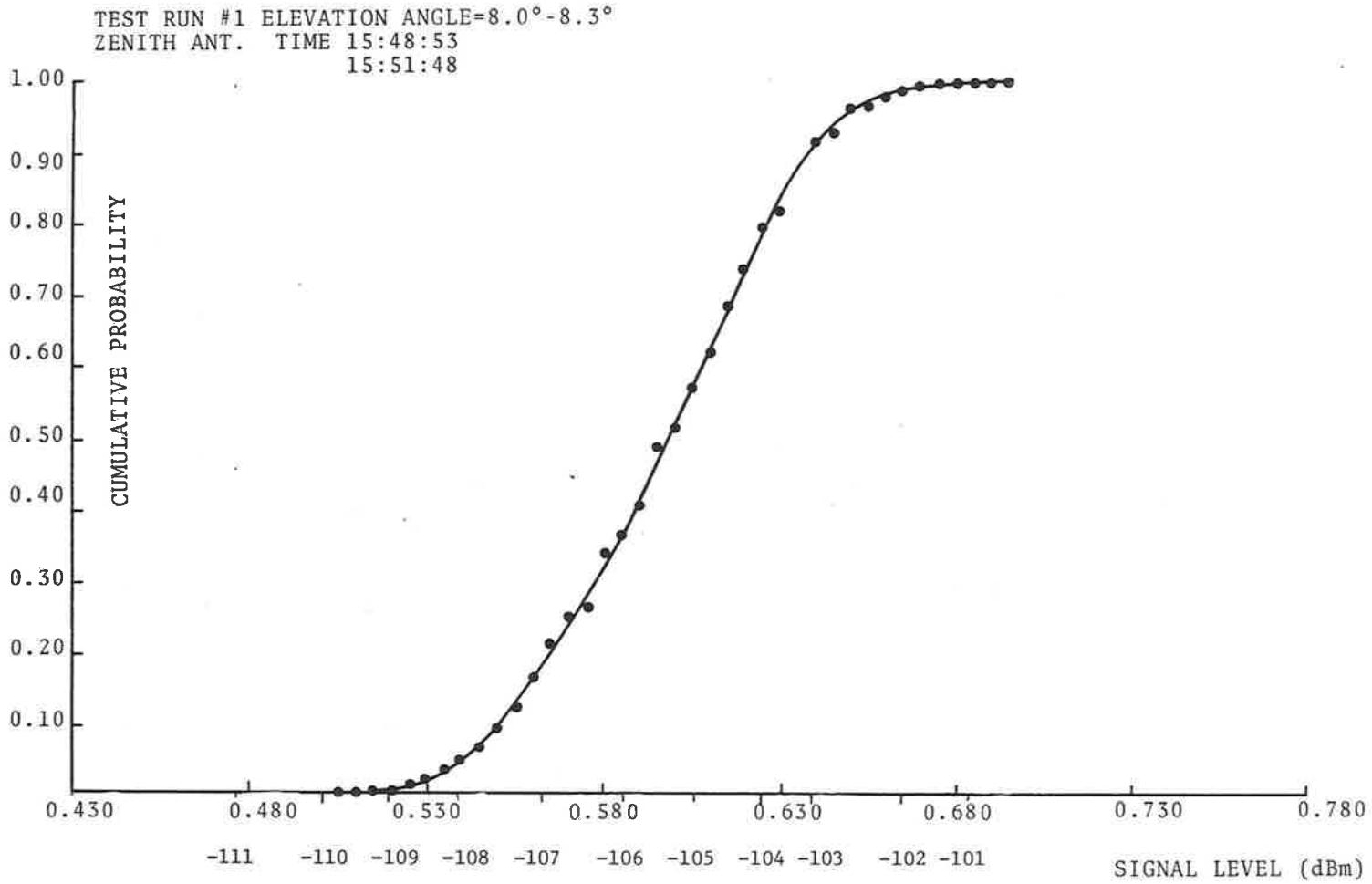

Figure 3-11. Cumulative Density of Signal, 8° Elevation Angles Test Run #1

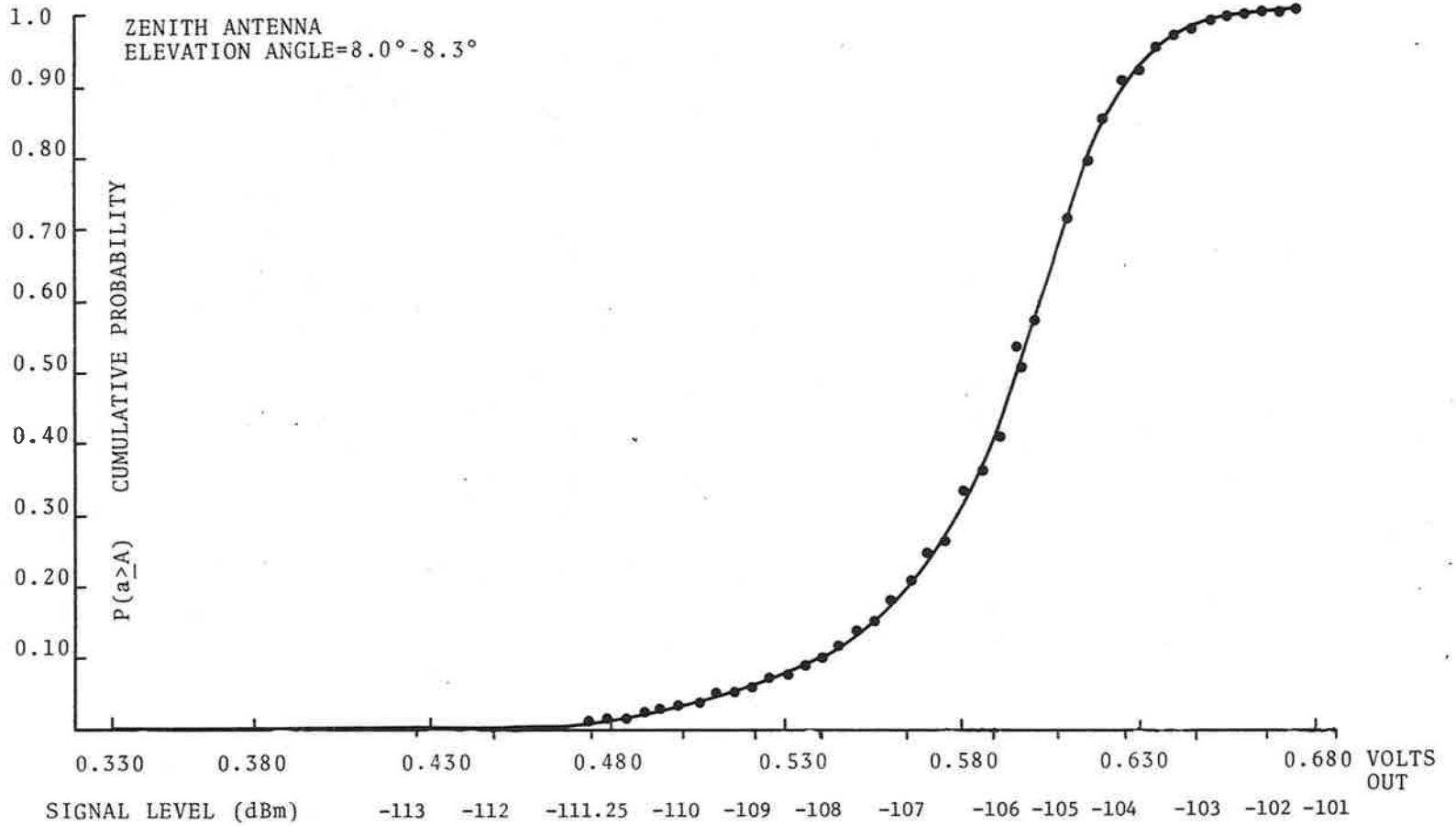

Figure 3-12. Cumulative Density of Signal, 8° Elevation Angle

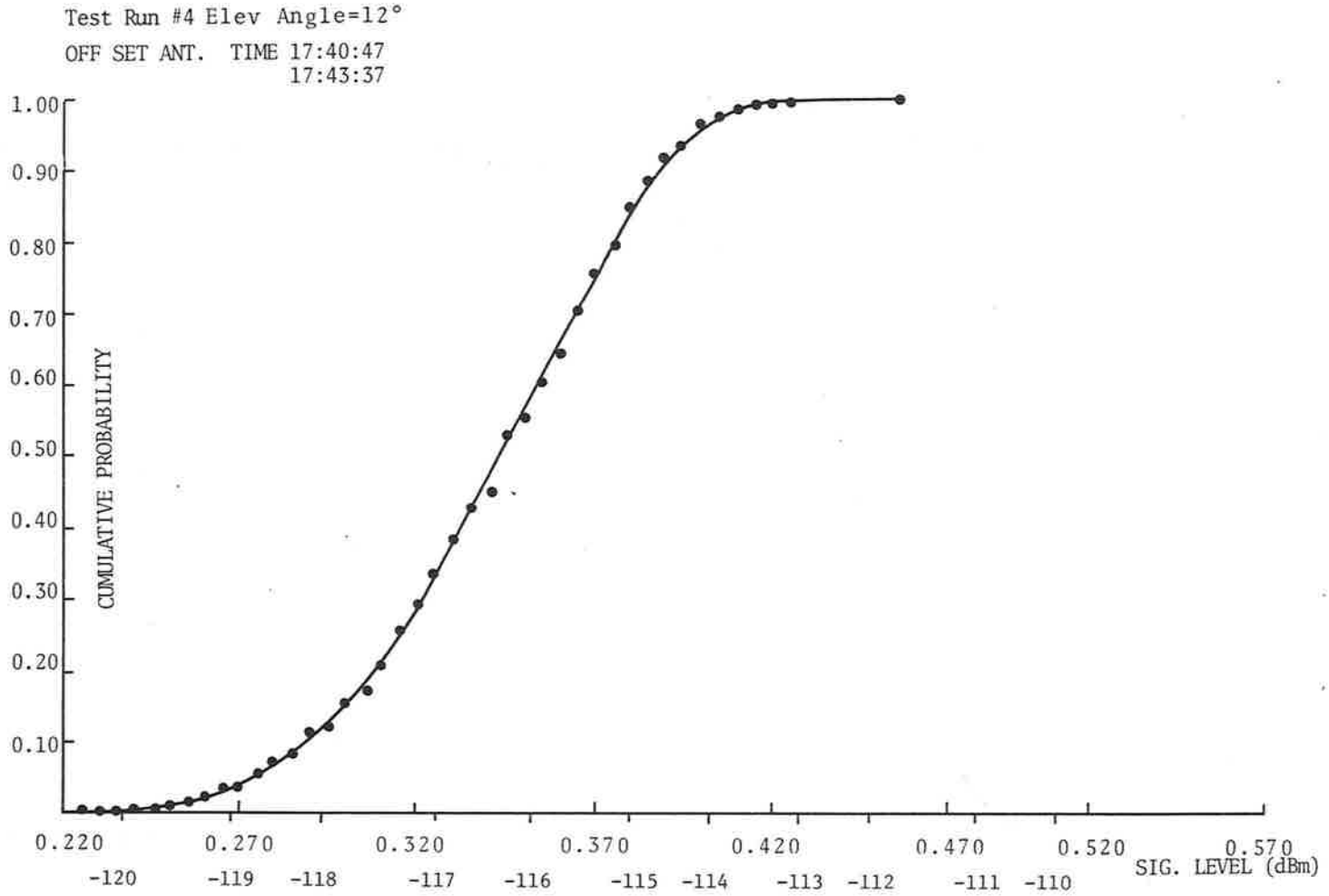

Figure 3-13. Cumulative Density, 12° Elevation Angle

TABLE 3-4. AVERAGE OBSERVED FADE LEVELS

ELEVATION ANGLE	FADE LEVEL - 1% OF TIME	ANTENNA
10°	3.5 dB	Zenith
12°	4.0 dB	Zenith
14°	3.5 dB, 6.0 dB	Offset

NOTE: Much Higher Fade Levels (6.0 dB, 1%) Were Observed at 14°, after Reflection Point Passed Into the Lee of an Offshore Island, and Encountered Much Smoother Sea Conditions

A. Examining the roll plane antenna pattern for the zenith mounted antenna presented in Figure 3-14, it is easy to see that aircraft roll of ±4° would result in less than 1 dB gain variation at 10° elevation angle in the direction of the direct signal. The change in gain in the direction of the multipath signal is somewhat greater varying from +2 dB to -4 dB. The change in the multipath rejection ratio, however, is from 2 dB to 7 dB ($G_{DIRECT}^{(dB)} - G_{INDIRECT}^{(dB)}$). Similarly, examining Figure 2-16 which is the role pattern for the R-35° antenna, the changes in gain at 10° elevation angle in the direct path for role of ±4° is ±1 dB.

The corresponding changes in gain in the indirect path are +8 to -10 dB, resulting in a variation of multipath rejection of 5 dB (min) to 21 dB (max). An investigation of roll data recorded during the CW tests performed on the West Coast in May 1971 revealed that the aircraft roll did not vary greater than ±4° throughout any one test run. This aircraft roll results in slow varying changes in signal level corresponding to the changes in gain described above. In the voice and data tests, an examination of roll data revealed that aircraft roll was on the average less than ±2°. In general, the flights during the French series of tests were straight line flights thus minimizing the roll which would occur from flying circular flight paths. The resulting change in gain in the direct path is negligible in comparison with the magnitude of C/No variation observed during the experiment.

B. Figure 3-15 is the cumulative density curve of the variation due to thermal noise of the L-band receiving equipment and the A/D conversion. It is expected that any CW measurements would result in variations of this order of magnitude even with a constant power received CW signal. An equivalent problem does not exist for the C/No measurements of the voice experiment. The technique of measurement and the calibration of the equipment in terms of C/No precludes any variations due to receiver thermal noise.

C. In both sets of experiments, real-time monitoring at the ground stations of balloon transponder power output was recorded. An examination of this data revealed essentially no change in

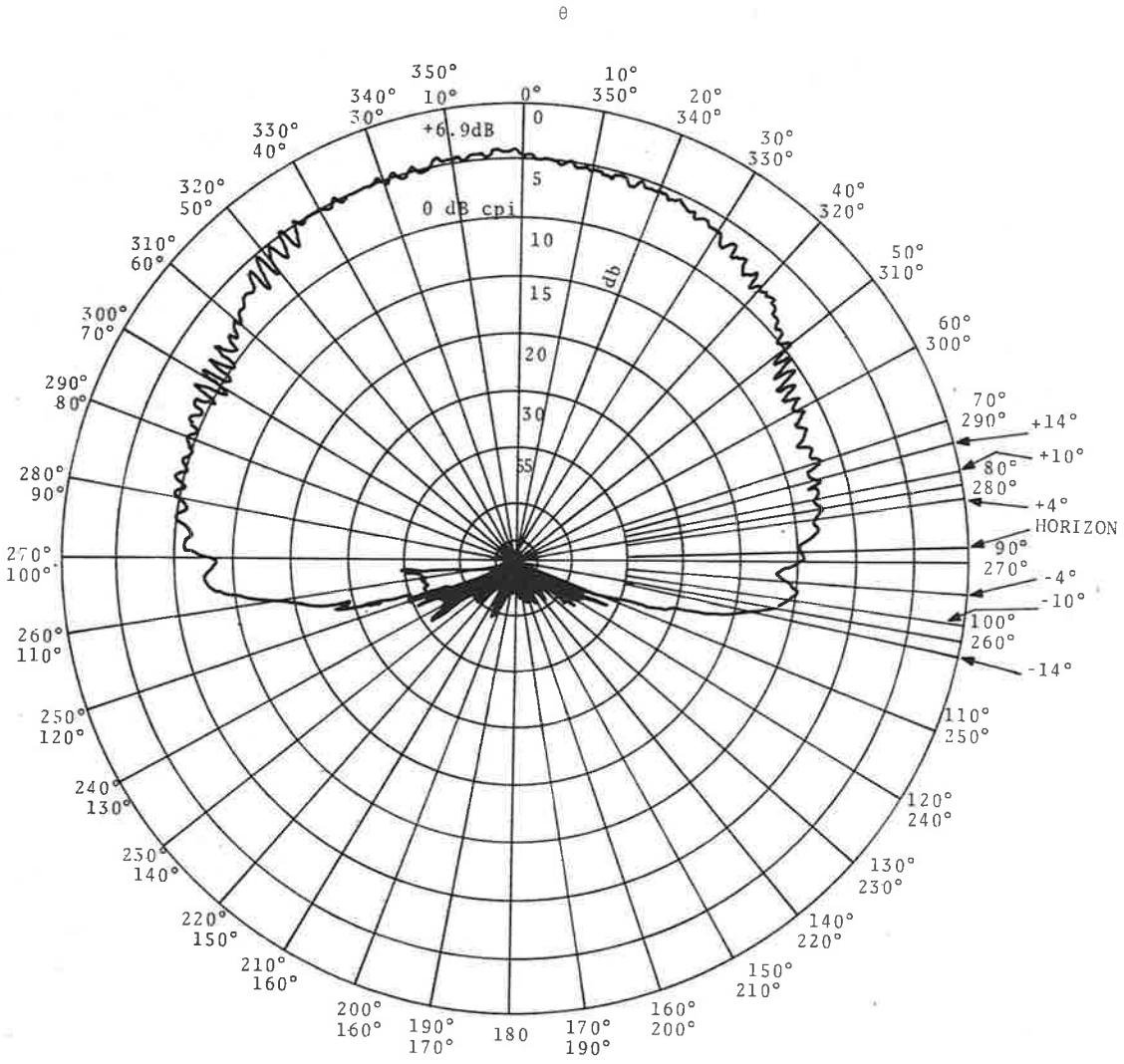

Figure 3-14. Roll Plane Pattern - Zenith Antenna

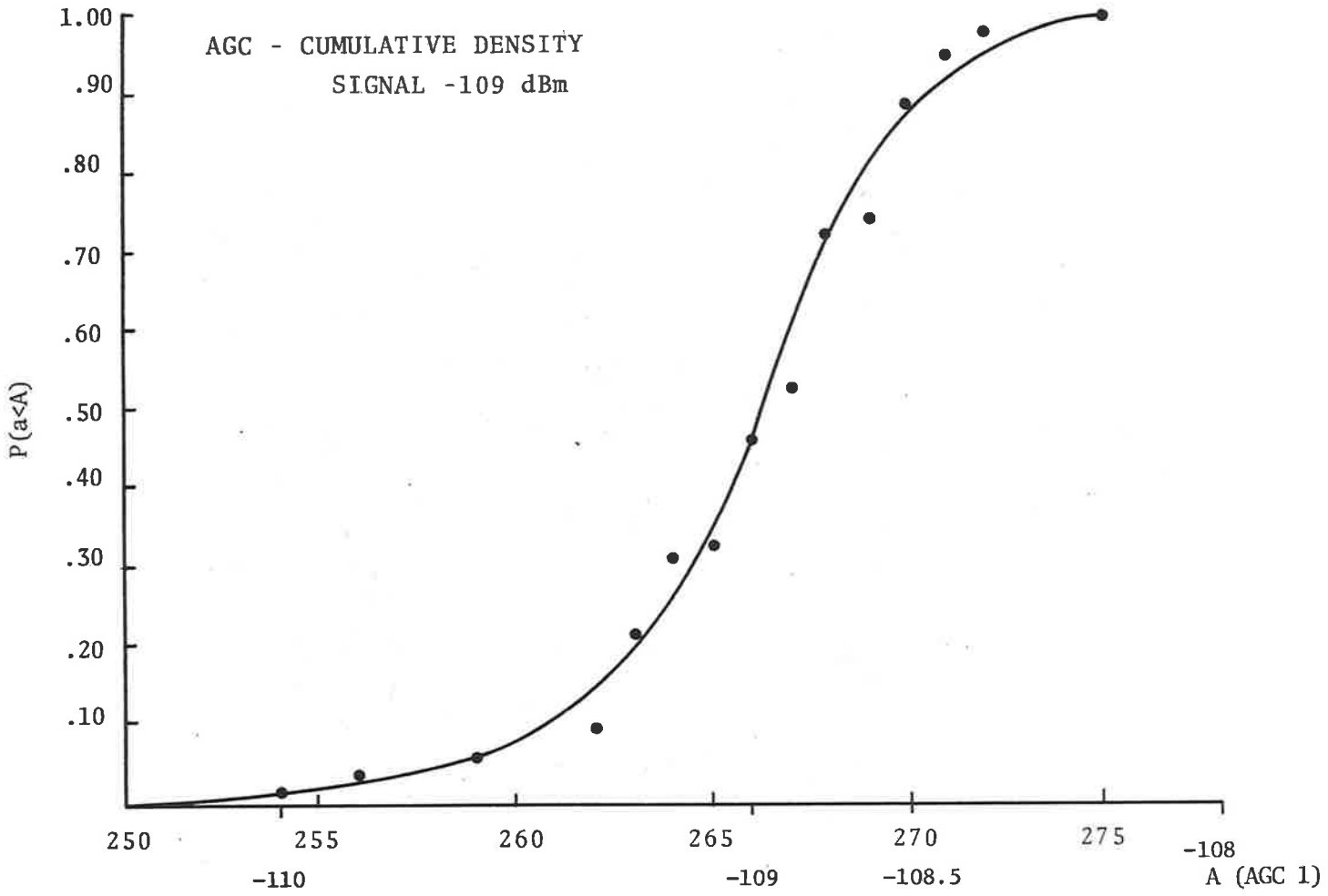

Figure 3-15. AGC - Cumulative Density - Curve

transponder power output during the CW tests. It is therefore concluded that the significant changes observed in the C/No measurements were primarily caused by multipath from the ocean and the aircraft surface.

4. RESULTS AND CONCLUSIONS

4.1 DISCUSSION OF RESULTS

The results of the voice experiment are presented as curves of intelligibility versus measured C/No. These curves represent a polynomial best fit to the actual data. The 1200 b/s digital data was not processed in the same manner. The small amount of digital measurements did not permit meaningful mathematical curve fitting. Instead, the test results for the data modem are presented as "eye-fit" curves. A detailed set of laboratory measurements was made on all three voice modems. The C/No was varied from 40 to 56 dB-Hz in two dB steps. The performance of each individual modem is given in Figures 4-1, 4-2, and 4-3. All three modems are compared in Figure 4-4.

From Figure 4-4 it can be seen that all three modems are within five percent of one another above 47 dB-Hz. Below this point the Delta Mod. System degrades rapidly. NBFM and PDM give very similar performance, with NBFM consistently better by a small amount (three-five percent). The laboratory data is summarized in Table 4-1. The second phase of the laboratory effort consisted of determining a relationship between the laboratory results for the 1000 pb word list, and message intelligibility. Using the data experimentally derived by Kryter (Reference 4), a curve was generated which relates intelligibility as measured using the 1000 word list, with that measured using Harvard sentences, with Articulation Index as an independent parameter. This curve is shown as Figure 4-5. The redundant structure of the sentence test represents a reasonable approximation to message intelligibility. Therefore, Figure 4-5 was used to transform the data presented in Figure 4-4 into an equivalent performance curve for sentence intelligibility. This is presented in Figure 4-6. It is apparent from this curve that, in terms of sentence (or message) intelligibility, which is the ultimate requirement of any voice modem, NBFM and PDM are virtually identical above 42 dB-Hz, and that Delta Mod. deteriorates drastically below 46 dB-Hz. From this data it is

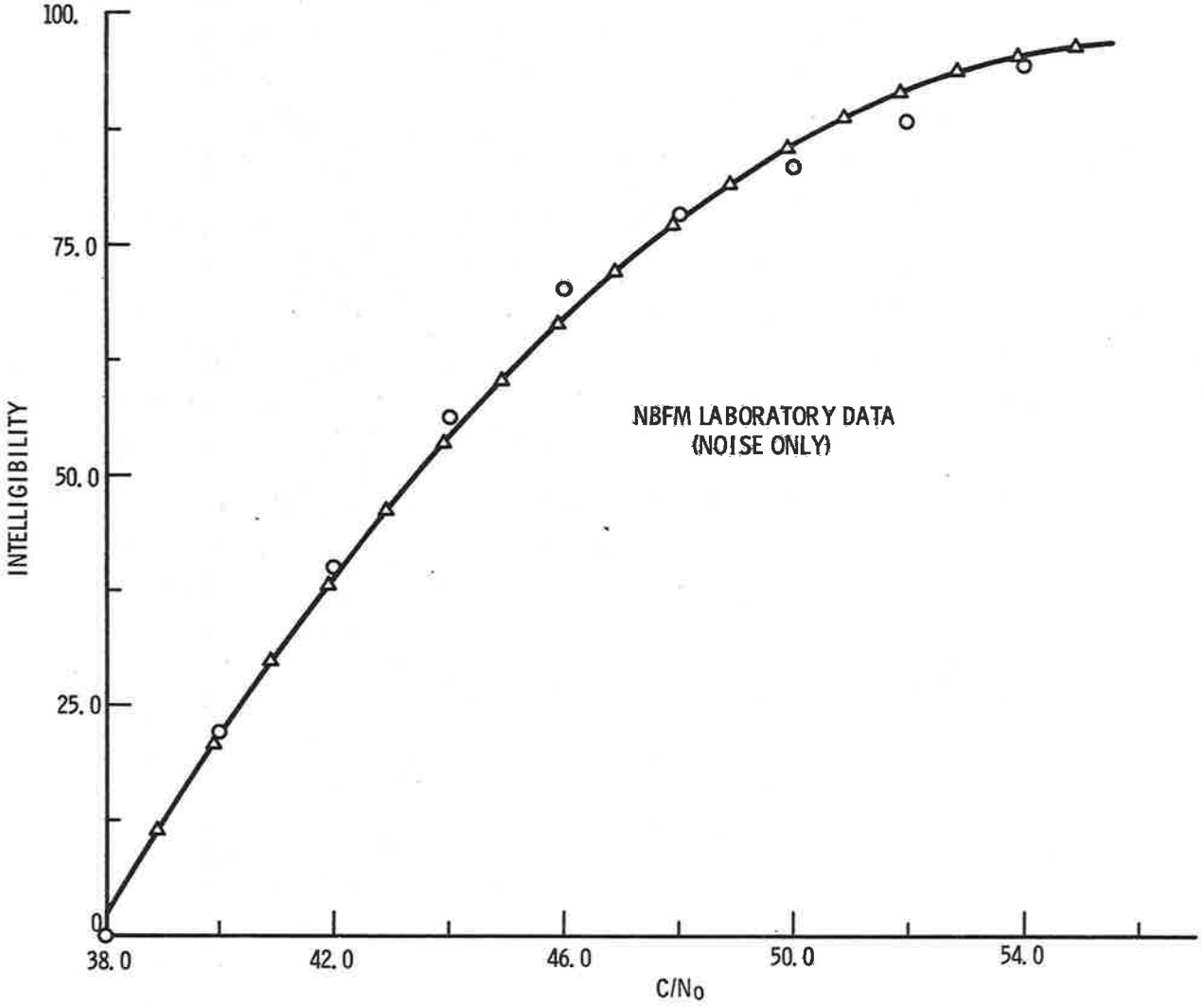

Figure 4-1. Laboratory Intelligibility Curve, ANBFM

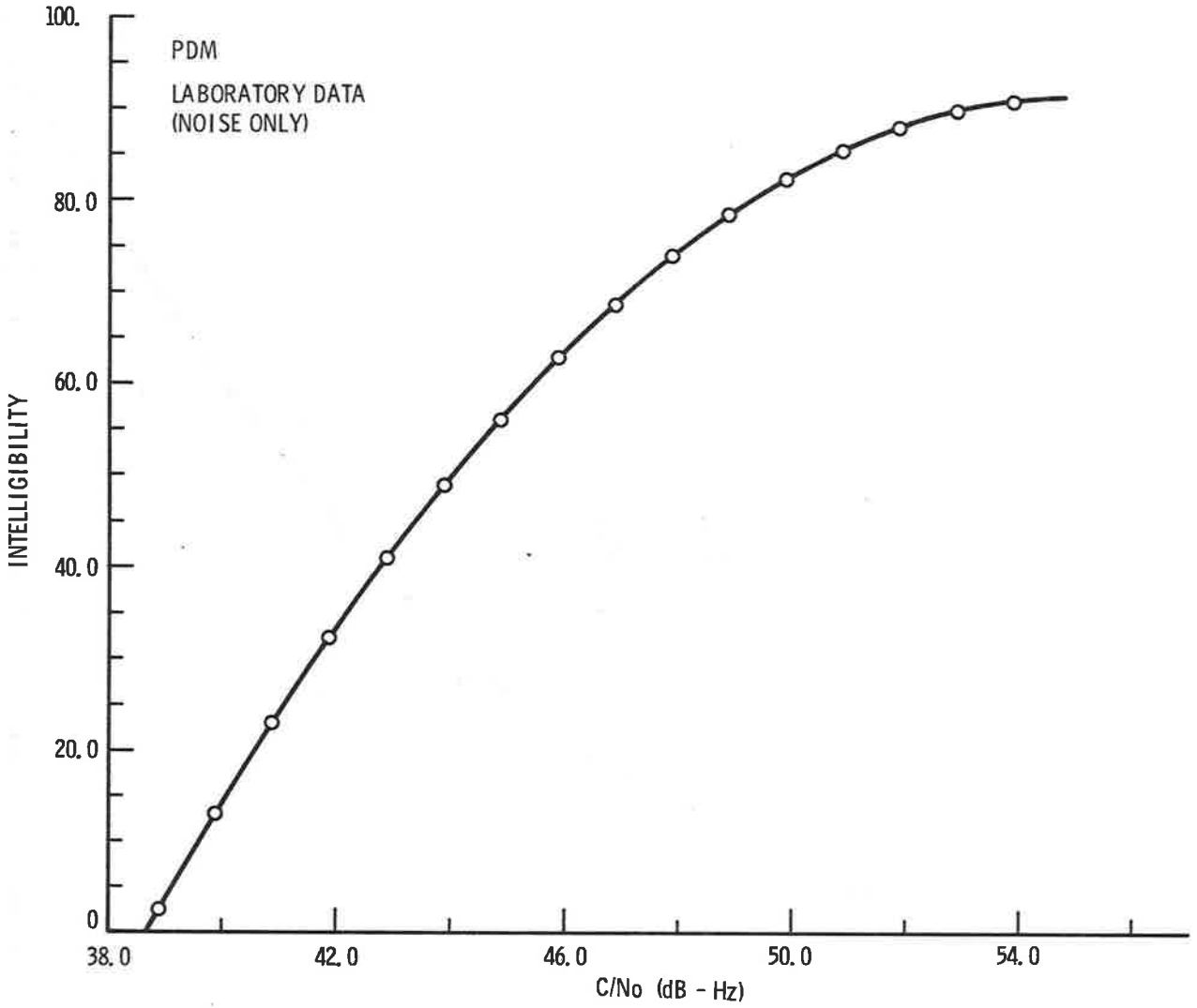

Figure 4-2. Laboratory Intelligibility Curve, PDM

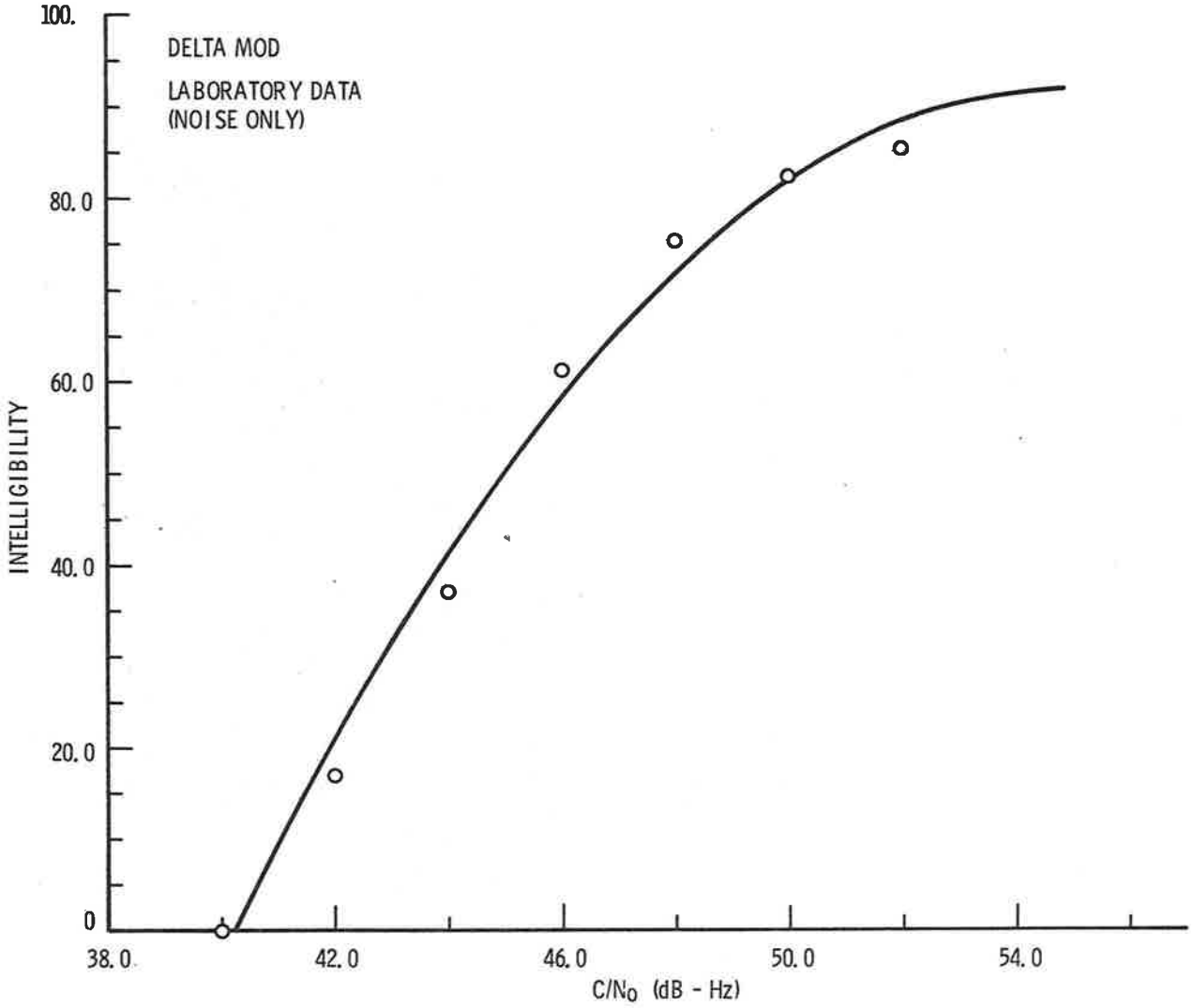

Figure 4-3. Laboratory Intelligibility Curve, Delta

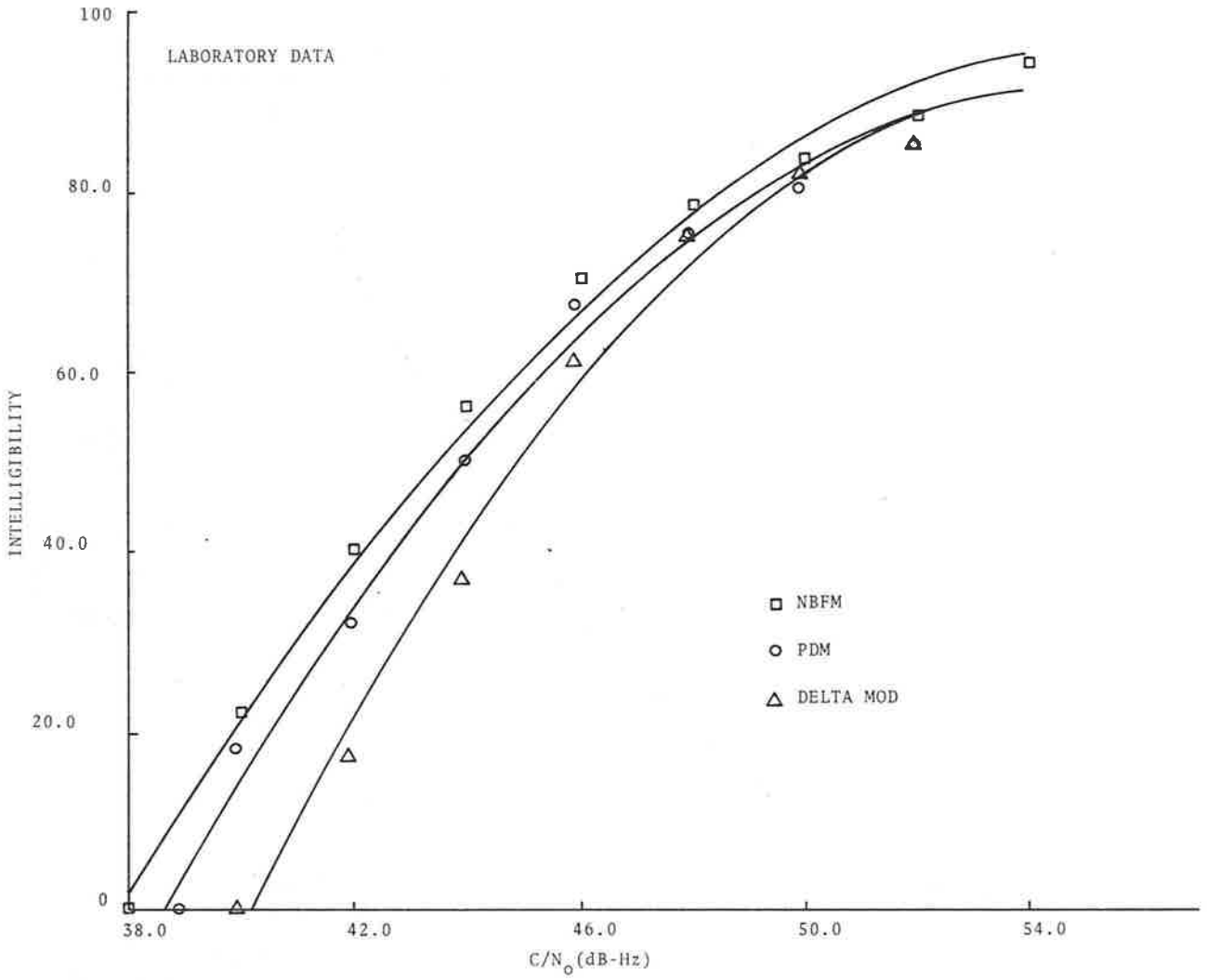

Figure 4-4. Comparison of Modem Performance

TABLE 4-1. C/NO VS INTELLIGIBILITY - LABORATORY DATA

C/No	NBFM	PDM	4-PHASE DELTA MOD
54	95	91	91
53	93	90	90
52	91	88	88
51	88	85.5	85.5
50	86	83	82
49	82	79	77
48	77.5	74.5	72
47	72	70	65.5
46	66.5	63	58
45	60	57	50.5
44	54	50	41
43	46	42	31
42	39	33	20.5
41	30	25	10
40	22	15	0
39	12	3	0
38	2	0	0

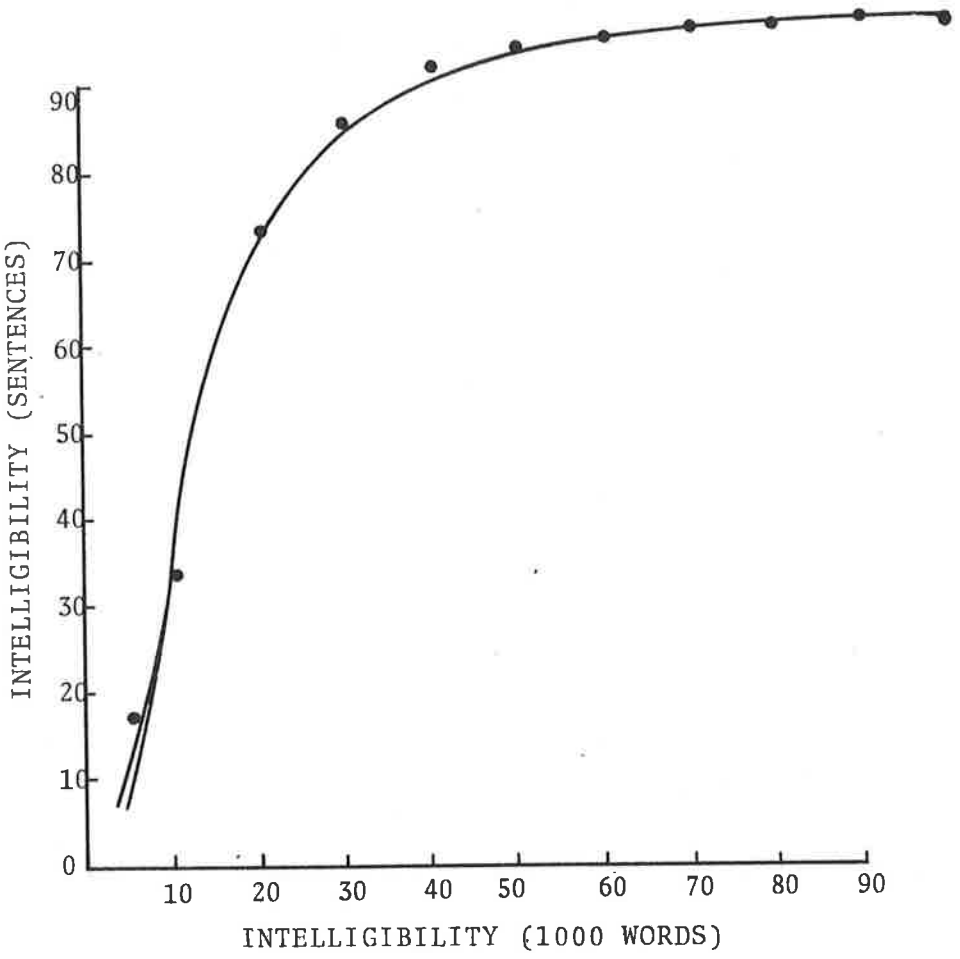

Figure 4-5. Harvard Sentence Intelligibility Vs. Word Intelligibility

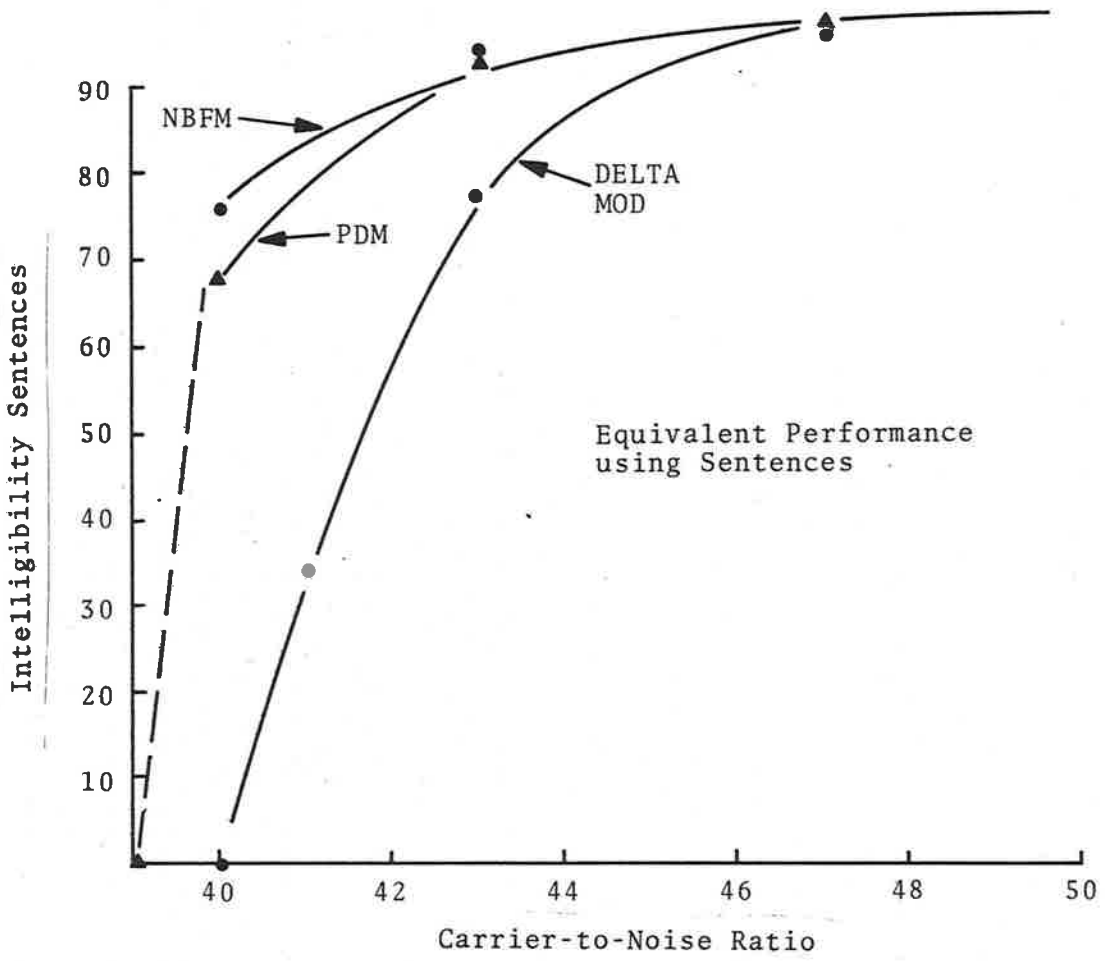

Figure 4-6. Equivalent Sentence Intelligibility Vs. Carrier-to-Noise Ratio

apparent that for the laboratory evaluation, where the only perturbation consisted of ideal white noise, performance of the NBFM and PDM modems was closely equivalent, with perhaps a slight but measurable advantage for NBFM. In all cases for C/No values below about 46-47 dB-Hz, performance of the four-phase Delta Modem was significantly poorer. However, in evaluating the relative performance of the four-phase Delta Modem used in this experiment, the discussion of its performance in Section 2.1.1 should be considered. In particular, it is important that the relatively poor performance of this modem should not be viewed as characteristic of Delta Modems in general.

Voice Modems - Field Results

The results of the intelligibility measurements of the voice recordings made during the field experiments are given in Figures 4-7 through 4-18. The recordings made during the field tests were obtained under conditions of widely varying C/No. The curves of intelligibility presented here were obtained from the curve fitting program described in Appendix A. Figures 4-7 through 4-10 are from recordings made at a 15° elevation angle to the balloon; Figures 4-11 through 4-14 are at 10° and 4-15 through 4-18 are at 7° elevation angle. Included in these figures of individual modem performance with elevation angle are the data points used to obtain the second order polynomial curve of performance. These data points were included to illustrate the "scattered" nature of the data obtained, and the necessity for the curve fitting used. As stated in the section on data reduction, after determining the polynomial of best fit for the data, a comparison of this curve with the actual input data points was made. This comparison was used to determine the rms deviation between the predicted performance (the curve) and actual measurements. This rms deviation then was a measure of the range over which each derived curve validly represents the measured data. The range of C/No values for which the deviation was minimum is given for each performance curve in Table 4-2.

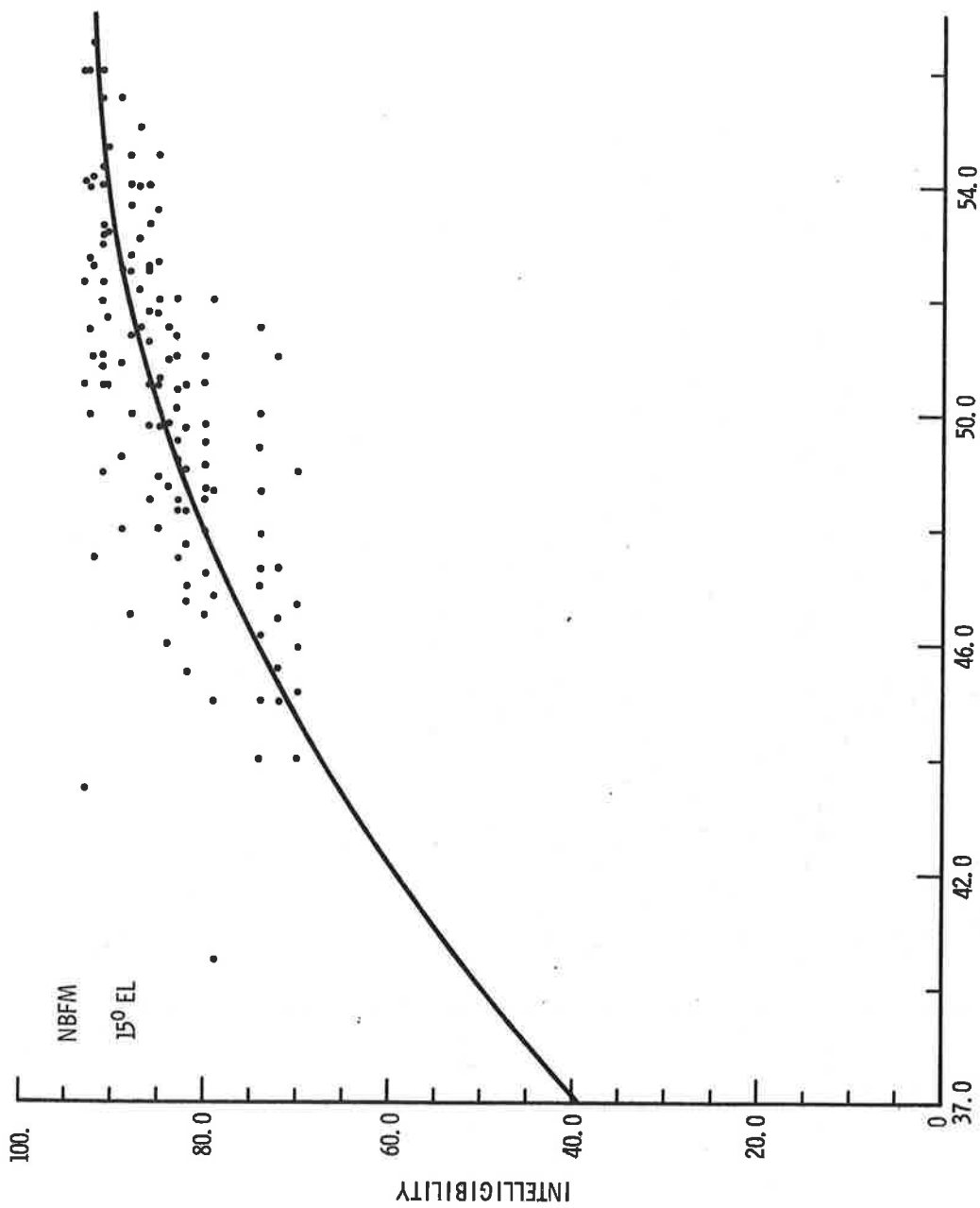

Figure 4-7. 15° Data, ANBFM

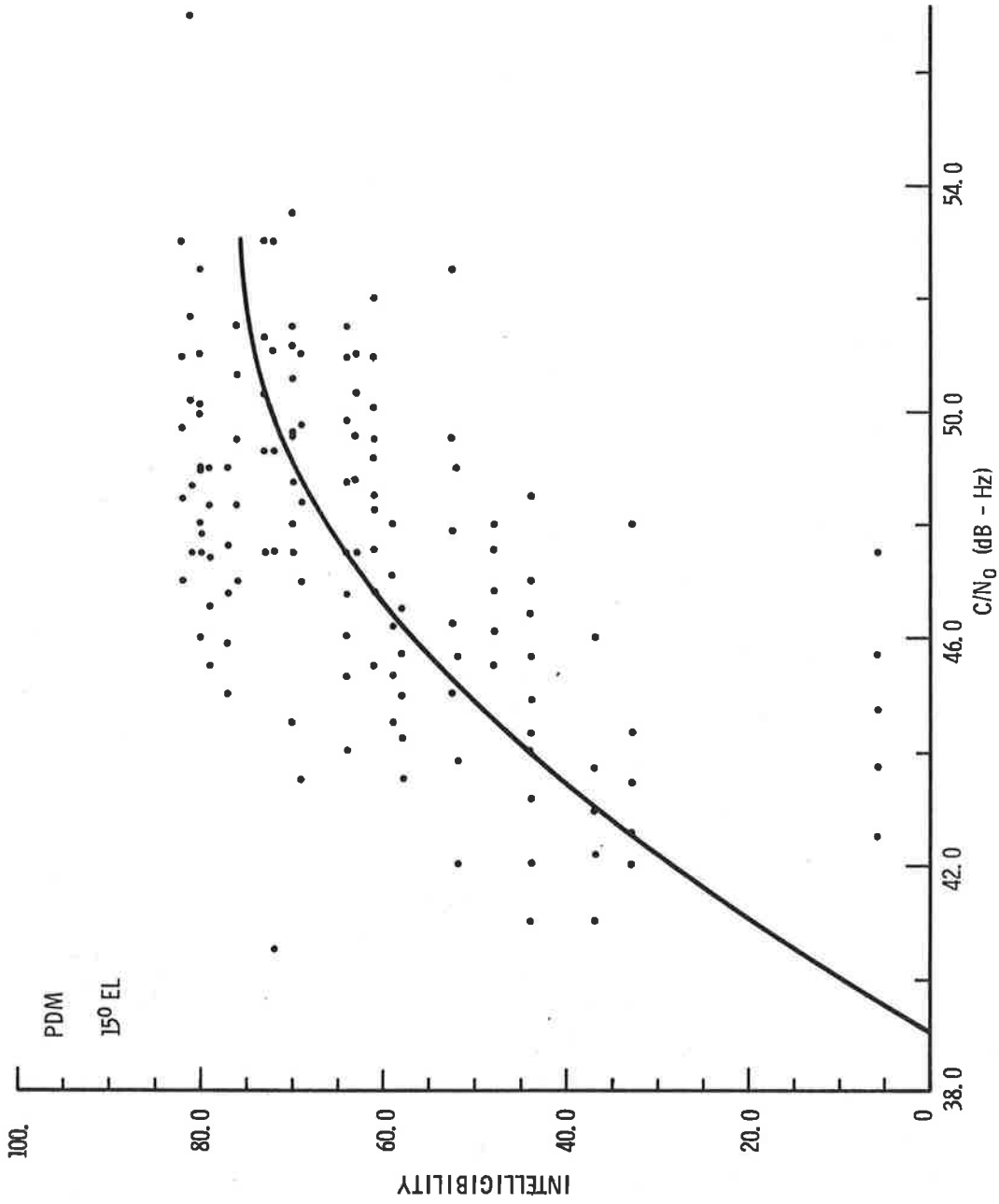

Figure 4-8. 15° Data, PDM

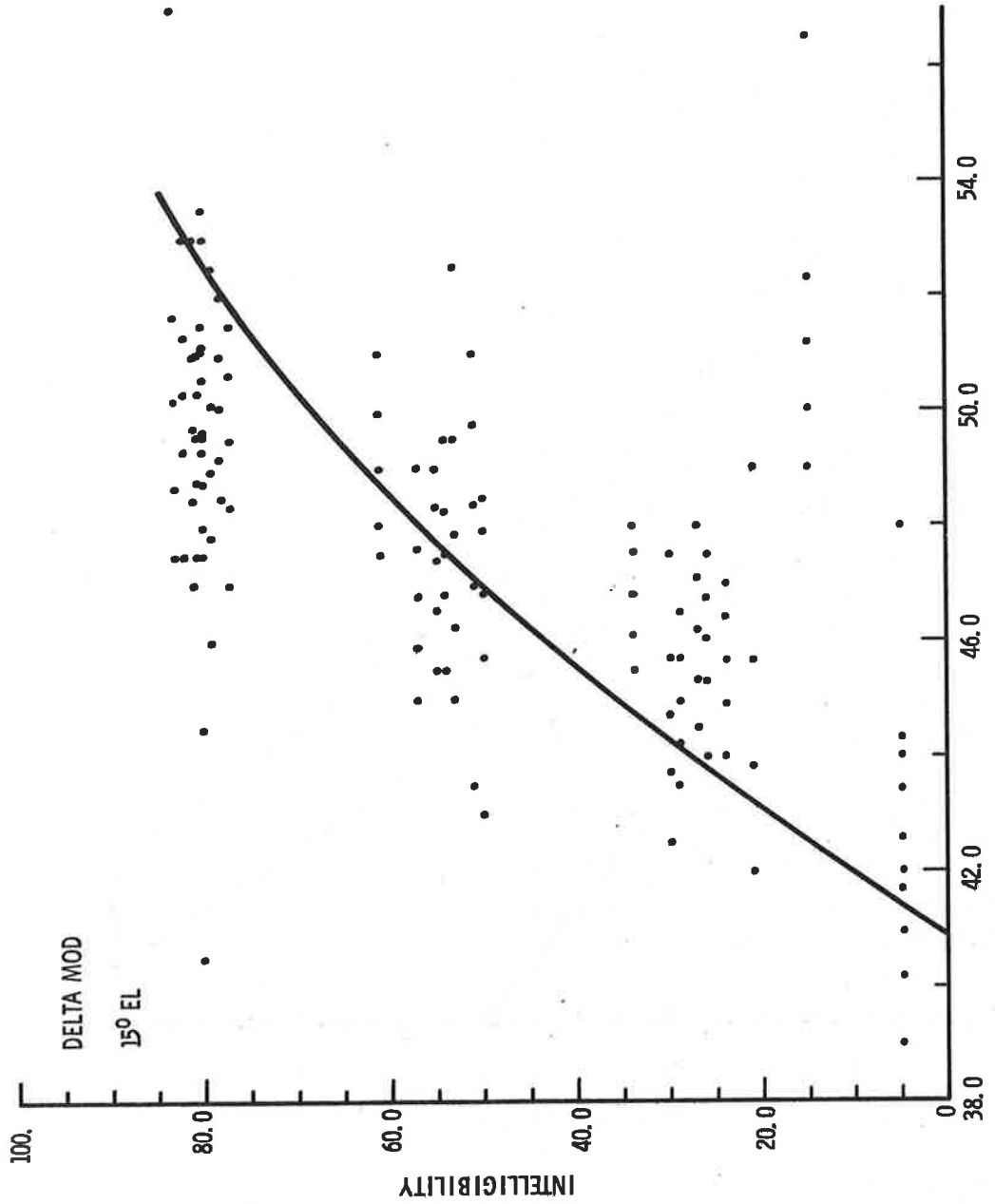

Figure 4-9. 15° Data, Delta-Mod

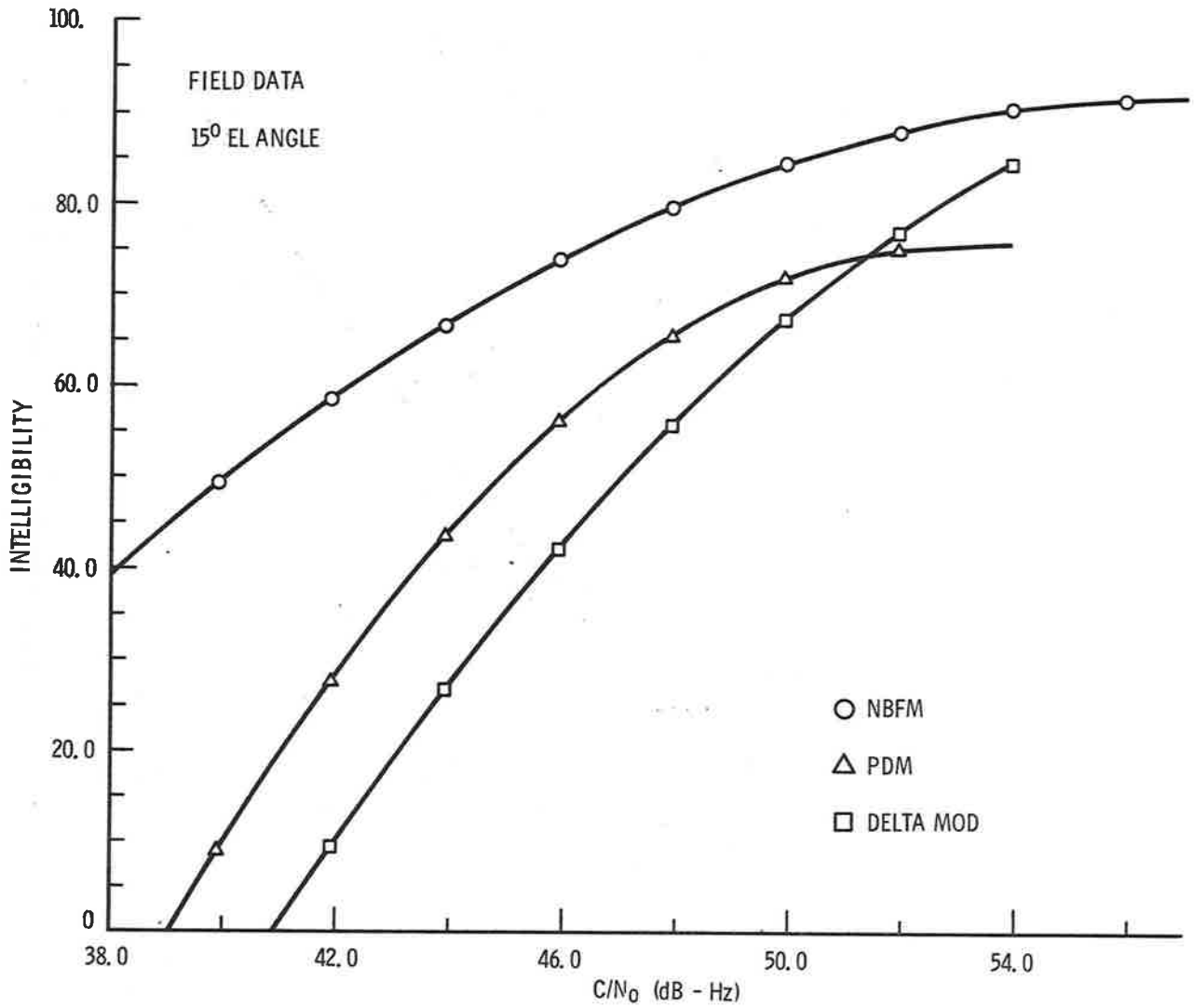

Figure 4-10. Comparison of 15° Data

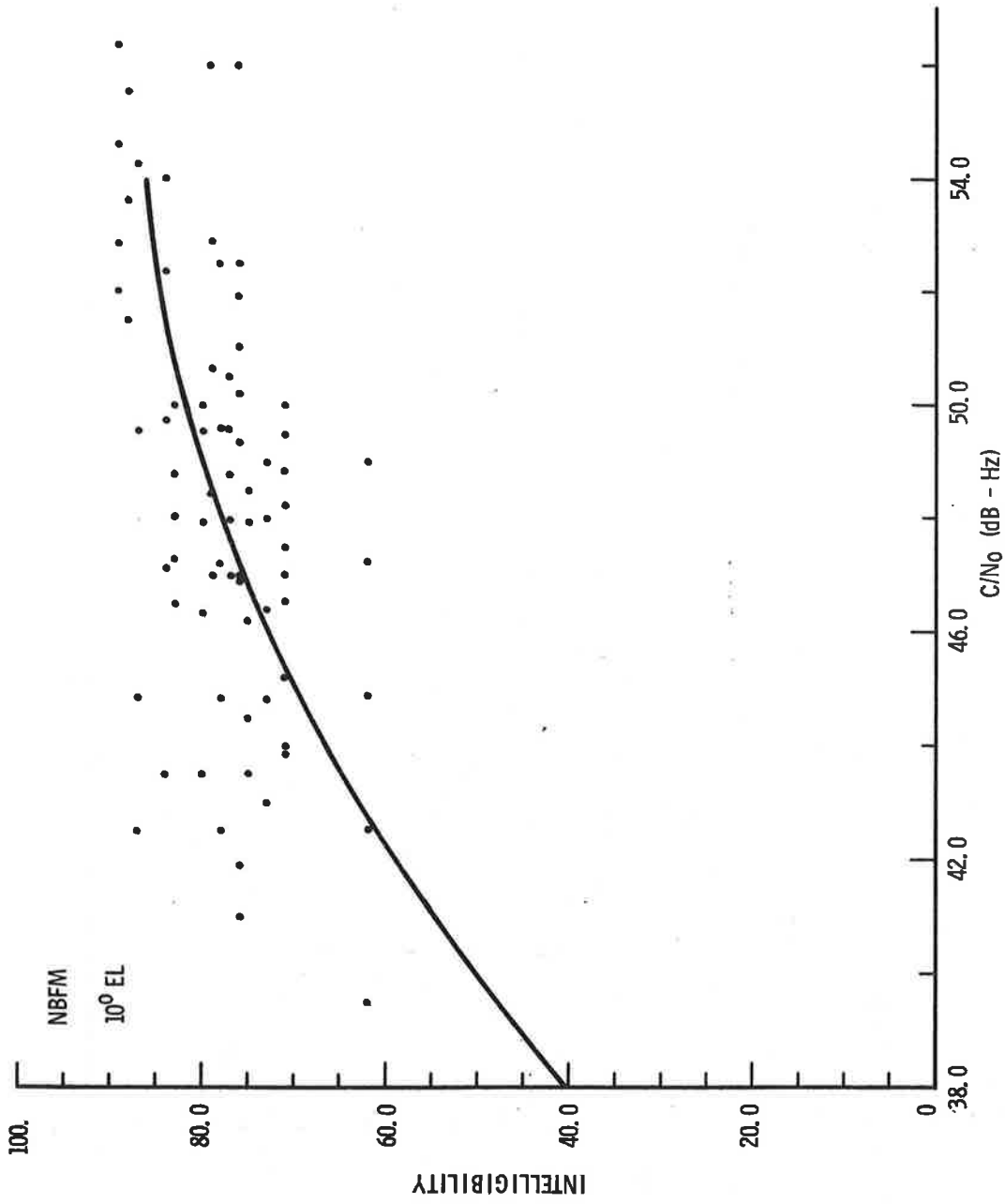

Figure 4-11. 10° Data, ANBFM

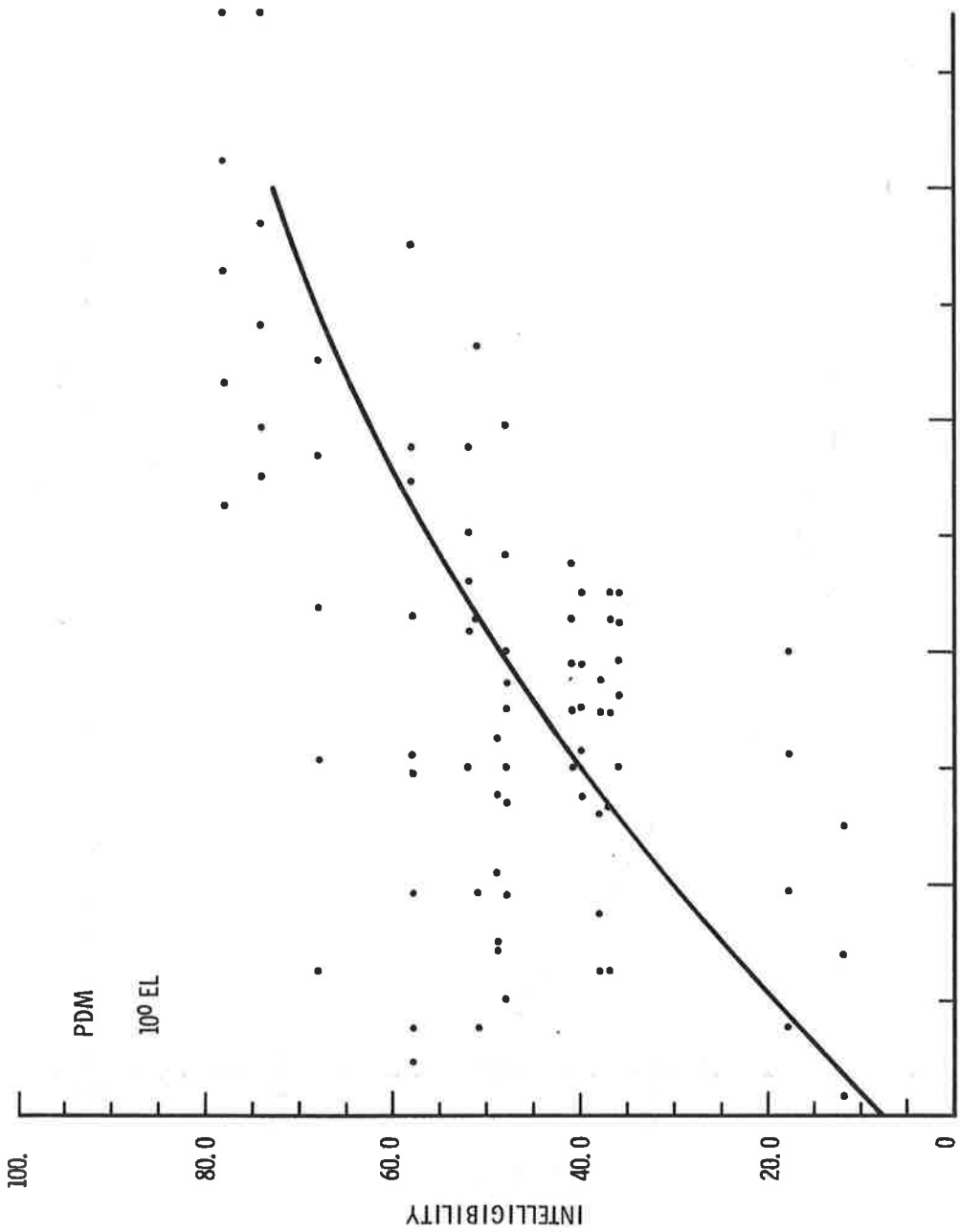

Figure 4-12. 10° Data, PDM

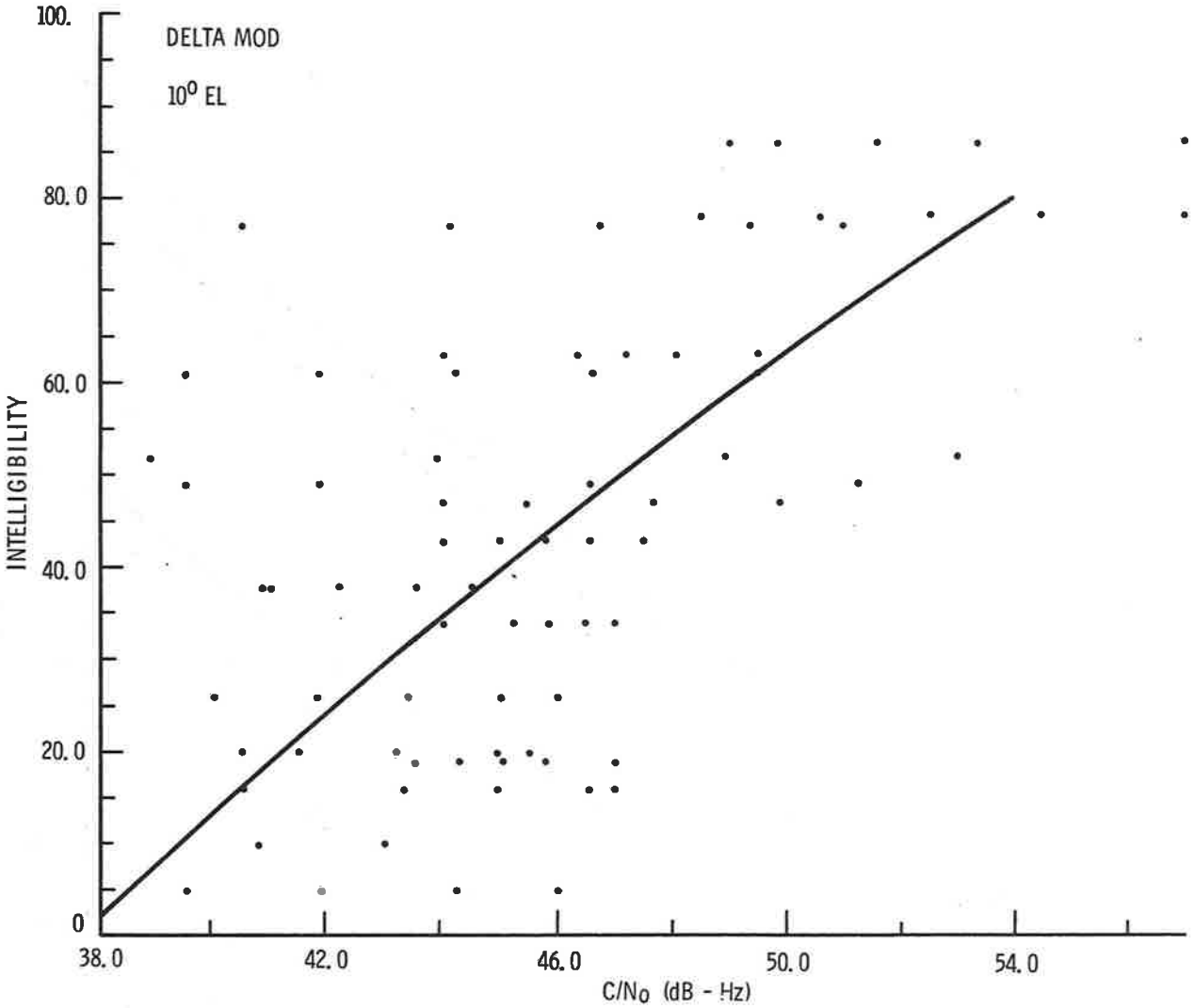

Figure 4-13. 10° Data, Delta-Mod

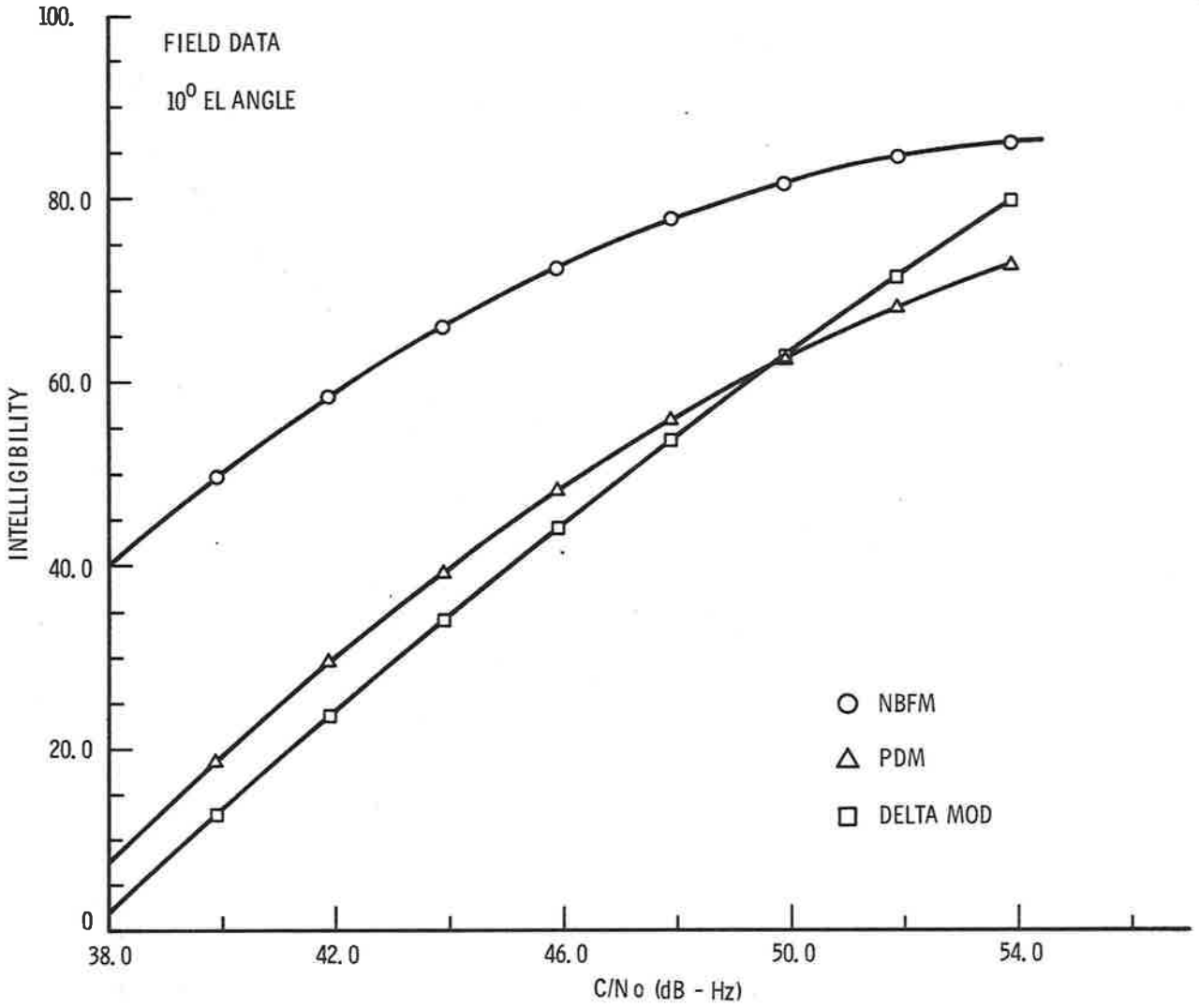

Figure 4-14. Comparison of 10° Data

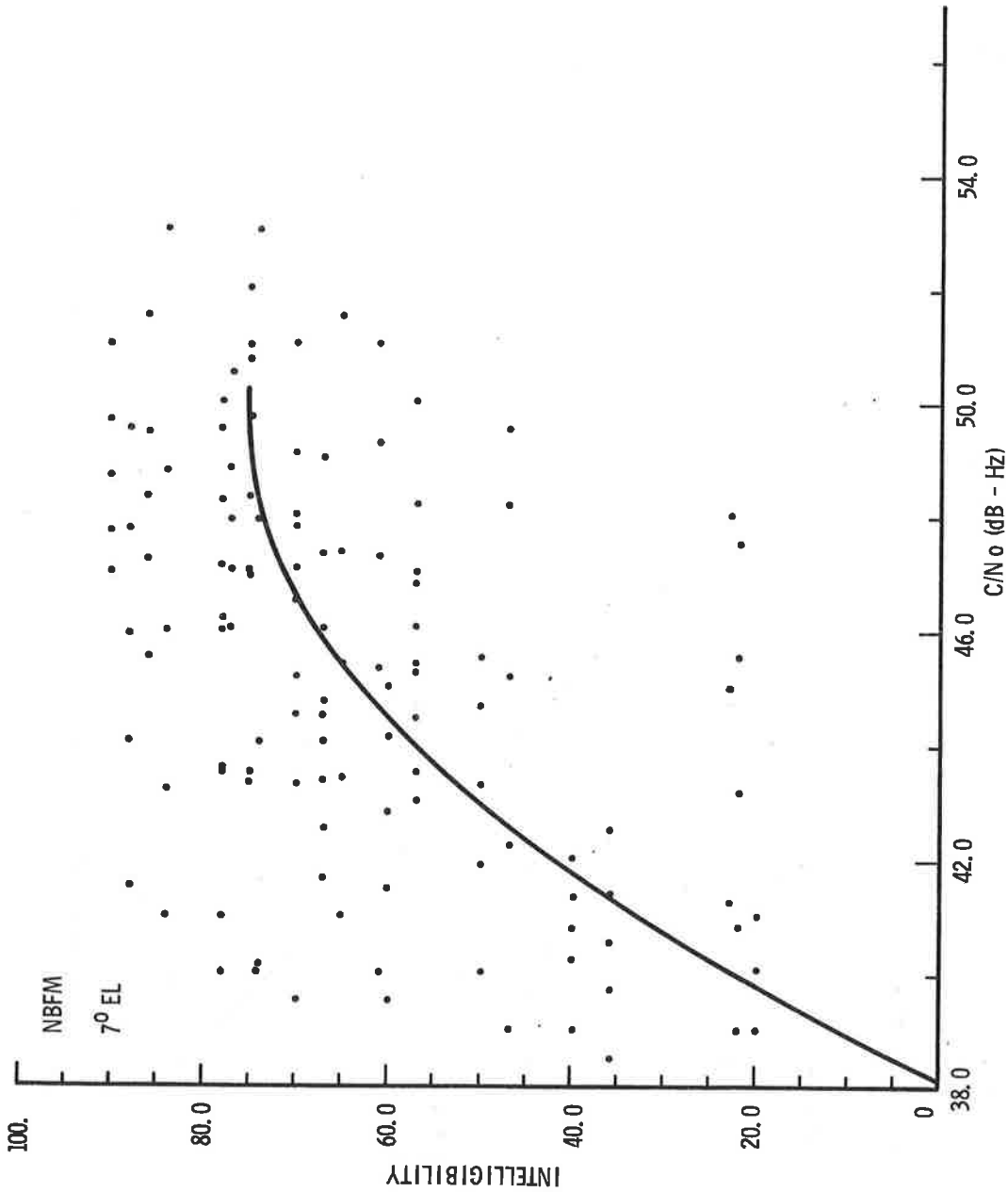

Figure 4-15. 7° Data, ANBFM

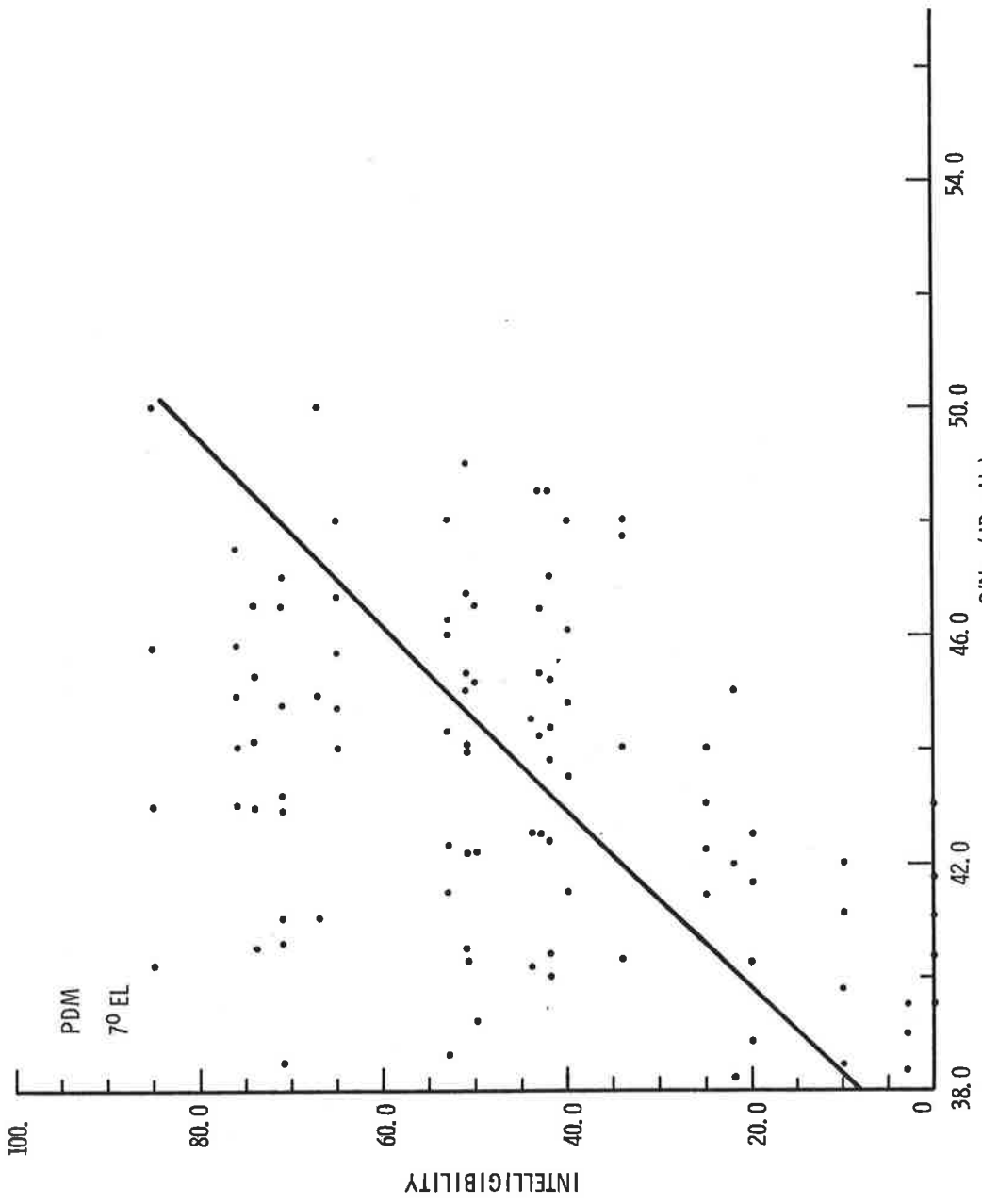

Figure 4-16. 7° Data, PDM

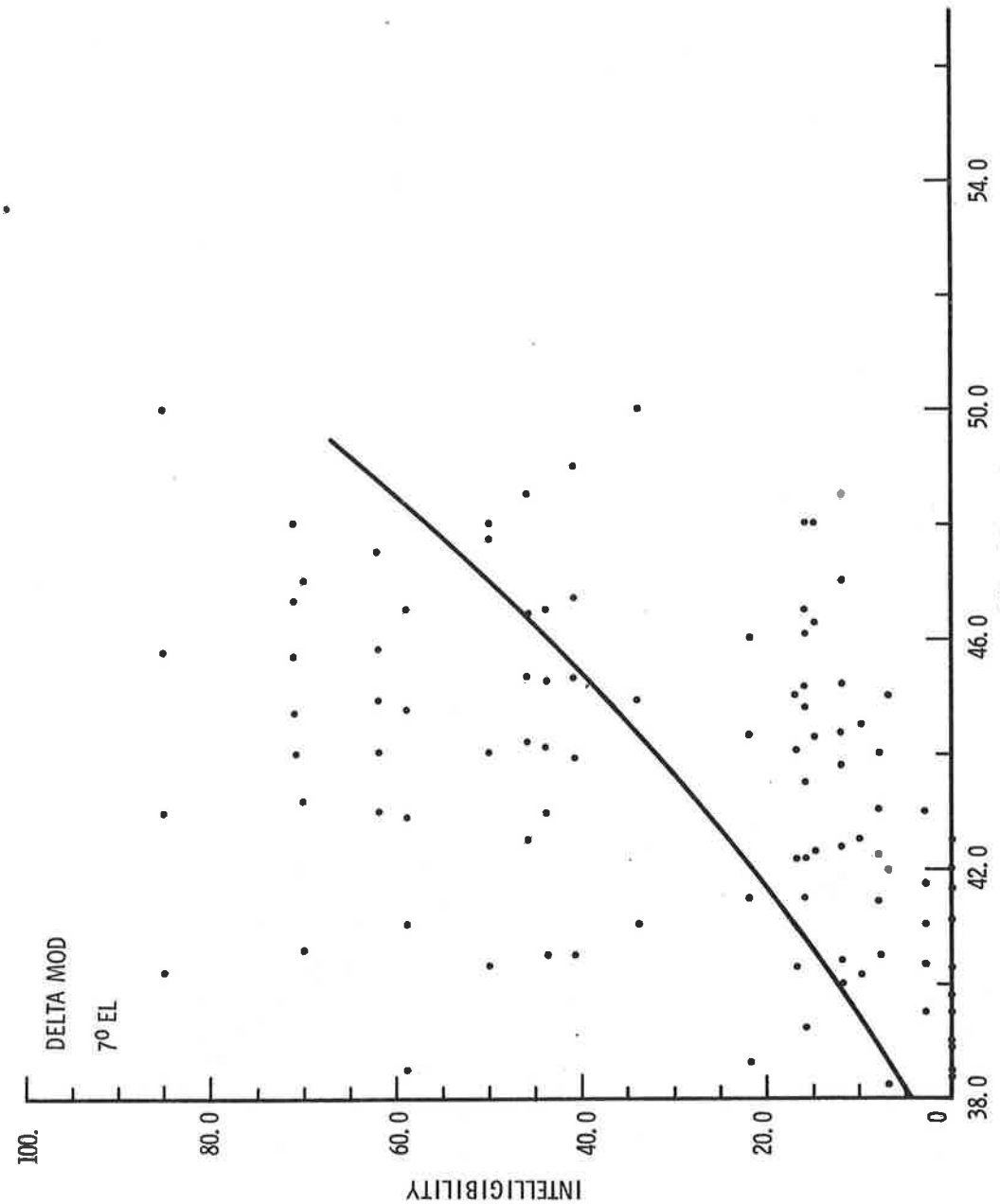

Figure 4-17. 7° Data, Delta Mod

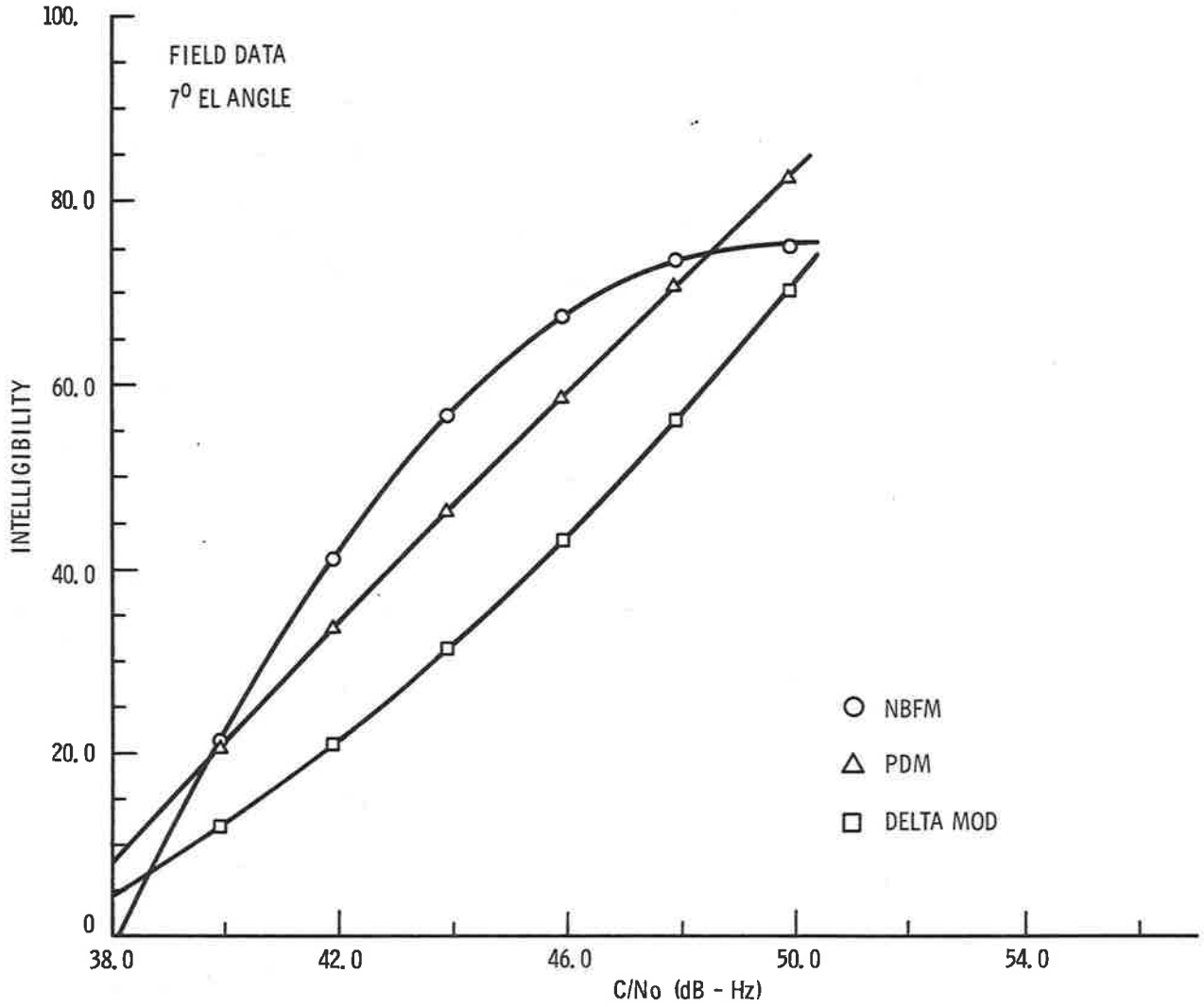

Figure 4-18. Comparison of 7° Data

TABLE 4-2. RANGE OF VALID DATA

SYSTEM	ELEVATION ANGLE	RANGE OF C/No (dB-Hz)	RMS DEVIATION (% INTELLIGIBILITY)
NBFM	15°	44 - 56	4%
	10°	42 - 56	5%
	7°	40 - 48	7%
PDM	15°	41 - 53	5%
	10°	43 - 55	7%
	7°	41 - 48	10%
DELTA MOD	15°	43 - 52	6%
	10°	42 - 49	9%
	7°	38 - 48	11%

Outside of these values either the ability of the curve to fit measured data worsened significantly or there existed little measured data; therefore, data outside of the range of C/No contained in Table 4-2 should be considered invalid. Figures 4-10, 4-14, and 4-18 compare the performance of the three systems for 15, 10, and 7° elevation angles respectively. The main conclusion from these curves is that the NBFM modem consistently exceeded the performance of the Delta Mod and PDM modems. Since Delta Mod and PDM both operated at 3 dB less carrier-to-noise density, more test time was available at lower C/No conditions than the PDM or Delta Mod. Thus, there was more high intelligibility data for the NBFM system than the other two systems. As a result, direct comparison of these curves on a one-to-one basis must be carefully done; the information of Table 4-2 must also be considered when comparing these curves. While keeping these considerations in mind, it appears that the same rank ordering of modems (NBFM, PDM, Delta Mod) as observed in the field intelligibility measurements were observed in the laboratory intelligibility tests.

Since the independent parameter of interest in all intelligibility tests is the Articulation Index, the data was next evaluated in terms of the C/No required to achieve A.I.'s of 0.3 and 0.19. Table 4-3 presents the required C/No to maintain an Articulation Index of 0.3 for the conditions tested. To obtain this table the field data was considered to be a limited vocabulary test of 256 words and the laboratory data to be 1000 words (see Figure 4-19). An Articulation Index of 0.3 is equivalent to 40% 100 pb word intelligibility, 80% 256 pb word intellibility and 93% sentence intelligibility.(5)

TABLE 4-3. REQUIRED C/NO FOR AI = 0.3

SYSTEM	LAB	15°	10°	7°
NBFM	42.0	48.0	49.1	no data
DELTA MOD	43.8	52.8	no data	no data
PDM	42.6	no data	no data	no data

Table 4-4 presents a comparison of system performance at an AI of 0.19 or 50% 256 pb word intelligibility.

TABLE 4-4. REQUIRED C/NO FOR AI = 0.19

SYSTEM	15°	10°	7°
NBFM	no data	no data	43.0
DELTA MOD	47.0	47.0	47.0
PDM	44.8	46.2	44.4

*The term "no data" in Tables 4-3 and 4-4 is used to indicate that the measured intelligibility never reached the levels of 80% (4-2) or 40% (4-3)

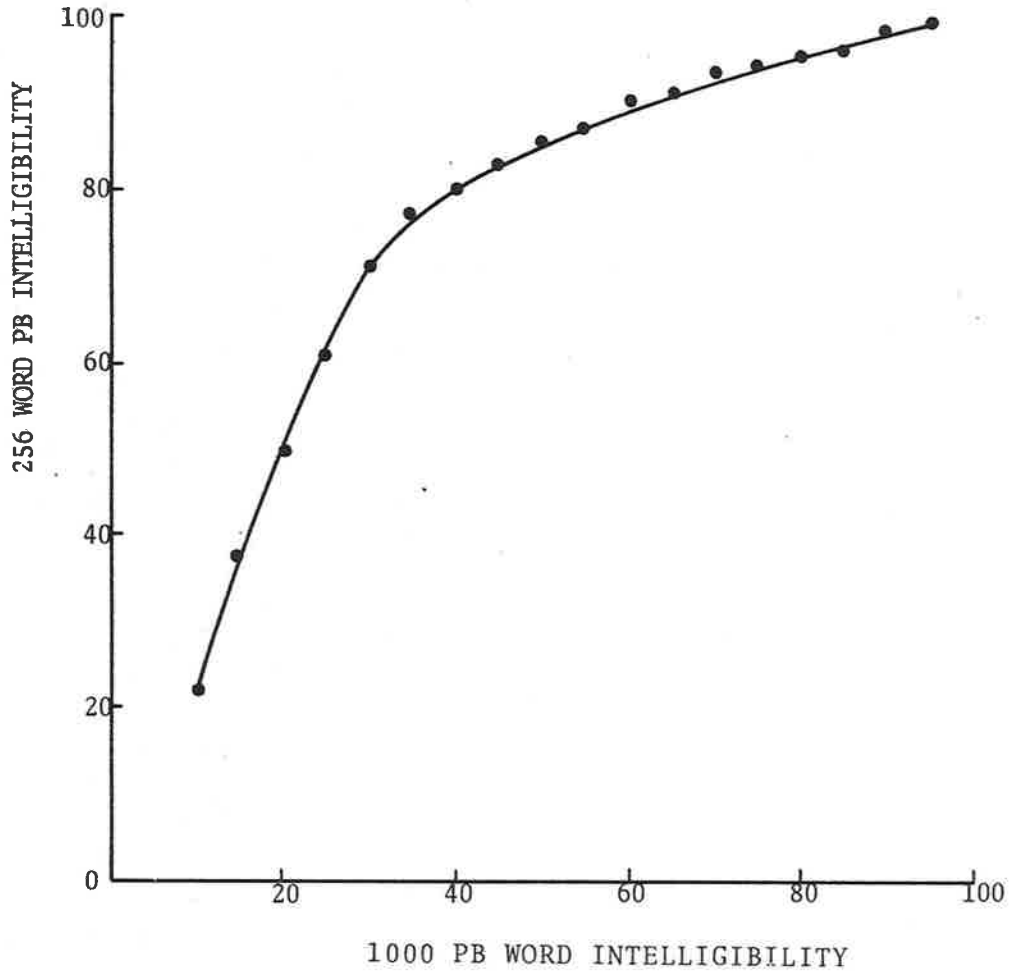

Figure 4-19. Intelligibility Comparison - 1000 Word List vs 256 Word List

It is evident from Tables 4-3 and 4-4 that the ANBFM modem requires the least power (or C/No) for a given AI.

4.2 CONCLUSIONS

From the data presented herein, the following conclusions are drawn:

a. In all tests the ANBFM modem was superior.

b. The ANBFM modem appears capable of providing a word intelligibility based on the 1000 word list, of 60% at 43 dB-Hz. This is equivalent to a sentence intelligibility of approximately 92%, and an AI of 0.42. This is very close to the desired performance of Section 2. Therefore, it is recommended that the ANBFM modem serve as a "baseline" modem for the AEROSAT program, and that modem development and test be expanded to derive data on new or improved modems.

c. During the field tests, large variations in received C/No were observed. These were frequently as large as 10 dB peak-to-peak. The standard deviation of C/No was significantly larger, as elevation angle decreased. An evaluation of known factors indicated that the most likely cause was multipath due either to reflections off the skin of the aircraft, or the surface of the ocean, or both.

d. The observed variations in C/No had relatively small effect on the average measured intelligibility. This was because the average intelligibility is the mean of a very large number of data points. Each point on the intelligibility curves (Figures 4-7 through 4-18) represents an average of several hundred data points. Looking at Figures 3-6, 3-7, and 3-8, one can see that the primary effect of the large C/No variations is to increase the standard deviation, without significantly affecting the mean.

e. The differences between the laboratory data and field data are primarily due to differences in the vocabulary length, insufficient data for some of the field test runs, and the effects of multipath. In order to resolve these differences, and determine in a quantitative manner the effect of multipath, large

quantities of data are necessary. Therefore, it is recommended that future test programs employ longer word lists (and uniform in length from test to test) and incorporate additional tests with simultaneous measurements of the multipath level, at different sea states and attitude angles.

4.3 DIGITAL DATA MODEM RESULTS

The field experiment time devoted to the two digital data modems was severely limited. Two flights had been scheduled for digital data; in the first, an extremely rapid balloon drift rate caused flight termination with a total of 37 minutes of usable data, at an elevation angle of 10°. The second flight never took place, as poor weather forced cancellation of the last balloon flight. Accordingly the field data presented herein must be viewed in the context of the following set of circumstances.

a. The data represents a total data time of 37 minutes, at an elevation angle of 10°.

b. During this time, the reflection point was over land, due to the drift of the balloon.

c. Subsequent to the experiment, the zenith antenna, which was used during the digital data test, was removed and examined. At this time it was discovered that a seal had failed, so that the antenna cavity was filled with water. It is unknown what effect this had on the antenna pattern; consequently, it is not possible to draw any conclusions regarding multipath or other propagation effects, or any recommendations based on relative performance. This antenna was not used for any voice tests.

With those three points in mind, the measured performance of the Magnavox data modem is presented in Figure 4-20, and that of the Bell modem in Figure 4-21. The performance of both modems, in the laboratory and in the field, is summarized in Table 4-5. In all cases, a theoretical value is included for comparison.

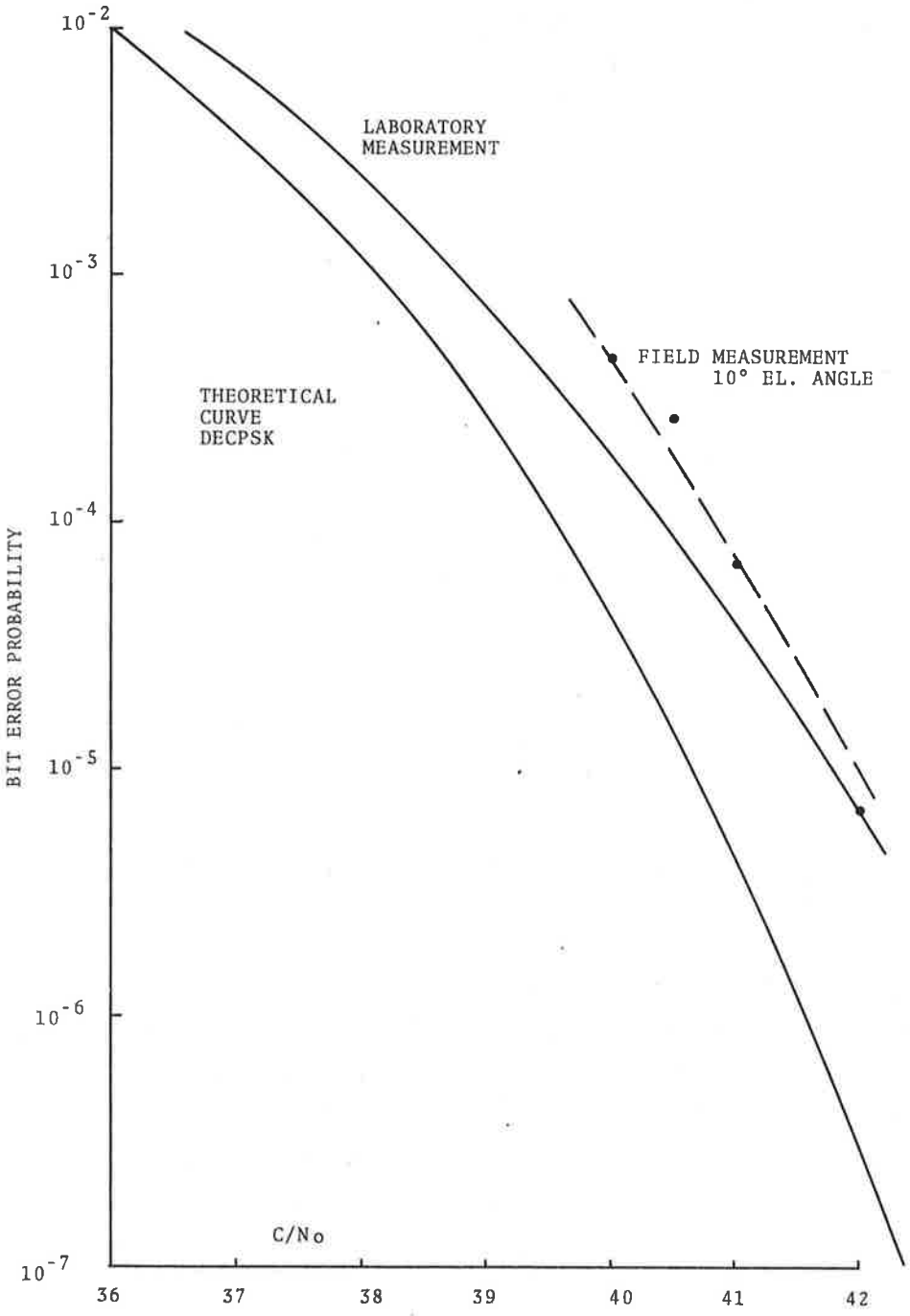

Figure 4-20. Magnavox Data Modem - Bit Error Rate vs C/No

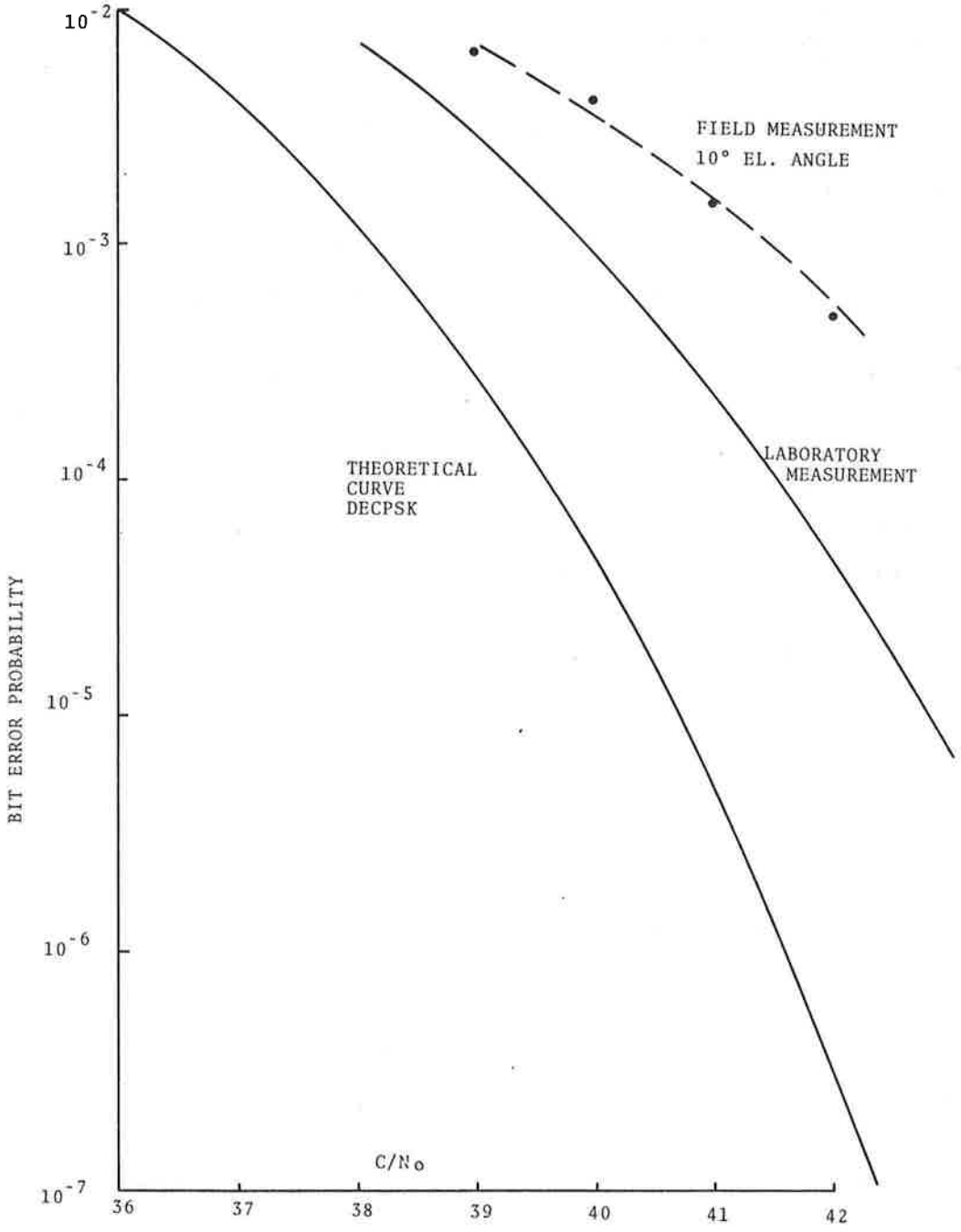

Figure 4-21. Bell Aerospace Data Modem - Bit Error Rate vs C/No

TABLE 4-5. BIT-ERROR RATE VS C/NO (dB-Hz)

BER	THEORETICAL C/NO (1200 b/s)	MAGNAVOX LAB	BELL LAB	MAGNAVOX FIELD	BELL FIELD
1×10^{-3}	38.1	38.8	39.9	No Data	41.4
1×10^{-4}	39.6	40.4	41.5	40.8	No Data
1×10^{-5}	40.7	41.8	42.8	42.0	No Data

It is apparent that the Magnavox modem, in a laboratory environment, performs with a degradation from theoretical of 0.7 to 1.1 dB, and that the Bell Modem performance is poorer (than Magnavox) by 1 dB. While no absolute statements can be made concerning the field data, it is apparent from the curves that the Magnavox modem performed reasonably close to its laboratory performance, particularly at higher C/No. The Bell modem however, exhibited a further deterioration of 1 to 1.5 dB. More field and laboratory data is needed to formulate a recommendation between these two modems.

APPENDIX A
MODEM DATA REDUCTION AND ANALYSIS

In order to facilitate an understanding of the results obtained by this experiment, this section includes a general discussion of intelligibility measurement techniques available and their features. Also discussed in this section are the preparation and form of the tests actually conducted, and the methods used to smooth the data and obtain the final curves of intelligibility as a function of carrier-to-noise ratio.

A.1 TSC VOICE TEST PROGRAM

The following is a discussion of the basic requirements and techniques for the measurement of voice modem performance.

The efficient transmission of voice signals has been the subject of intensive research for many years. The difficulties which have beset all investigations are traceable primarily to the non-deterministic nature of speech. Human speech consists of a highly variable combination of noise like signals, together with a fundamental (the "pitch") and its harmonics. This non-deterministic signal structure is also responsible for the difficulties which are encountered when attempting a quantitative, objective evaluation of the communicability of a voice modem.

There are three general categories into which nearly all voice evaluation techniques can be classified - intelligibility measurement, preference testing, and Articulation Index measurement. These are discussed below. (Also see References 6, 7, and 8.)

1. Intelligibility Measurement

The measurement of voice intelligibility provides the truest, and least misinterpreted measure of voice communicability. This is so because such measurement classically requires the transmission of actual words or voice sounds, pronounced by a human speaker. These measurements are then listened to by human listeners, and

their results appear as a percent of words correctly understood. Because this is an expression of actual intelligibility, all other methods of voice modem evaluation are eventually evaluated in terms of their relationship to some type of intelligibility measurement.

2. Preference Testing

There is an extensive literature on the subject of preference testing. Speech quality measurements, of the type known as preference measurements, are measurements of the "preferability" of a system in terms of its "appeal" to a human listener. In other words, how well does the listener "like" a particular modem, viewed as an information source.

Preference testing is fraught with many complex problems. There appears to be no general agreement on an approach which best represents the problem or its solution. In general, most evaluation procedures eventually attempt a relation to actual intelligibility measurement, as a primary parameter. Because of these reasons, preference testing was discarded as an evaluating tool for this program.

3. Articulation Index Measurement

The concept of automated Articulation Index testing grew out of the work of French and Steinberg (reference 6), published in 1947. In this classic paper, the authors demonstrated that a voice signal could be divided into 20 frequency bands, each of which independently contributed five percent to the intelligibility of the original signal. Consequently, if one were to measure the signal-to-noise ratio in each band, and combine the measurements appropriately, the result would be an electrical measurement which is directly related to intelligibility. Such an approach is very attractive since such measurements are, in principle, much easier to make than actual intelligibility measurements. Consequently, a number of techniques for making such measurements have been proposed, and at least three are available as hardware today.

Because Articulation Index measurements rely on a specific relationship between frequency, signal-noise ratio and

intelligibility, any processing of the voice signal which alters this relationship will cause erroneous results. Specifically, altering the spectrum or the ratio of peak-to-average power of the speech signal will alter the relationship of Articulation Index to intelligibility. Since most voice modems attempt to improve the efficiency of voice transmission by low pass filtering and peak clipping, the Articulation Index measurement must be recalibrated for each such modem, in order to reestablish the relationship to measured intelligibility. In addition, the effect of multiplicative disturbances have not, in general, been evaluated; this is, in fact, a very difficult task.

It is for these reasons that intelligibility measurements were chosen by TSC for the evaluation of experimental modems. A large number of different tests are available for intelligibility testing; they can be divided into three categories as follows:

NONSENSE SYLLABLES	WORD TESTS	REDUNDANT TESTS
Consonant Recognition Test	Harvard PB word list	Sentence Tests
Nonsense Syllable Test	Modified Rhyme Test Fairbanks Rhyme Test Diagnostic Rhyme Test	Message Tests

Although a number of other tests are available, they can be considered as variations of the ones listed.

The criteria used for evaluation of test performed were:

1. Sensitivity - ability to discern changes due to small variations in signal-noise ratio.
2. Discrimination - the ability to discern statistically small differences in modem performance.
3. Immunity to learning - In a test involving much repetition, memorization of the test material by the listeners can result in erroneous data. Each of the testing techniques listed was evaluated; it is beyond the scope of this

document to describe the details, advantages and disadvantages of each technique. However, two techniques were clearly superior in terms of all three criteria. They were the Consonant Recognition Test (CRT), and the Harvard 1000 Phonetically Balanced Word Test (PB Test).

CRT is a very sophisticated, computerized testing technique. Its primary disadvantage lies in the fact that the expertise necessary to conduct and evaluate the test exists at only one facility - Fort Monmouth, New Jersey. The PB test, on the other hand, is widely used (we have used the services of three different test facilities, with equivalent results). The PB test is equal or superior in performance to all other word tests. In addition, it is widely accepted as a standard test, as it is the basis for the American National Standards Institute (ANSI) "Method for Measurement of Monosyllabic Work Intelligibility" (Reference 7). For these reasons, this test has been chosen at TSC to be used for all evaluation of experimental voice modems.

A final word should be mentioned concerning sentence and message testing. These tests contain a high degree of redundancy; as a result, they provide relatively little sensitivity of discrimination. Typically, the measured intelligibility of sentences will remain above 90% until very near system threshold, at which point it will abruptly decrease to 10% or less with a signal level change of only three dB. If one has an operational system to demonstrate, this type of test is ideal. If, however, one is attempting to experimentally evaluate a variety of modems over a wide range of conditions, sentence or message tests are worthless, as there will be little or no measurable change over most of the test conditions.

A.1.1 Voice Tape Processing

Two distinct and independent scorings were performed on the voice tapes obtained in the flight tests. These scorings were performed at separate facilities and under different conditions. Following the return from France, a program was begun to obtain immediate scorings of the voice tapes to determine an initial rank

ordering of the three voice systems. This first evaluation was performed at Regis College. The scoring was obtained using tapes which were direct transcriptions of the master tapes reocrded during the experiment. These tapes had a minimum 1.5 second spacing between words. The scoring was accomplished by the individuals hand writing the words heard on these tapes. Because these scores were obtained with tapes with such short pauses between words, and because the training and scramblings of word order were minimal, the results obtained were used only for an initial rank ordering of the system. No laboratory tapes were available for scoring at that time. For the above reasons and to obtain an evaluation of the modem performance in the laboratory, a second program of intelligibility measurements was begun. For this evaluation, the chosen facility was the Electromagnetic Environmental Test Facility (EMETF) of the U.S. Army Electronic Proving Ground, Fort Huachuca, Arizona. The EMETF is a contractor-operated facility located in Tuscon, Arizona. This facility and the personnel operating it have been involved in performing intelligibility tests for the Army and other government agencys (NASA, Houston) for over seven years. They have a long record of reliability and repeatability in the scoring of voice tapes.

The tapes to be scored were re-recorded on 1/4" magnetic tape. A total of five speakers produced the laboratory and field master tapes. Four speakers were used for laboratory evaluation and one speaker was used for field evaluation. The start of a word group was signified by the statement "Would you please record the word," and was followed by the 50 PB words. There were no other carrier sentences with the words. Each speaker recorded the entire list of 1000 PB words, each with different word orders. When the testing was conducted, a minimum three-day spacing was used before a word group was repeated to prevent any listener memorization. The material for a testing session was also scrambled between laboratory and field conditions and C/No presented. Thus during a typical testing session, a variety of conditions was always scored. A total of approximately 750 word-groups were scored using the three systems and varying conditions.

A total of 24 listeners were used in scoring the voice tapes. These 24 persons were equally divided between male and female. They were broken into three juries of eight each. These crews were used only for scoring TSC material. The listeners were University of Arizona students. They were all given audio examinations to guarantee they met the hearing requirements. If any listener was absent for a prolonged time or too frequently, they were dropped and replacements were recruited and trained. Listeners were not used more than 16-18 weeks. Each listener received approximately 20 hours of standard training and eight hours of specialized training.

In addition to the standardized training period, a second specialized training was given each listener crew. This specialized training consisted of tapes recorded at TSC. This training included listening and scoring tapes recorded with all speakers under totally clear conditions and tapes recorded using all three voice systems at 56 dB-Hz, 48 dB-Hz and 44 dB-Hz. Their training started them with a clear channel and moved progressively to the noisy channel. One day was spend with each modem and one day with a combination of all three modems. This training program thus accomplished the basic requirements for listener training as stated in the American National Standard; that is, stability of results over successive tests, familiarity with the word lists and the scoring technique, and exposure to material recorded with typical test conditions.

A.1.2 Interpretation of Intelligibility Scores

The intelligibility scoring of the laboratory and field test material at the EETF was in the form of percentage of words correct per fifty-word group per listener and per crew. Each word group had been recorded over a particular communications channel, with one of the three modems under evaluation. These channels represented either laboratory conditions of varying carrier-to-noise power density ratios or field conditions of varying elevation angles, sea states and carrier-to-noise power densities. The

intelligibility scores were then grouped according to test conditions (i.e., modem, C/No, elevation, sea state, etc.). Laboratory scores were separated by modem and C/No value. For the score obtained from field data, the separation was again in terms of modems, mean C/No observed during the recording of the particular word group and elevation angle. Precise measurements of sea state were never available; however, the information available indicated that during all test flights, sea conditions were "relatively calm." Thus, we were unable to separate the field data by sea state conditions.

Examination of the intelligibility scores from the field data showed large variations (10 dB peak-peak) in the received carrier-noise density ratio. Because of this large variation, the data was not reduced by the same technique used to evaluate the laboratory data (simple averaging). Instead, it was felt that the observed values of intelligibility should be treated as a probability factor. We will define this probability as the word score obtained for the word group associated with the particular C/No measurement of interest.

The voice data as reduced, represents a measure of percentage of words scored correctly by between 10 and 20 listeners for a group of fifty words. This percentage is herein defined as the probability of scoring a word correctly during that word group. This will then be associated with all the C/No measurements for that word group. Figure A-1 illustrates how this technique for handling the data was implemented. This technique more completely describes the data obtained and with the curve-fitting technique used removes some of the original anomalies in the data.

The process diagrammed in Figure A-1 can be described as follows. Assume an independant random variable C/No associated with a dependant random variable I. Then for each modem and the four experimental conditions (i.e., field conditions at 0°, 10°, 15° elevation angle and laboratory condition) generate a set of points of the form $(C/No_i, I_i)$, where I_i is the measured intelligibility of a particular word group and C/No_i are the values of C/No measured during the recording of that word group.

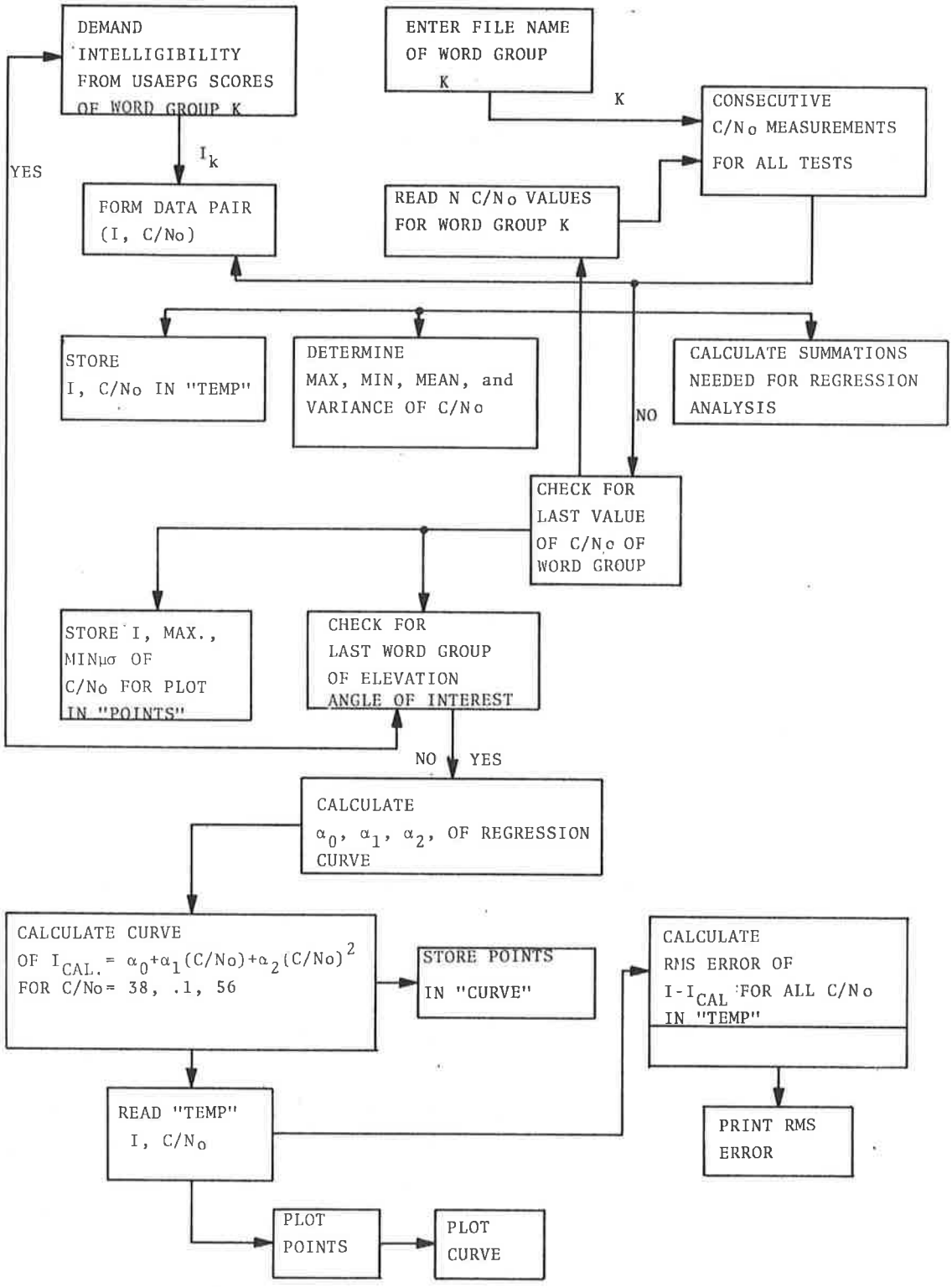

Figure A-1. Voice Data-Curve Fitting Algorithm

Next, it was necessary to choose a curve which would best fit the data. For the selection of this curve, only the laboratory data was used, as it was more "well-behaved" than the field data. Although it is expected that the performance in the field would be different than in the laboratory the nature of performance of the system as a function of C/No should not change significantly. Thus, a technique which could accurately describe the laboratory data would be a best guess for also describing the field data.

Many types of curves were fitted to the laboratory data including a linear expression, exponential expression, and polynomials to degree 10. It was found that a second-order polynomial best fit the data. This is defined by two variables called Y (= intelligibility) and X (= measured C/No), and a random sample (X, Y); then determine a set of constants α_i i = 0, 1, 2 such that

$$E(Y/X = X) = \alpha_o + \alpha_1 X + \alpha_2 X_2 \qquad (1)$$

Given a particular value of carrier to noise density, the mean intelligibility is given by the polynomial expression on the right in Equation 1. The α_i's are determined such that one minimizes the sums of the squares of the deviations of the observed Y's from the sample curve.

$$S = \sum_{i=1}^{N} Y_i - \left[\left(\alpha_o + \alpha_1 X_i + \alpha_2 X_i^2\right)\right]^2 \qquad (2)$$

That is, S is a minimum for all choices of α_i. The solution for α_i's is accomplished by setting the partial derivatives of S with respect to α_i to zero and solving for α_i. Equation 1 then is the regression curve of Y on X and is the best estimator of Y in the sense of least squares.

APPENDIX B
A COMPARISON OF SATELLITE-TO-AIRCRAFT, BALLOON-TO-AIRCRAFT AND AIRCRAFT-TO-AIRCRAFT MULTIPATH TESTS

B.1 INTRODUCTION

In order to define the suitability of a replacement experiment for a satellite-to-aircraft link an evaluation of certain multipath related parameters is necessary. Three cases are evaluated, the satellite-to-aircraft, a balloon-to-aircraft and an aircraft-to-aircraft link. The parameters considered are relative doppler between direct and indirect signals, fading bandwidth due to scattering of the multipath signal and space loss difference between the direct and indirect signals for the three cases. Also given is the rate of change of elevation angle; this is of importance in determining how long measurements can be made without a significant change in elevation angle. This is particularly important since multipath measurements are felt to be closely related to being able to maintain an elevation angle over a long interval.

The relative doppler between the direct and indirect paths is expected to be particularly significant in the VHF voice link since it will determine the fade rate and thus have an effect on the intelligibility of the received signal. Fading bandwidth determines the spectrum associated with an L-band multipath signal. Relative space loss should, for any alternate experiment, be kept to a minimum, this loss is essentially zero for a satellite-to-aircraft link. Large values for this loss will tend to minimize the effects of multipath which occur in actual space link.

B.1.1 Relative Doppler Shift

Figure B-1 defines the geometry used to determine the relative doppler shift for a satellite, balloon or aircraft-to-aircraft link. In this diagram point A is the receiving aircraft and point B either a satellite, balloon, or aircraft, R_D is the direct path length and $R_1 + R_2$ the multipath length. The relative doppler

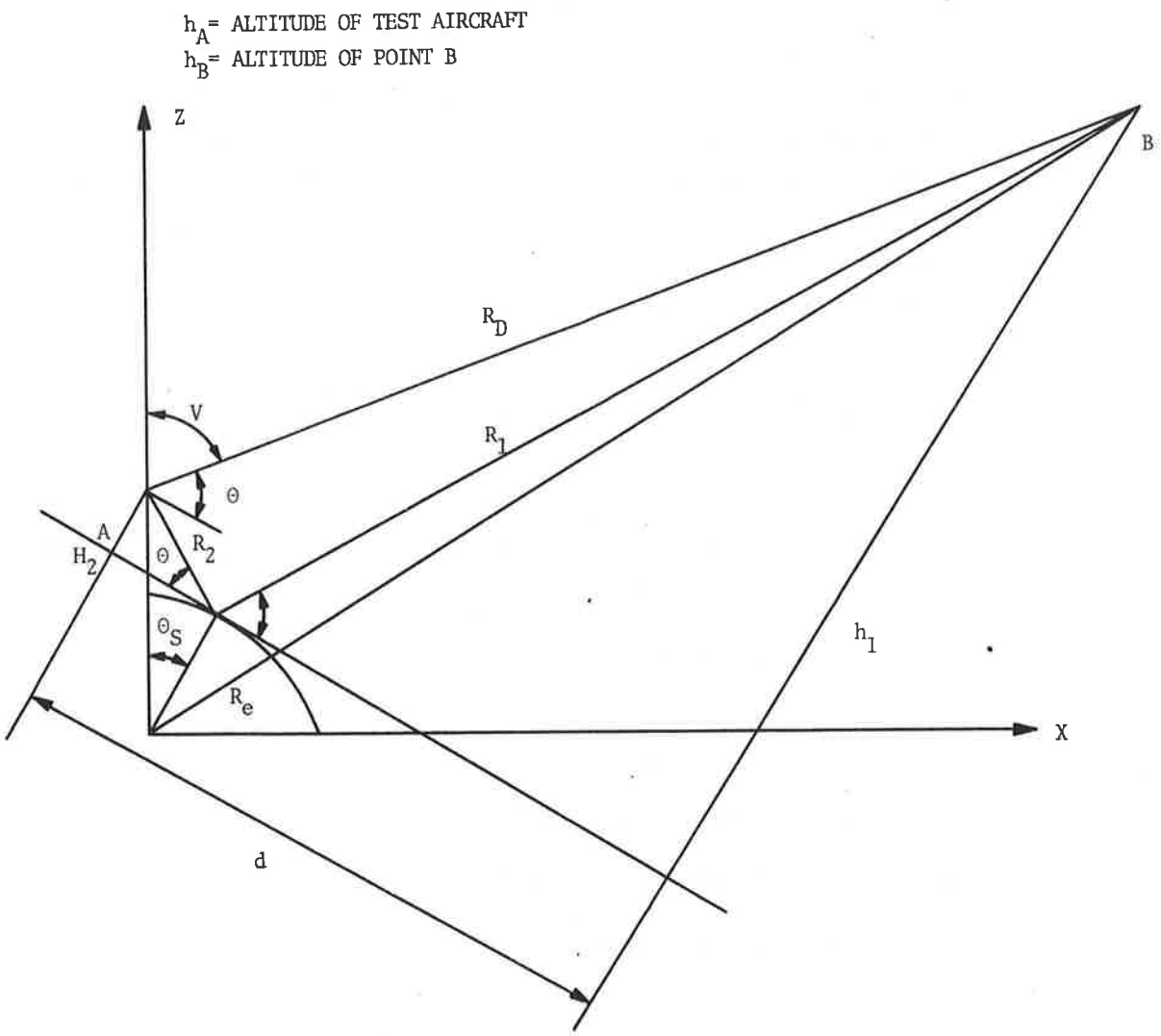

Figure B-1 Aircraft-Balloon Geometry

shift is the time rate of change of the path length difference $R_D - (R_1 + R_2)$ divided by the wavelength λ of the incident signal. Equation 1 is the path length difference obtained from Appendix E of TRW's Test Plan for Navstar Navigation System (See Section C.1).

$$R_D - R_1 + R_2 = \Delta = \frac{(K-1)h_2}{\sin\theta}\left\{\sqrt{1 + \frac{4K}{(K-1)^2}\sin^2\theta} - 1\right\} \qquad (1)$$

At this point TRW used the binomial approximation to the radical in the above expression and then took the derivative of Δ using this approximation. This approximation is valid only when the relative altitudes differ by a factor of five or more, which is not the case for aircraft/aircraft and balloon/aircraft tests. Thus we took the derivative of the exact expression of Δ and this is given in equation 2 which is valid for all cases.

$$\dot{\Delta} = \frac{\left[\dot{h}_1 - \dot{h}_2 - \left(\dot{H}\cos^2\theta - \frac{d}{2}\sin 2\theta\right)\right]\left[\sqrt{(K-1)^2 + 4Kv^2} - (K-1)\right]}{v(K-1)}$$

$$+ \frac{2(K-1)\left(\dot{h}_1 - K\dot{h}_2\right)V + 4VK\left(\dot{H}\cos^2\theta - \frac{\dot{d}}{2}\sin 2\theta\right) - 4Kv\left(\dot{h}_1 - K\dot{h}_2\right)}{\sqrt{(K-1)^2 + 4Kv^2}\,(K-1)} \qquad (2)$$

where θ = elevation angle

$K = \frac{h_1}{h_2}$

$\dot{h}_1$ = time rate of change of h_1

$\dot{h}_2$ = time rate of change of h_2

$\dot{d}$ = time rate of change of d

$\dot{H} = \dot{h}_1 - \dot{h}_2$

In equation 2 it is important to note that for low elevation angles $\dot{d}$ is not the true ground velocity but contains a component of vertical velocity equal to $v(\sin\theta_s)$, where θ_s is shown in Figure B-1. This vertical component must be considered in calculation of Δ.

From equation 2 Figures B-2, B-3, and B-4 were generated which compare the relative doppler from the specular reflecting region of the case of a transmitting satellite, balloon or aircraft operating in conjunction with a test airplane. Table B-1 summarizes these calculations for low elevation angles.

B.1.2 Fading Bandwidth

For a multipath signal reflected from the earth's surface (in particular reflected off the sea) the received multipath signal will be composed of not only a specular component but also scattered components which will not only beat with the direct signal to cause fading but also with each other. Thus the fading will occur at various rates.

Durranni (reference 7) gives the fading or scatter bandspread as $B_s \simeq \frac{1}{2\tau_o}$ where τ_o is the time at which $C(\tau)$ the time autocorrellation function is $\frac{1}{e}$ of its maximum value $C(0)$. Using this definition for B_s we find that

$$B_s \approx kv\left(\frac{\sqrt{2}\sigma}{T}\right) \frac{\left(1-H \tan^2 A\right) \cos A}{1-H \tan^2 A + 4\theta_{s/\sin 2A}} \qquad (3)$$

when the motion of the test aircraft is in the xz plane of Figure B-1 and

$$B_s \approx kv \left(\frac{\sqrt{2}\sigma}{T}\right) \frac{\sin A}{\tan B} \qquad (4)$$

when the motion of the test aircraft is perpendicular to the XZ plane.

In equations 3 and 4:

$K = \frac{2\pi}{\lambda}$, the wave number

v = velocity of the test plane

$H = h_a/R_e$

V = tangent aspect angle (defined in Figure B-1)

$A = V - \theta_s$

TABLE B-1. CALCULATIONS FOR LOW ELEVATION ANGLE

θ elevation angle	H_B	Ground Speed between A and B	Vertical motion of test craft Point A	Vertical motion of transmitter Point B	Δf in hertz transmitting at L-Band	Δf in hertz transmitting at Vhf (120 mHz)
10°	19,323 nm	400 knots	0	0	2.45	0.18
20°	"	"	"	"	2.29	0.17
30°	"	"	"	"	2.05	0.15
10°	120,000 ft	400 knots	0	0	21.99	1.64
20°	"	"	"	"	78.97	5.92
30°	"	"	"	"	124.03	9.30
10°	60,000 ft	50 knots	0	0	11.01	0.82
20°	"	"	"	"	25.47	1.90
30°	"	"	"	"	35.82	2.68
10°	19,323 nm	0	5 ft/sec	0	3.09	0.23
20°	"	"	"	"	5.82	0.43
30°	"	"	"	"	8.37	0.62
10°	120,000 ft	0	5 ft/sec	0	3.72	0.27
20°	"	"	"	"	7.15	0.53
30°	"	"	"	"	9.35	0.70
10°	60,000	0	5 ft/sec	0	5.15	0.38
20°	"	"	"	"	8.06	0.60
30°	"	"	"	"	10.97	0.82
10°	120,000 ft	0	0	5 ft/sec	0.75	0.05
20°	"	"	"	"	1.21	0.09
30°	"	"	"	"	1.31	0.09
10°	60,000	0	0	5 ft/sec	1.96	0.14
20°	"	"	"	"	2.59	0.19
30°	"	"	"	"	2.50	0.18

In the above table H_B = 19,323 nm the satellite case, 120,000 ft. for the balloon 60,000 ft. for the aircraft. The test aircraft is at 25,000 ft. Ground speed is the velocity of the approach of point A to B in Figure B-1.

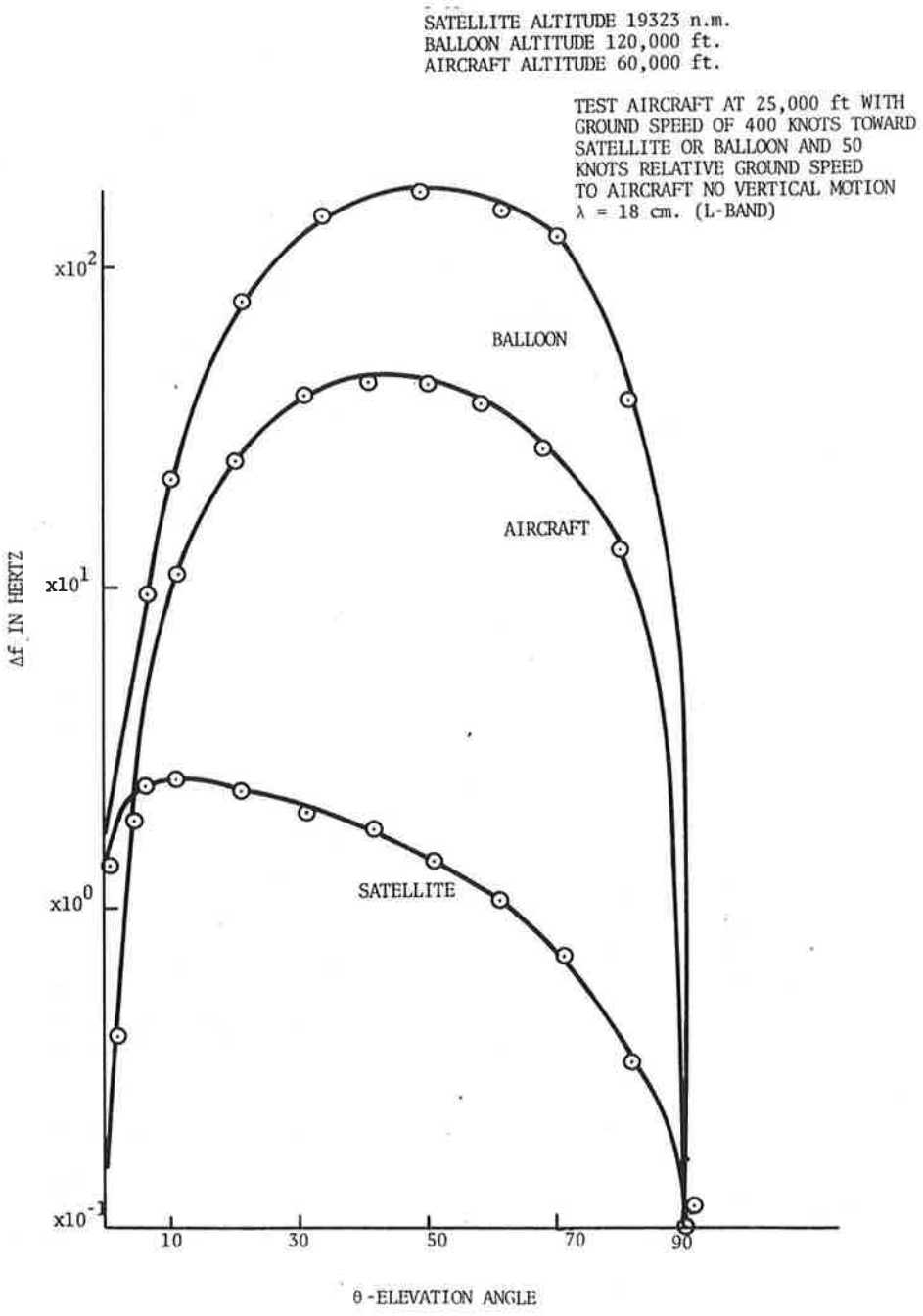

Figure B-2a. F-Relative Doppler Shift Vs. θ Elevation Angle
λ = 18 cm. (L-Band)

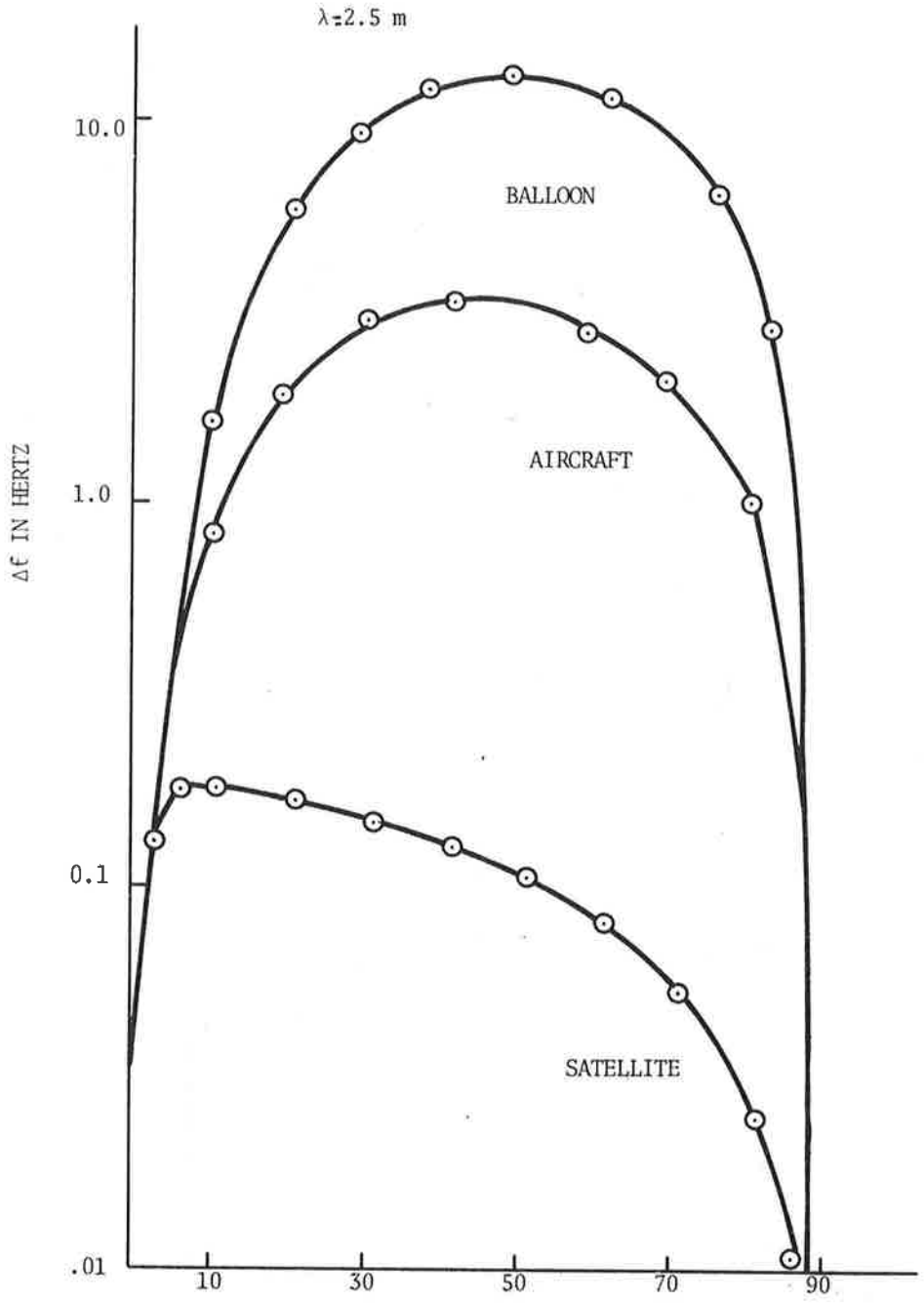

Figure B-2b. F-Relative Doppler Shift Vs. θ Elevation Angle (Same as B-2a) λ = 2.5 m (VHF)

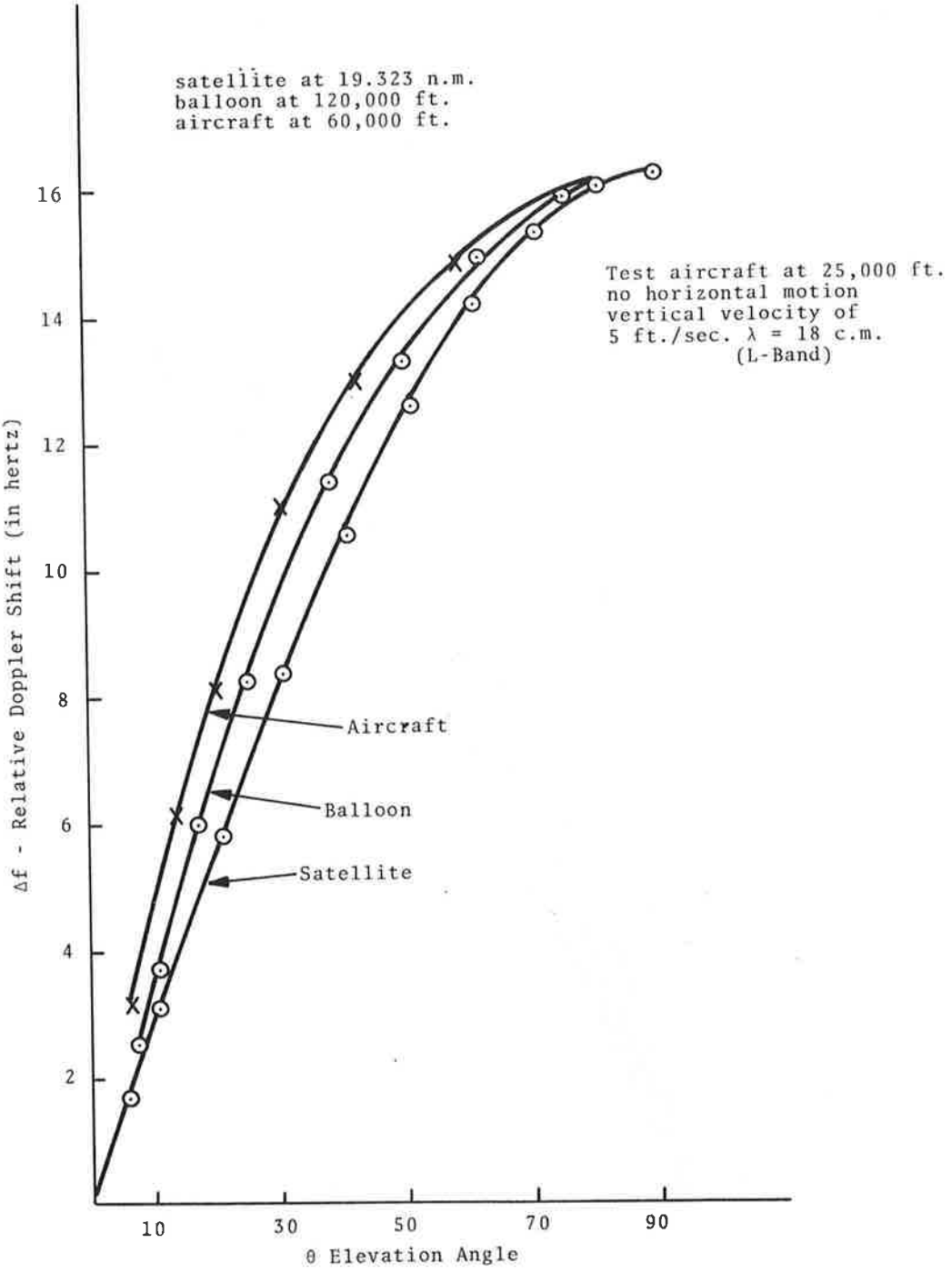

Figure B-3a. Δf Doppler Shift Vs. Elevation θ. λ = 18 cm (L-Band)

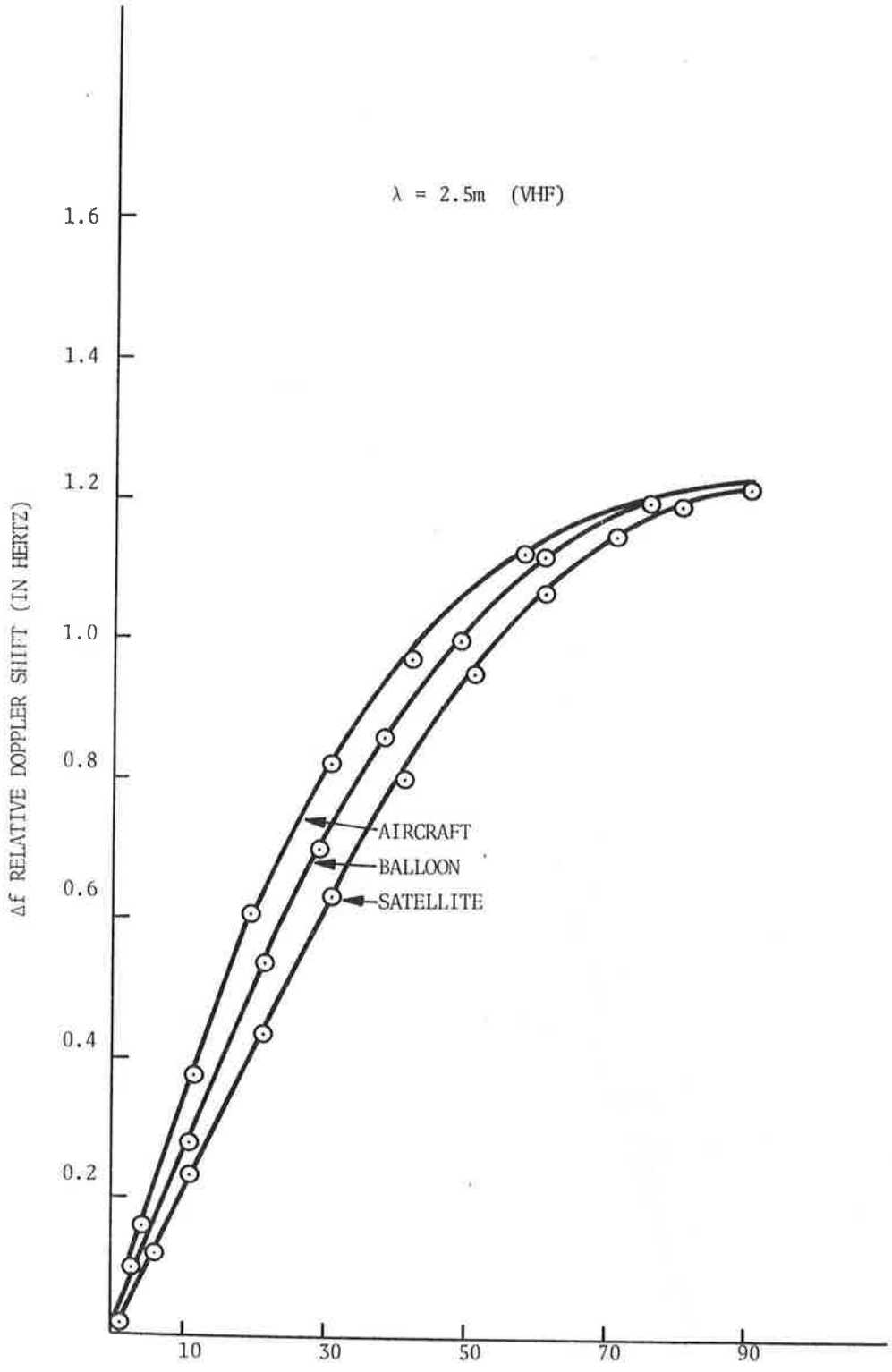

Figure B-3b. Δf Doppler Shift Vs. Elevation θ. (Same as B-3a)
λ = 2.5 m (VHF)

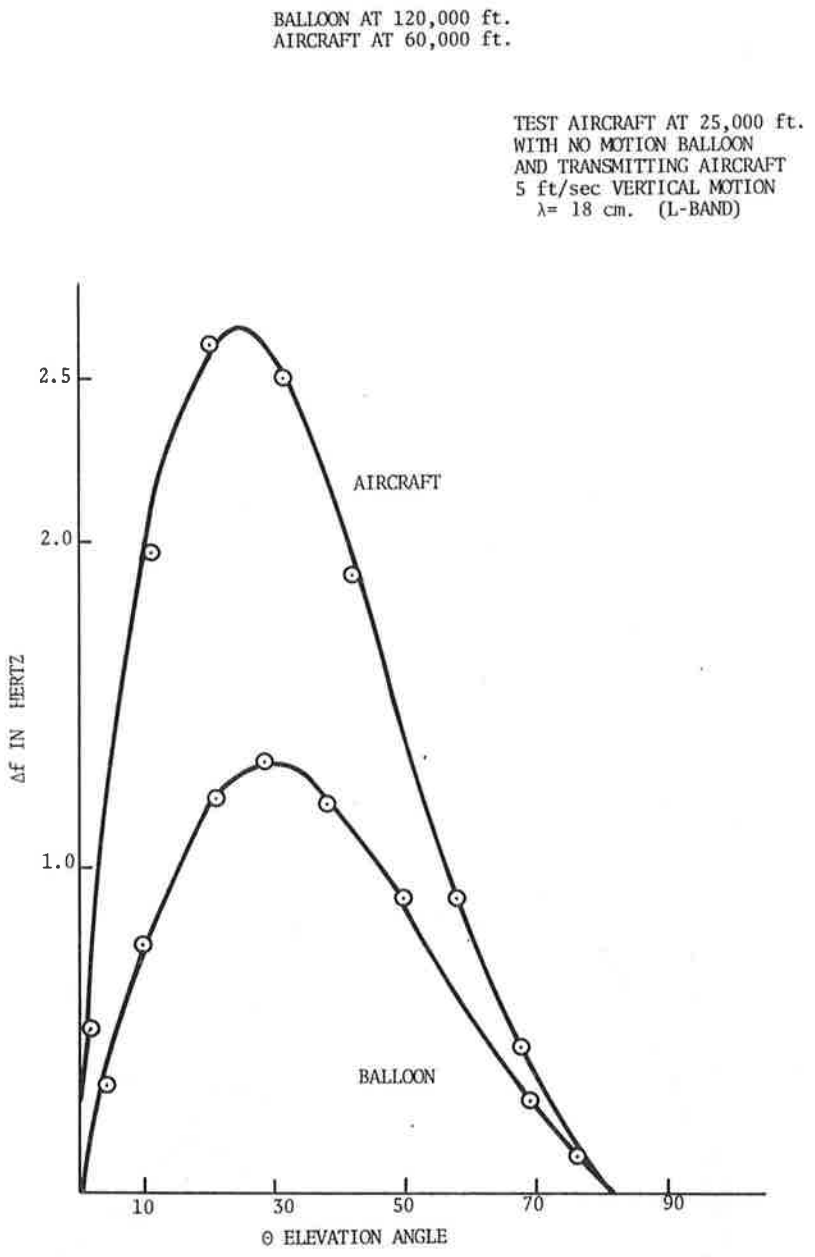

Figure B-4a. Relative Doppler Shift Vs. Elevation Angle. λ = 18 cm. (L-Band)

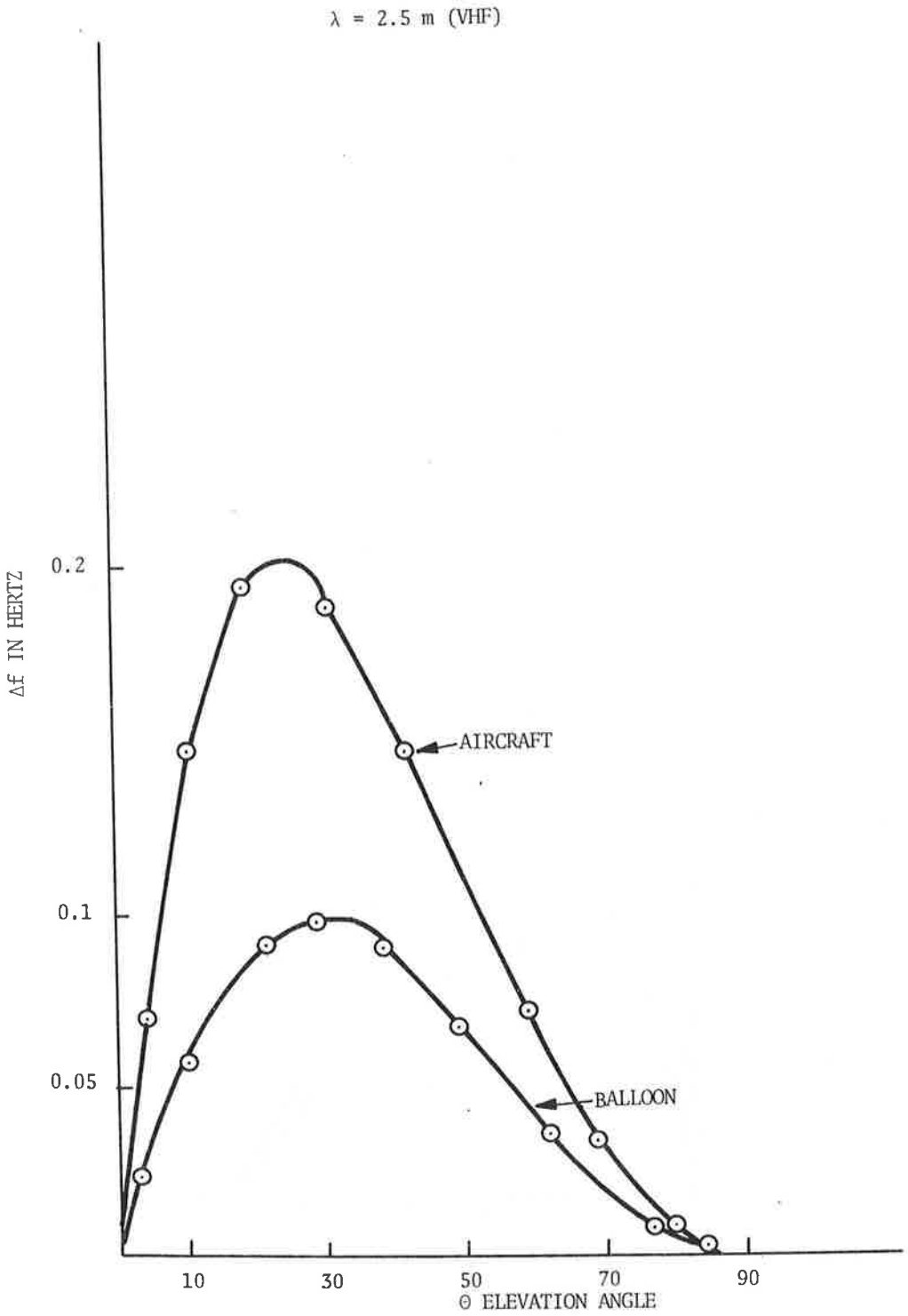

Figure B-4b. Relative Doppler Shift Vs. Elevation Angle. (Same as B-4a) λ = 2.5 m (VHF)

$B = V - 2\theta_s$

$\frac{\sqrt{2}\sigma}{T}$ = measure of the rough reflecting surface slope

σ = RMS surface irregularities height

T = surface correlating distance and corresponds to a distance between irregularities.

The Durranni and Staras Model for scatter bandwidth is based on the following assumptions:

1) The surface undulations can be described by a two dimensional Gaussian distribution

2) σ/T is fairly small

3) σ/λ is fairly large

4) The auto correlation of the surface fluctuation is an analytic function

5) The transmitting source "does not change its position in the period τ."

These conditions hold for an L-band, satellite or balloon link and sea surface conditions existing most of the time in the North Atlantic. The results of calculations made with equations 3 and 4 showed very little difference between the case of the aircraft flying at the source and perpendicular to the source (circular flight around the source). For the satellite-to-aircraft and balloon-to-aircraft cases it was found that there was no discernable difference in the bandwidth of the scattered signals. Table B-2 shows the normalized bandwidth ($NB_s = B_s/k\sqrt{2}\sigma/T$) and Table B-3 gives B_s for L-band for these two cases.

Calculations of B_s versus elevation angle are given in Figures B-5 and B-6.

B.1.3 Space Loss Difference

Space loss difference is the difference of the space loss of the direct signal to the multipath signal and is given by

TABLE B-2. NORMALIZED BANDWIDTH

θ	NB_s V=400 knots Satellite	NB_s V=400 knots Balloon
5	16.1	16.6
10	34.0	34.7
20	69.3	69.8
30	102.0	102.0
50	157.0	157.0
70	193.0	193.0
85	204.0	205.0

TABLE B-3. SCATTER BANDWIDTH FOR L-BAND ELEVATION ANGLE AND SURFACE ROUGHNESS

θ	Satellite $\frac{2\sigma}{T} = .1$	Balloon	Satellite $\frac{2\sigma}{T} = .2$	Balloon	Satellite $\frac{2\sigma}{T} = .3$	Balloon
5	38.1	39.3	76.2	78.6	114.4	117.9
10	80.7	82.3	161.4	164.6	242.2	246.9
20	164.3	165.4	328.6	330.8	492.8	496.2
30	241.8	242.8	483.8	485.6	725.6	728.4
50	372.0	372.8	744.0	745.6	1116.0	1118.4
70	456.8	457.5	913.6	915.0	1370.4	1372.5
85	484.4	485.2	968.7	970.4	1453.1	1455.6

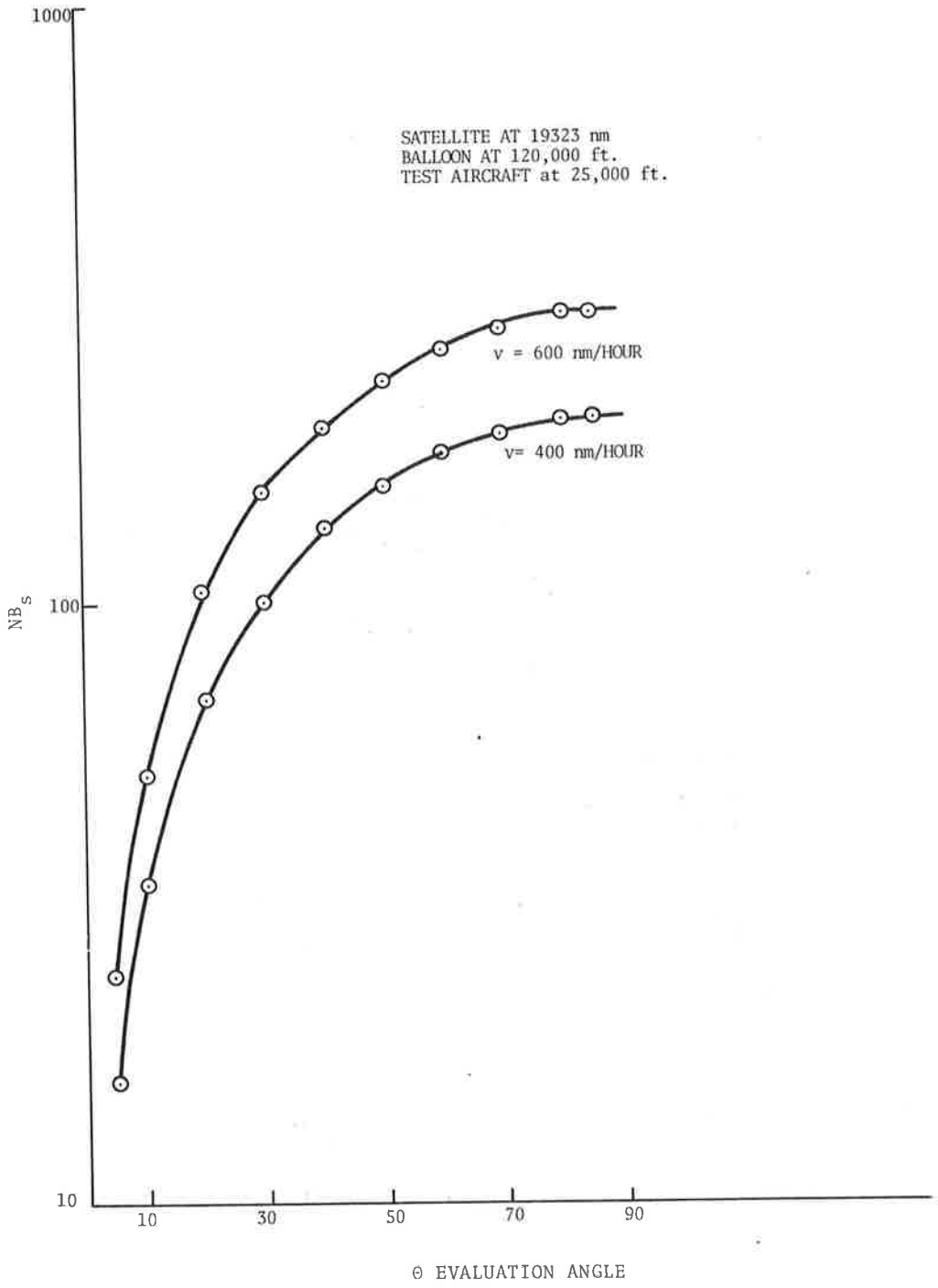

Figure B-5. Normalized Fading Bandwidth Vs. Elevation Angle

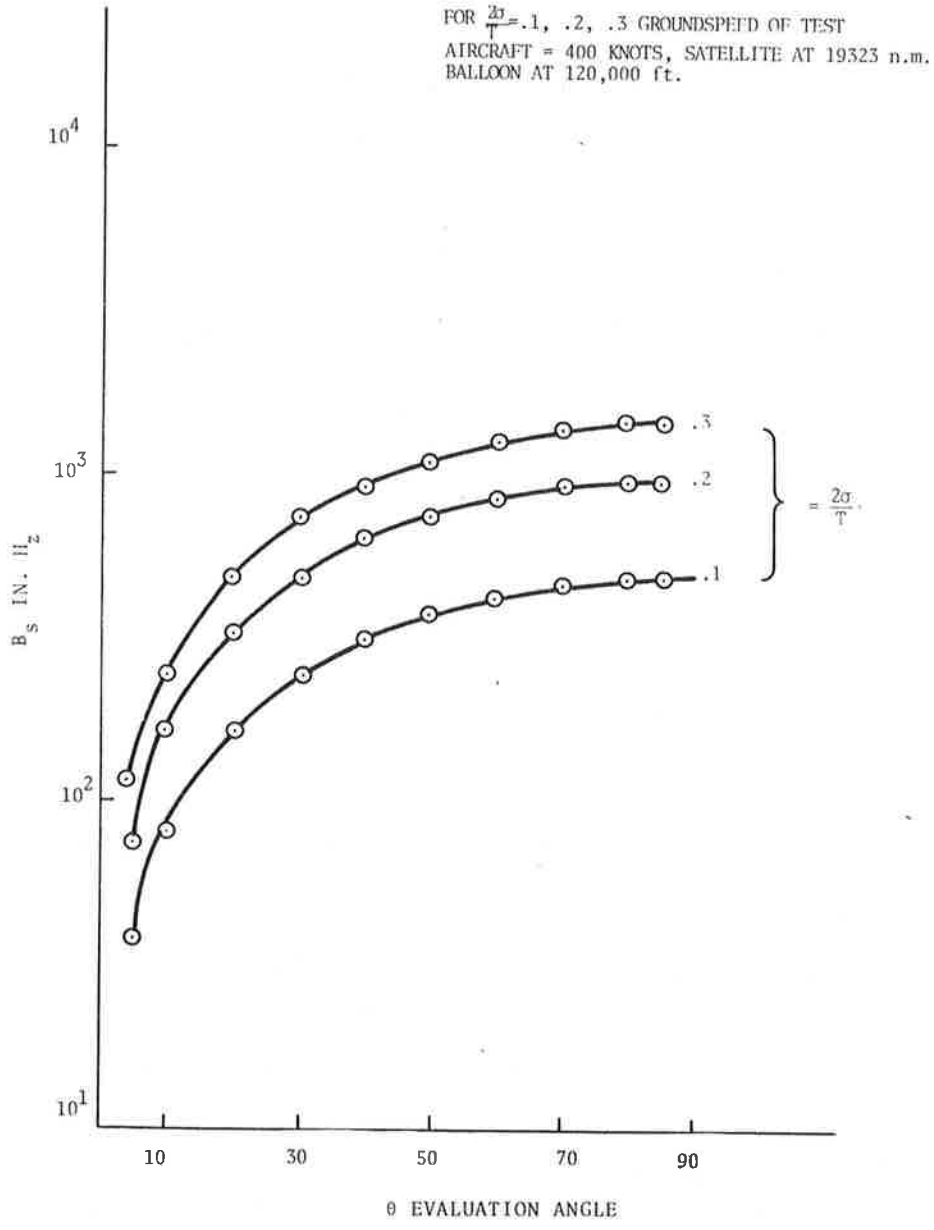

Figure B-6. B_s Fading Bandwidth Vs. Elevation Angle

$$\left(R_1 + R_2\right)^2 / R_D^2 = 1 + \frac{4K}{(K-1)^2} \sin^2 \theta$$

A plot of this space loss difference is given in db in Figure B-7.

B.1.4 Time Rate of Change of Elevation Angle - $\dot{\theta}$

It is of interest to know how long it is possible to maintain a particular elevation angle for each of the three cases being studied.

Given $\tan \theta = \frac{h_2 - h_1}{d}$

Then $\dot{\theta} = \frac{1}{2} \sin 2\theta \frac{\dot{d}}{d}$ where h_1, h_2, d are shown in Figure B-1 and $\dot{d}$ is the time derivative of d. Figure B-8 gives $\dot{\theta}$ vs θ elevation angle.

B.2 LIST OF GRAPHS FOR RELATIVE DOPPLER SHIFTS

Figure B-2: Δf - relative doppler shift vs θ, elevation angle with the following conditions: satellite at synchronous altitude.
balloon at 120,000 feet
aircraft at 60,000 feet
test plane at 25,000 feet
ground speed for the test plane of 400 knots towards the satellite or balloon, relative ground speed of 50 knots between the test plane and transmitting aircraft both flying parallel flights. No vertical motion considered.

Figure B-2a λ = 18 cm (L-Band)

Figure B-2b λ = 2.5 m (VHF)

Figure B-3: Same as conditions of Figure B-2 except ground speed is zero and the vertical velocity is 5 feet/sec at the test plane.

Figure B-4: Same as conditions of Figure B-2 except no motion considered for test plane. A vertical velocity of

5 feet/sec exists at the balloon and aircraft.

Figure B-5: Normalized fading bandwidth NB vs θ elevation angle. This normalized B_s - is $NBs = {}^{Bs}/k\sqrt{2}\cdot\frac{\sigma}{T}$ and is plotted for a test aircraft ground speed of 400 knots and 600 knots. Satellite at synchronous altitude, balloon at 120,000 feet, test aircraft at 25,000 feet.

Figure B-6: - fading bandwith vs θ elevation angle for $\frac{2\sigma}{T}$ = .1, .2, .3 and V=400 knots altitudes same as IV.

Figure B-7: Space loss difference in dB versus θ elevation angle. Satellite at synchronous altitude, balloon at 120,000 feet, Aircraft 60,000 feet. Test aircraft at 25,000 feet.

Figure B-8: $\dot{\theta}$ rate of change of θ vs elevation angle θ for satellite at 19,323 nm, balloon at 120,000 ft aircraft 60,000 ft, test aircraft at 25,000 ft. Ground speed 400 knots.

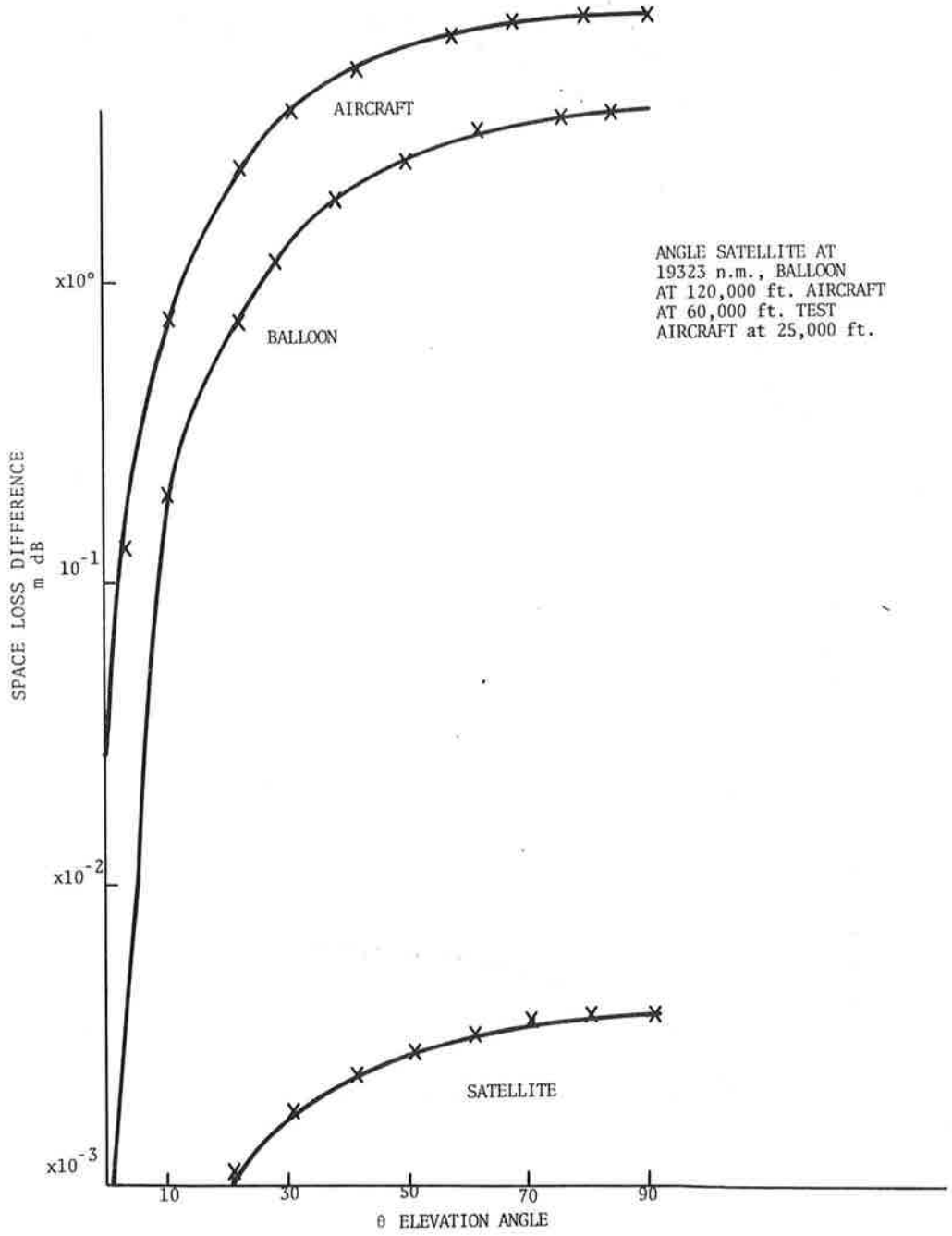

Figure B-7. Space Loss Difference in dB Vs. Elevation

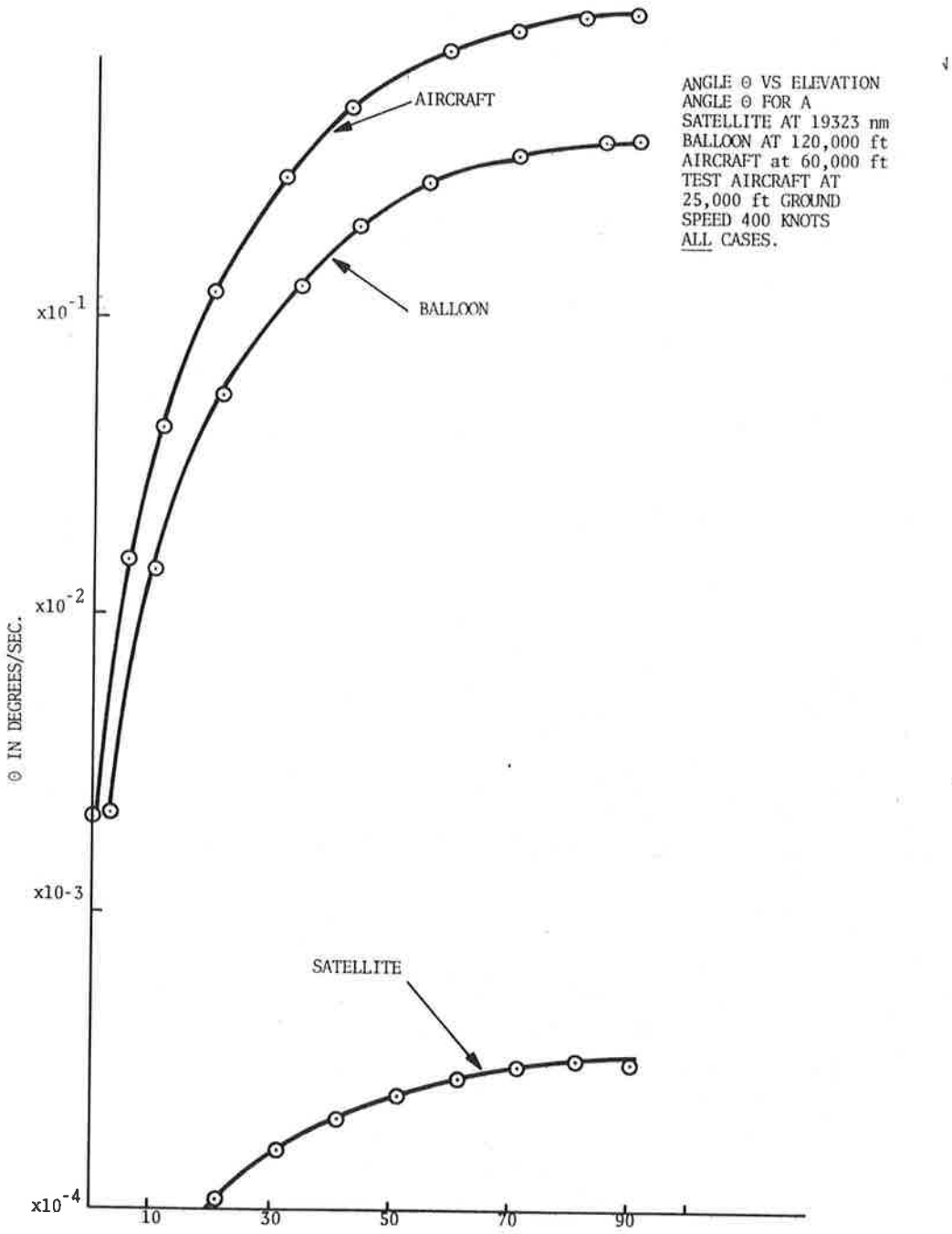

Figure B-8. Rate of Change of Elevation

APPENDIX C
CONCLUSIONS

Complete calculations of all possible parameters of multipath, particularly for the aircraft-to-aircraft tests has not been performed. Obtaining expressions for scattered bandwidth for this case require extensive modification of the Durranni and Staras results. This modification was attempted at ERC but at the present time no firm analytic result exists for this parameter. However, investigation of the model leads to a heuristic argument which indicates that it is difficult to conceive of a useable flight plan for the two aircraft which will achieve a fading bandwidth comparable to a satellite-to-aircraft link.

On the other hand it is shown that the fading bandwidth for the balloon aircraft tests is nearly identical to that expected for a satellite-to-aircraft link. The major discrepancy for the balloon aircraft link is the sensitivity of the relative doppler to horizontal motion which will effect fading and intelligibility of a voice signal, particularly at VHF. This discrepancy may be removed by choosing a near circular flight path around the balloon. This approach has the further advantage that a relatively constant elevation angle can be maintained.

Perhaps most significant is the relative space loss for the two cases considered. This loss is essentially zero for a satellite-to-aircraft link. The balloon-to-aircraft result gives a little over 1 dB loss at a 30° elevation angle. This is not expected to be very significant, since it does not supress multipath interference; however the aircraft-to-aircraft result is nearly 4 dB below the satellite-to-aircraft value, which seems excessive and may seriously effect the multipath results.

This it is apparent that the balloon aircraft simulation most represents the operational aircraft-to-satellite link.

BIBLIOGRAPHY

1. TRW, Test Plan For Navstar Navigation System, NASA contract 12-539, Appendix E.

2. Durranni and Staras, "Multipath Problems in Communications Between Low Altitude Spacecraft and Stationary Satellites," RCA Review March 1968. NASA contract NASW-1447.

APPENDIX D
SIMULATION OF FADING BANDWIDTH WITH AN AIRCRAFT-TO-AIRCRAFT LINK

Calculations were made of angular deviation from a perfectly circular flight around the balloon necessary to obtain the same specular doppler shift as in the case with the satellite link. This angular deviation is a function of the elevation angle and is given below along with the rate of change of elevation angle.

Elevation Angle	Deviation Angle	Relative Doppler Shift	Rate of change of elevation θ Angle
θ			$\dot{\theta}$
11°	6.41°	2.45 Hz at L-band	1.56×10^{-3}
21°	1.66°	2.29 Hz at L-band	1.62×10^{-3}
31°	0.95°	2.05 Hz at L-band	1.82×10^{-3}

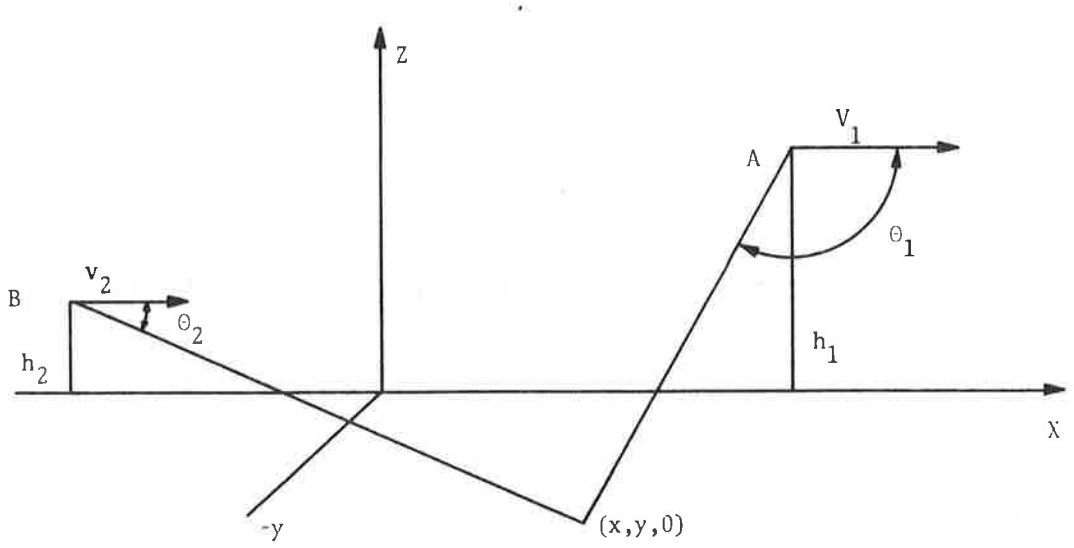

Figure D-1. Geometry of Aircraft-to-Aircraft Link

In the following discussion, we shall try to show heuristically that the fading bandwidth of a high altitude aircraft-to-aircraft link will not closely simulate the fading bandwidth obtained with a satellite-to-aircraft link.

Given diffuse multipath, the received signal at an aircraft will be composed of a direct component, specular component and components reflected from all points in the scatter region. Also each component is doppler shifted proportional to the individual geometry. All of these signals beat with each other to provide a bandwidth of fading. A reasonable criterion for equivalent fading then would be that the doppler shifted return from any point in the scatter plane for an aircraft-to-aircraft link closely approximate the doppler shifted return for a satellite-to-aircraft link at the same point.

Consider the flat earth geometry of Figure D-1. The frequency f_m of the doppler shifted signal from S is given as:

$$f_{M_{A/A}} = f_c - \frac{f_c V_1 \cos \theta_1}{C} + \left(f_c - \frac{f_c V_1 \cos \theta_1}{C}\right)\left(\frac{V_2 \cos \theta_2}{C}\right) \qquad (1)$$

where f_c - carrier frequency

V_1 - speed aircraft 1

V_2 - speed aircraft 2

C - speed of light

θ_1, θ_2 - shown in Figure D-1.

The doppler shifted signal from point A for a satellite-to-aircraft link will be

$$f_{M_{S/A}} = f_c + \frac{f_c V_2 \cos \theta_2}{C} \qquad (2)$$

We are interested in

$$f_{M_{A/A}} - f_{m_{S/A}} = 0 \qquad (3)$$

for as close a simulation of the satellite-to-aircraft link as possible.

$$f_{M_{A/A}} - f_{M_{S/A}} = 0 = \frac{f_c V_1 \cos \theta_1}{C} \left(1 + \frac{V_2 \cos \theta_2}{C} \right) \qquad (4)$$

Equation D-2 is satisfied if any of the following conditions are true:

$$V_1 = 0,\ V_2 = -C,\ \theta_1 = 90°,\ \theta_2 = 180°$$

Obviously, $V_1 = 0$ or $V_2 = -C$ is impossible but flight paths can be chosen such that $\theta_1 = 90°$ or $\theta_2 = 180°$. However, for the simulation to be close to the satellite case Equation D-2 must be satisfied for all points in the scatter plane and clearly choosing a flight path such that $\theta_1 = 90°$ or $\theta_2 = 180°$ for all points is impossible.

APPENDIX E
ELEVATION ANGLE θ VS ANGLE OF INCIDENCE ϕ

For a stationary satellite-to-aircraft link it can be shown that the elevation angle θ and angle of incidence ϕ at the specular point are essentially equal, see Figure D-1. This follows from the altitude of the satellite 19,323 nm which allows one to consider paths R_1 and R to be parallel. However in the case of balloon-to-aircraft or aircraft-to-aircraft these paths are not parallel and we must derive a means for determining ϕ given θ for various altitudes of the balloon or aircraft.

Now it can be proven that

$$\tan\theta = \frac{K-1}{K+1}\tan\phi \quad \text{where } K = \frac{h_1}{h_2} = \frac{r_1}{r_2} \tag{1}$$

From the law of cosines

$$(h_a+R)^2 = r_1^2 + R_e^2 + 2Rer\sin\phi \tag{2}$$

$$(h_s + R_e)^2 = r_2^2 + R_e^2 + R_e r_2 \sin\phi \tag{3}$$

$$r_1 = R_e \sin\phi \pm R_e^2 \sin^2\phi + 2R_e h_a + h_a^2$$

$$r_2 = R_e \sin\phi \pm R_e^2 \sin^2\phi + 2R_e h_s + h_s^2$$

$$\frac{r_1}{r_2} = K = \frac{1 - \sqrt{1 + \frac{2h_a}{R_e\sin\phi} + \left(\frac{h_a}{R_e\sin\phi}\right)^2}}{1 - \sqrt{1 + \frac{2h_s}{R_e\sin\phi} + \left(\frac{h_s}{R_e\sin\phi}\right)^2}} \tag{4}$$

Now using equations 2 and 3 we can obtain θ as a function of ϕ and values of ϕ for various values of θ when this function is plotted. This value of ϕ is used in determining B_s or relative doppler shifts. These results are given in graph A-1, for two altitudes of the test aircraft.

Error in considering θ as elevation angle:

In examining Figure D-1 it may be noticed that θ is not measured from a perpendicular to the aircraft's position vector but rather from a line parallel to the position vector of the specular point. Thus it is of concern how close the value of δ is to 90°.

$$\delta = \frac{\pi}{2} - \theta_s \tag{5}$$

Figure E-1 is θ_s versus θ and shows that at 5° θ_s=1° at 10° = .5° and decreases exponentially so that at angles greater then 5°,θ is very close to being the true elevation angle. The plot given in A-2 is for the satellite-to-aircraft but is very similar for balloon and aircraft links.

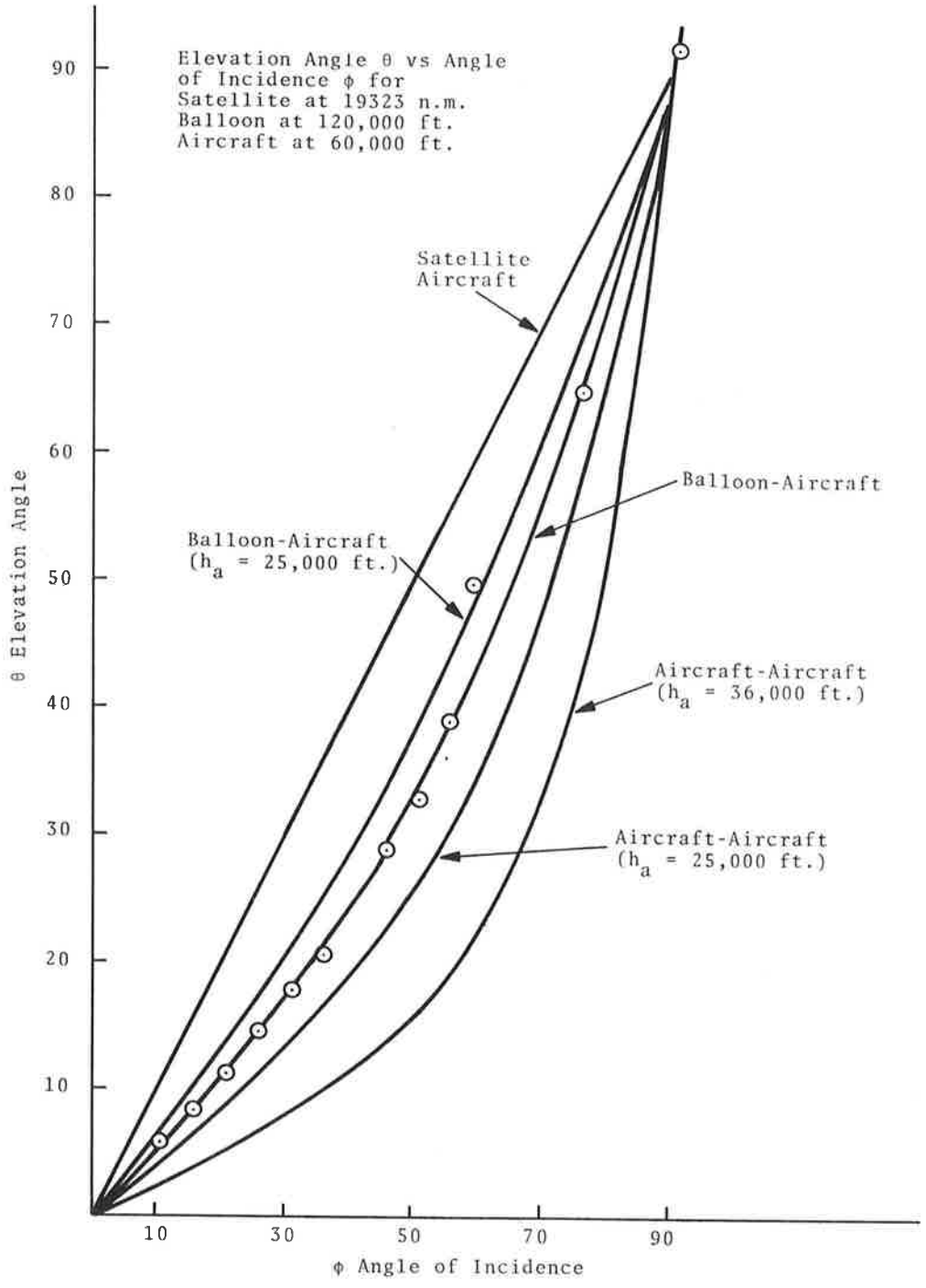

Figure E-1. Elevation Angle θ vs Angle of Incidence for Satellite at 19323 n.m.

APPENDIX F
REFERENCES

1. Personal Communication, Dr. Campanella of COMSAT Labs, to R. Wilson, March 1972.

2. European Space Research Organization, "ESRO ATC Balloon-Aircraft Satellite Simulation Experiment 1971," D.L. Brown, Editor, European Space Research and Technology Center, Noordwijk, Holland, March 1972.

3. Gardner, F.M., "Phaselock Techniques," John Wiley & Sons, NY, 1966.

4. Kryter, K.D., "Validation of the Articulation Index," J. Acous. Soc. Am., November 1962.

5. ERC Phase A Analytical Report, "Navigation/Traffic Control Satellite," Prepared by the Satellite Programs Office, NASA Electronics Research Center #PM-62, May 1970.

6. French, N.R., and Steinberg, J.C., "Factors Governing the Intelligibility of Speech Sounds," JASA, Vol. 19, #1, January 1947.

7. The American National Standards Institute, "Method for Measurement of Monosyllabic Work Intelligibility," Report #S 3.2, 1960.

8. Birch, J.N. and Getzin, N., "Voice Coding and Intelligibility Testing for a Satellite-Based Air Traffic Control System," Magnavox Co., Report NASA contract no. NAS5-20168, April 1971.